UNIVERSITY OF CALIFORNIA SAN DIEGO

Activation and regulation of mRNA decay by the inflammatory response factor, Tristetraprolin

A dissertation submitted in partial satisfaction of the
requirements for the degree Doctor of Philosophy

in

Biology

by

Alberto Carreño

Committee in charge:

Professor Jens Lykke-Andersen, Chair
Professor Eric Bennett
Professor Matthew Daugherty
Professor Amy Pasquinelli
Professor Miles Wilkinson

2022

The dissertation of Alberto Carreño is approved, and it is acceptable in quality and form for publication on microfilm and electronically.

University of California San Diego

2022

DEDICATION

This thesis is dedicated to my family.

TABLE OF CONTENTS

LIST OF FIGURES AND TABLES

Chapter 2

Chapter 3

ACKNOWLEDGEMENTS

Chapter 2, in full, has been submitted for publication of the material. Carreño, Alberto; Lykke-Andersen, Jens. The dissertation author was the primary investigator and author of this material.

VITA

2013	Bachelor of Science, University of California Santa Barbara
2013-2014	Laboratory Technician, Santa Barbara City College
2013-2014	Volunteer Researcher, University of California Santa Barbara
2014-2015	Laboratory Technician, BTS Research
2015-2022	Graduate Student Researcher, University of California San Diego
2022	Doctor of Philosophy, University of California San Diego

PUBLICATIONS

Alberto Carreño and Jens Lykke-Andersen. 2022. The Conserved CNOT1 Interaction Motif of Tristetraprolin Regulates ARE-mRNA Decay Independently of the p38 MAPK-MK2 Kinase Pathway. bioRxiv doi: 10.1101/2022.02.15.480631

ABSTRACT OF THE DISSERTATION

Activation and regulation of mRNA decay by the inflammatory response factor Tristetraprolin

Alberto Carreño

Doctor of Philosophy in Biology

University of California San Diego, 2022

Professor Jens Lykke-Andersen, Chair

The RNA binding protein tristetraprolin (TTP) is an mRNA destabilizing factor that regulates the stability of transcripts involved in promoting inflammation. TTP regulates mRNA stability through recruitment of decay factors involved in deadenylation, decapping, exonucleolytic decay, and translation repression. TTP activity is regulated by post-translational modifications with nearly 30 reported sites of phosphorylation; however, the functional effects of only two sites are well characterized. Previous work revealed the conserved TTP CNOT1 Interaction Motif (CIM) is an important structural element that promotes the association with the major deadenylase complex, CCR4-NOT.

In the work described in Chapter 2, I studied how the TTP CIM promotes mRNA decay cooperatively with other regions of the TTP protein. Using tethered decay assays, I find that mutation of conserved tryptophan residues, which associate with the CCR4-NOT subunit CNOT9, in addition to removing the CIM causes stabilization of target mRNA. Pull-down assays of TTP mutants reveal that CCR4-NOT recruitment is facilitated in a cooperative manner by the TTP-CIM and tryptophan residues. Furthermore, I find, contrasting previous reports, that the p38 MAPK pathway does not target a conserved serine residue within the TTP-CIM and that the CIM remains active in conditions where TTP is targeted by the downstream p38 MAPK kinase, MK2. These results suggest that efficient regulation of TTP requires multiple signaling pathways.

Difficulties examining TTP under native conditions has been a limitation of previous studies. In the work described in Chapter 3, to facilitate studies of TTP in a more endogenous setting, I generated $TTP^{-/-}$ RAW 264.7 mouse macrophage cells using a CRISPR-Cas9 targeting approach. These were used to generate lentiviral add-back cells expressing TTP from the endogenous TTP promoter. Unfortunately, exogenous TTP expression was unable to reach the levels seen from the endogenous locus in RAW 264.7 cells suggesting that additional enhancer element(s) acting on the TTP locus are necessary to produce an efficient TTP-expression response. Additional repair template-mediated CRISPR-Cas9 gene editing techniques using selectable markers are also reported here as a promising tool to generate endogenous TTP mutants in RAW 264.7 macrophage cells.

Chapter 1. Post-transcriptional gene regulation by the ZFP36 protein family.

1.1 Post-transcriptional gene regulation

Proper gene regulation is of vital importance for maintaining homeostasis of the cell and preventing the occurrence and progression of pathologies. In addition to gene expression being regulated at the transcriptional level, post-transcriptional regulation of protein coding genes provides an additional layer for fine-tuning protein output.

The generation of a mature mRNA includes the addition of a 7-methylguanosine cap at the 5' end and a poly-A tail at the 3' end where these two modifications protect the newly generated transcript from degradation. The co-transcriptionally added 5' cap protects mRNA from 5' to 3' exonucleases and serves as a binding site for the eukaryotic translation initiation factor eIF4E (1). The poly-A tail of mRNA serves as a binding site for Poly-A Binding Proteins (PABPs) that protect from mRNA decay by reducing deadenylation and by preventing decay-promoting TUT4/7 mediated uridylation (2–4). Removal of these binding factors is a critical step in promoting mRNA decay.

Cytoplasmic mRNA decay relies on the coordination of various decay factors. The decay process is most often initiated by deadenylation and proceeds either by 3' to 5' exonucleolytic decay or by removal of the 5' cap by decapping factors, followed by 5' to 3' decay pathways (5). The major pathway of mammalian mRNA decay first requires the removal of the poly-A tail of an mRNA transcript, which is often the rate-limiting step of mRNA decay. Following deadenylation, mRNA decay can proceed through 3'-5' exonucleolytic decay by the exosome or by removal of the 5' cap by a process known as decapping (6, 7). Removal of the 5' cap first requires the displacement of the cap-binding protein eIF4E. Upon removal of the 5' cap, degradation by the 5'-3' exonuclease XRN1 can proceed. Although they have sometimes been portrayed as two disparate forms of mRNA decay, decapping and deadenylation have been observed to be linked by factors such as

LSM1-7 and DDX6 (8–12). Although decapping and XRN1-mediated decay has been demonstrated to be the major pathway of mRNA degradation, deadenylation is generally a pre-requisite for mRNA decay (13).

Studies in human cells suggest that mRNA deadenylation undergoes a biphasic form of poly-A tail removal, where the long mRNA tail is first trimmed by the PAN2-PAN3 deadenylase complex to a size of about 110 nucleotides (nts) (14), followed by the removal of the remaining tail by the CCR4-NOT deadenylase complex (15). The CCR4-NOT complex is an approximately 1 MDa complex composed of seven shared core components in flies, yeast and humans (15), which is able to promote deadenylation through its DEDD-domain containing CNOT7/CNOT8 proteins, also known as CAF1, and the EEP domain containing CNOT6/CNOT6L proteins, also known as CCR4 (16, 17). The overexpression of Ccr4p in budding yeast was capable of promoting deadenylation in conditions where Caf1p was mutated, suggesting some degree of functional redundancy (16). Further investigation into these two deadenylase subunits of the CCR4-NOT complex have demonstrated that although they both function to remove terminal adenosines, there exist some functional differences. PABPs, which have been shown to associate with eIF4G as well as with ribosomes to promote efficient translation of the encoded protein (18–20), are displaced from the polyA-tail by CCR4, but not CAF1, allowing for downstream exonucleolyic events to occur (21, 22). Altogether, these findings reveal a major role for the CCR4-NOT deadenylation complex in mRNA decay.

The purpose of mRNA is to serve as a template for protein production by translating ribosomes. The process of translation itself appears to stabilize transcripts (23). Indeed, the codon usage within mRNAs affects the translocation by ribosomes and it has been found that transcripts containing optimal codons, codon sequences for which there are more abundant tRNAs, causes more stable transcripts (21, 23–26). Furthermore, inefficient translation is sensed by the CCR4-NOT complex which can initiate the process of mRNA degradation

(24). Translation repression has been demonstrated to promote decay events, such as decapping (10). Disruption of translation initiation has been a demonstrated function of mRNA destabilizing factors that affect the association of eIF4E to the 5' cap (27–30). For example, the translation repression factor GIGYF2-4EHP directly associates to the 5' cap through the cap binding protein 4EHP (also known as eIF4E2), sterically preventing the association of eIF4E (31, 32). These interactions prevent the recruitment of ribosomes to eIF4F which is unable to associate with the 5' cap. These findings reveal that the process of mRNA decay is an intricate and coordinated event, orchestrated by a variety of destabilizing elements with unique functions that promote the efficient disposal of mRNA.

1.2 mRNP granules

The dynamic environment of the cell requires an ability to quickly react to instances of molecular stress to preserve the integrity of the cell. The costly processes of translation and protein maintenance must be tightly regulated to prevent unnecessary expenditure of cellular resources while also retaining the ability to resume promptly to maintain homeostasis. While translation inhibition is reported to promote mRNA decay, during times of stress, translationally silenced mRNAs form mRNP granules called stress granules (SGs) (33, 34). SGs have been considered as sites of triage whereby mRNA transcripts can be released back into the cytoplasm to re-engage in translational activity, or be shuttled to undergo mRNA decay, possibly in association with another variety of granules called processing bodies (PBs), which are enriched in mRNA decay factors (33, 34). Interestingly, the localization of SGs and PBs relative to each other differs according to conditions in the cell.

1.3 The AU-rich element (ARE) affects mRNA stability

Despite the almost universal presence of the 5' cap and poly-A tail, half-lives differ greatly between mRNAs, which can range from the order of minutes to several hours (35,

36). This difference in transcript stability is attributed to sequences found within the mRNA transcripts. These intrinsic stability or instability elements can include *cis*-elements located in untranslated regions (UTRs) or codon compositions of the coding regions (25, 37, 38). *Cis*-elements within UTRs serve as binding sites for *trans*-acting factors which can control the stability of transcripts.

A well-studied 3'UTR *cis*-element is the Adenylate-Uridylate rich element (ARE) present in the 3' UTRs of many cytokine and proto-oncogene mRNAs (39–41). The regulation of mRNAs by their AREs have been shown to affect several aspects of cell function including cell growth, cell differentiation, and response to external stimuli (42, 43). AREs were first demonstrated to serve as mRNA instability elements when the decay of a stable mRNA species was dramatically reduced upon addition of the ARE-containing GM-CSF 3' UTR (44). Much of the destabilizing effects of AREs is seen to be regulated by signaling events such as the p38 MAPK pathway (45). AREs serve as binding sites for RNA-binding proteins involved in mRNA decay and genes encoding mRNAs with AREs have been estimated to comprise ~8% of the genome (46). Notably, ARE-mediated mRNA regulation has been shown to be important for the regulation of inflammation whereby following activation, ARE-containing pro-inflammatory transcripts are transiently expressed and facilitate the initiation and propagation of the inflammatory response (47). In order to prevent chronic inflammatory pathologies from developing, the pro-inflammatory, ARE-containing, transcripts are seen to be rapidly degraded following a short period of increased stability (48). These changes in stability are now understood to be regulated by the RNA destabilizing factor tristetraprolin (TTP) (49).

1.4 TTP is a critical cytokine mRNA destabilizing factor in inflammation

Tristetraprolin (TTP), which contains three tetra-proline motifs awarding its name, was first discovered in mouse NIH 3T3 fibroblast cell lines as a protein whose expression was

responsive to insulin treatment (50). Although not readily detectable in serum-deprived cells, the rapid expression of TTP was detected within 10 minutes of stimulation with insulin, classifying it as an immediate-early response gene.

TTP was found to contain two conserved CCCH zinc-finger domains, each with two sequence stretches of C8xC5xC3xH (C=Cysteine; H=Histidine; x=any amino acid) that are separated by 18 amino acids, and was found to be expressed at low levels in the nucleus in fibroblasts, but was readily induced upon treatment with growth factors, serum, phorbol 12-myristate 13-acetate (PMA) and Lipopolysaccharide (LPS) (50–53). The promoter region of TTP has been shown to serve as a binding site for several transcription factors, including EGR-1, AP2, SP1, and NF-κB (54, 55). Upon induction, TTP was found to be translocated to the cytoplasm and post-translationally modified (51, 56–58).

The physiologic relevance of TTP was demonstrated by the chronic inflammatory phenotype that developed in TTP knockout (KO) mice, which developed myeloid hyperplasia, cachexia, dermatitis, and arthritis (57). Termed “TTP-deficiency syndrome”, these TTP KO mice were observed to have a lifespan of less than 8 months. The inflammatory phenotype was attributed to an excess of circulating TNF-α cytokines (52, 57), which was supported by the appearance of a normal phenotype when TTP KO mice were treated with antibodies for tumor necrosis factor α (TNFα). Evidence supporting the role of TTP in regulating TNF-α expression was demonstrated in macrophages lacking TTP, which more than doubled the half-life of TNFα mRNA, from 35 min to 85 mins (59). TTP’s CCCH zinc finger domains were found to bind the ARE within the 3’ UTR of mRNAs for early immediate genes, including TNF-α, as well as other pro-inflammatory transcripts (49, 52, 59–65). The importance of the TTP zinc finger domain (ZFD) was noted in knock-in ZFD mutant mice that developed a severe inflammatory phenotype caused by TTP’s inability to bind to target mRNA (66). Supporting the paradigm of inflammation being a tightly controlled process, it has been

observed that he mRNA for TTP itself contains an ARE in its 3' UTR and it was shown that TTP mRNA lacking its own ARE protects mice from inflammatory pathologies (67, 68).

Novel high-throughput methods have now revealed the network of transcripts that are targeted by TTP. In addition to its role in inflammation, TTP is observed to regulate processes such as iron homeostasis, cell division, adipogenesis, and TTP mis-regulation has been shown to be a contributing factor to diseases such as cancer of various tissues and neurodegenerative diseases (46, 69–72). In addition to its noted physiological role, studies into TTP-mediated mRNA decay offer an understanding of fundamental processes involved in mRNA decay and its regulation.

1.5 TTP interacts with multiple mRNA destabilizing factors

Having established its targets and physiologic role, efforts to understand the molecular mechanism by which TTP regulates mRNA decay have contributed to our understanding of the activation and regulation of mRNA decay. TTP interacts with factors involved in all facets of mRNA decay, including those involved in deadenylation, decapping, exonucleolytic decay, and translation repression (73–79). Decay assays monitoring truncation mutants revealed that TTP can promote mRNA decay through both of its N- and C-terminal domains, suggesting that TTP contains decay promoting redundancies.

Work done towards understanding the association of TTP with decay factors have revealed conserved motifs that are responsible for its interaction with critical factors involved in mRNA decay. The tetraproline motifs, responsible for the naming of the protein itself, have been shown to be responsible for the association of TTP with the 4EHP-GYF2 translation repression complex (32, 77). The ability of TTP to promote translation repression has also been shown to require the association of the RNA helicase DDX6 (80). Notably, recent studies examining TTP's structure revealed a highly conserved C-terminal CNOT1-interacting motif (CIM) that associates with the CCR4-NOT scaffold protein, CNOT1.

Because of its critical role in promoting mRNA decay, the loss of association with the CCR4-NOT complex would be predicted to lead to a dramatic stabilization of targeted mRNAs. However, both *in vitro* and *in vivo* experiments have revealed that deletion of the TTP CIM led to only a mild stabilization of target mRNAs (76, 81), suggesting that TTP promotes mRNA decay through additional interactions. In addition to the CIM, TTP has been demonstrated to associate with the CCR4-NOT deadenylase complex through its conserved tryptophan residues, which interact with the CNOT9 subunit (82). These findings suggest a functional redundancy in TTP's ability to stabilize associations with critical deadenylase factors. Indeed, the N-terminal domain of TTP has been demonstrated to associate with factors involved in decapping, exonucleolytic decay and, surprisingly, deadenylation factors (74). These findings suggest that TTP can stabilize associations with decay factors through seemingly disparate motifs and reveals a functional redundancy in decay-promoting activities.

As an mRNA repression factor, TTP has unsurprisingly been found to associate with sites of translationally repressed mRNAs such as stress granules and p-bodies (83–85). With the exception of the conserved ZFD, TTP is largely composed of intrinsically disordered regions which may contribute to its association with these granules and may in part explain how both TTP termini can intrinsically associate with decay factors.

Although several key discoveries have been made toward understanding TTP-mediated mRNA decay, much is still unknown. Despite observations that reveal that both domains of TTP are sufficient to promote mRNA decay, it is still unclear how the full-length protein utilizes both domains to coordinate the process of translational repression and mRNA decay.

1.6 TTP is a post-translationally modified protein

TTP has been shown to be a target of several kinase pathways including the p38, ERK, and JNK mitogen activated protein kinase (MAPK) pathways (56, 86). Upon LPS induction, TTP is shown to receive a generous amount of phosphorylations, as initially seen in experiments where phosphatase treatment leads to a faster migrating species from 50 kDa to its predicted 34 kDa migration pattern, in SDS-polyacrylamide gels (87–90). TTP has been reported to contain around 30 sites of phosphorylation, as determined by mass-spectrometry experiments in HEK 293 cells transfected with TTP (91). Notably, the p38 MAPK pathway has been demonstrated to contribute to the inflammatory response by stabilizing cytokines/stress-induced genes through MAPK-activated protein kinase 2 (MK2) (92). Indeed, phosphorylation of TTP by MK2 has been shown to be a critical regulator of TTP stability, localization, and function.

Although TTP is targeted by several pathways, the functional consequence of each is still largely unknown. An example of this is seen in investigations looking at the role of the p38 and ERK MAPK pathways on TTP. Activation of p38 MAPK helps stabilize TTP mRNA (67): phosphorylation of TTP's serine residues 52 and 178 (mouse numbering) by MK2 of the p38 MAPK pathway has been shown to promote localization from the nucleus to the cytoplasm, inhibit the association of decay factors, recruit association with 14-3-3 adaptor proteins, and protect TTP from degradation by the proteosome (83, 90, 93–95). Furthermore, TTP protein is rapidly degraded upon inhibition of the p38 MAPK pathway and TTP mRNA stability is decreased. In contrast to the effects of p38 MAPK pathway modulation on TTP, inhibition of the ERK pathway did not influence TTP expression or its mRNA stability, suggesting that the targeting of TTP by distinct pathways may have unique consequences and roles. Although the ERK pathway does not appear to affect TTP function, inhibition with drugs potentiated the nuclear localization of TTP when co-treated with p38 and ERK inhibitors while treatment with ERK inhibitors alone did not retain TTP in the nucleus upon induction (94).

Targeting of TTP by MK2 has been demonstrated to affect its localization within the cytoplasm. While TTP can be observed to associate with stress granules upon carbonyl cyanide-*p*-trifluoromethoxyphenylhydrazone energy deprivation treatment, activation of MK2 through arsenite treatment reduced TTP association to SGs (83). These results suggest TTP localization to SGs are context specific and is affected by post-translational modifications.

Of particular interest, is a highly conserved serine residue residing within the conserved CNOT1-interacting motif (CIM) of TTP. Phosphorylation of this serine residue has been previously shown to reduce the association of CNOT1 to a synthetically produced CIM peptide, suggesting a critical site of regulation (76). Indeed, mutation to this conserved serine residue to an alanine led to an increased rate of TTP-mediated mRNA decay (96). Interestingly, others have demonstrated that while TTP loses its association to CNOT1 upon phosphorylation of this serine, the mutation of the serine to aspartate led to an increased association to the decapping factor DCP1a in the TTP homolog BRF1 (97). Clearly, the functional effect of TTP-phosphorylation is still poorly understood and efforts made toward elucidating these dynamics will help uncover the role that signaling events have in the regulation of mRNA decay.

1.7 The ZFP36 protein family: Similarities and differences of TTP with its paralogs BRF1 and BRF2

As part of the ZFP36 protein family, Tristetraprolin (ZFP36) shares similarities with the proteins butyrate response factor-1 (BRF1, ZFP36L1) and -2 (BRF2, ZFP36L2). Members of the ZFP36 family encode for RNA destabilizing proteins that contain the C8xC5xC3xH zinc-finger domain that targets ARE-containing transcripts. Despite sharing a nearly 70% sequence identity in the zinc-finger region, TTP, BRF1, and BRF2 share little sequence identity in the domains upstream and downstream of this RNA-binding motif (98). Despite targeting similar ARE-containing transcripts (53) due to the presence of the

conserved zinc-finger domain, knockout experiments reveal different physiologic consequences between ZFP36 members in mice. As discussed above, knockout of TTP yields chronic inflammatory phenotypes (57, 59). Disruption of BRF1 is embryonic lethal due to aberrations in placental function (99–101). BRF2 ablation in mice led to defective hematopoiesis leading to perinatal mortality (102). BRF2 has also been demonstrated to play a role in oocyte meiotic maturation through its regulation of luteinizing hormone receptor (LHR) mRNA (103). Furthermore, conditional knockouts of BRF1 and BRF2 in lymphocytes led to disruptions in the proper development of B-cells and T-cells (104, 105). Interestingly, although all members of the ZFP36 family are induced in RAW 264.7 macrophage cells, myeloid specific knockouts of BRF1 did not lead to an increase in inflammatory markers (106). Lastly, TTP, but not BRF1 or BRF2, sensitizes cells to apoptosis by TNF-α treatment (89).

Aside from the conserved zinc-finger domain, few sequence similarities exist between ZFP36 family members. Despite this, TTP and BRF1 have been demonstrated to associate with several similar mRNA decay factors and contribute to the formation of p-bodies (74, 85). The one other feature that is highly similar between ZFP36 family proteins is the conserved C-terminal CNOT1 interaction motif, critical for the association with the CCR4-NOT complex (76, 107). Similar to the TTP-CIM, the BRF1-CIM was demonstrated to promote the association with CCR4-NOT (97, 108). Research into BRF1 also revealed another potential function mediated by the CIM, where it was found to promote translation repression (109). Whether translation repression can be mediated by the TTP-CIM remains to be explored.

As discussed for TTP, BRF1 and BRF2 activities are also regulated by post-translational modifications from several disparate kinase pathways (110–113). As mentioned above, the ZFP36 proteins are highly dissimilar, and this is also reflected in their sites of phosphorylation. Although several sites of phosphorylation are not conserved, two serine residues, and their surrounding sequences, corresponding to the MK2-targeted TTP-Ser 178

and the TTP CIM-Ser 316 (mouse numbering), are conserved in BRF1 and BRF2. Indeed, BRF1 has been demonstrated to be a target of MK2 at Ser 203, corresponding to TTP-Ser 178, which is also a reported target of the Protein Kinase B (PKB) pathway (110, 112). Lastly, the conserved serine residue within the BRF1-CIM, corresponding to TTP-Ser 316, was demonstrated to be a target of Protein Kinase A (PKA) (97). Although this phosphorylation resulted in a decrease in the association with CNOT1, phosphorylation of the BRF1-CIM led to an increase in BRF1-mediated mRNA decay which was explained by increased association with decapping factors. Altogether this adds a layer of complexity between how BRF1, and perhaps BRF2, regulate the association of decay factors according to post-translational modifications which may also be relevant to TTP-mediated mRNA decay mechanisms. Clearly, many questions remain to be addressed about how the ZFP36 protein family of proteins activate mRNA degradation and how their activities are regulated by signaling events.

Chapter 2 The Conserved CNOT1 Interaction Motif of Tristetraprolin Regulates ARE-mRNA Decay Independently of the p38 MAPK-MK2 Kinase Pathway

2.1 Abstract

Regulation of the mRNA decay activator Tristetraprolin (TTP) by the p38 mitogen-activated protein kinase (MAPK) pathway during the mammalian inflammatory response represents a paradigm for the regulation of mRNA turnover by signaling. Phosphorylation of TTP by p38 MAPK-activated kinase 2 (MK2) inhibits the association of TTP with the CCR4-NOT deadenylase complex and represses TTP-mediated mRNA decay. In this chapter, I present evidence that TTP remains active in the presence of activated MK2 due to its highly conserved CNOT1 Interacting Motif (CIM), which remains unphosphorylated and capable of promoting deadenylation and decay. The CIM recruits the CCR4-NOT complex cooperatively with previously identified conserved tryptophan residues of TTP and deletion of the CIM strongly represses residual association with the deadenylase complex and activity of TTP in conditions of active MK2. A conserved serine in the CIM is not a target of MK2 but is instead phosphorylated by other kinases including the PKCa pathway and regulates TTP activity independently of MK2. These results suggest that kinase pathways regulate TTP activity in a cooperative manner and that the p38 MAPK-MK2 pathway relies on the activation of additional kinase pathway(s) to fully control TTP function.

2.2 Introduction

mRNA turnover is a critical step in the regulation of gene expression and improper regulation of mRNA stability can promote the development of pathologies including neurodegenerative disorders, cancer, and chronic inflammation (7). mRNA degradation occurs by a multistep process that generally initiates with the removal of the poly(A)-tail,

followed by decapping of the 5' 7-methylguanosine cap, and exonucleolytic decay from either the mRNA 3' or 5' end (6, 7). Transcriptome-wide analyses have revealed considerable differences in stability between mRNAs with half-lives in mammals ranging from minutes to hours or days (36, 114). Factors that affect the stability of mRNAs include sequences found within the 3' or 5' untranslated regions (UTRs), and the codon usage within the open reading frame (6, 7, 26, 114). Importantly, there are transcripts whose stability change in accordance with signaling events in the cell. These transcripts are often regulated by RNA-binding proteins, which are themselves targets of post-translational modification. The general principles by which these post-translational modifications affect the activation of mRNA decay remain poorly defined.

The RNA binding protein Tristetraprolin (TTP; also known as ZFP36 or TIS11) is an mRNA destabilizing factor that recruits factors promoting translation repression, deadenylation, decapping, and exonucleolytic decay (74, 76, 82, 115). TTP is a highly regulated protein whose post-translational modifications have been shown to affect its stability, localization, and decay activity (83, 93, 94, 116). TTP is best known for its role in resolving the inflammatory response by promoting the degradation of pro-inflammatory cytokine mRNAs that contain adenosine-uridine rich elements (AREs) in their 3' UTRs (52, 59, 61, 88, 117). Structurally, TTP consists of a zinc-finger domain responsible for RNA binding, flanked by amino- (N-) and carboxy- (C-) terminal domains, each of which are capable of promoting mRNA decay (74). Two vertebrate paralogs of TTP, BRF1 (also known as ZFP36L1 and TIS11b) and BRF2 (also known as ZFP36L2 and TIS11d), which also mediate degradation of ARE-containing transcripts, contain zinc finger domains that are highly similar to that of TTP, but N- and C-terminal domains that are distinct, except for a highly conserved region at the extreme C-terminus (93, 107, 109, 110).

Recent attention has been turned towards the conserved C-terminal region of the TTP protein family. Studies examining the structural basis of TTP's association with the central cytoplasmic deadenylase, the CCR4-NOT complex, revealed an interaction with the CCR4-NOT scaffold protein, CNOT1, and this C-terminal region of TTP, which was therefore named the CNOT1-Interacting Motif (CIM) (76, 118). Supporting the importance of the CIM, deletion of the TTP CIM led to a stabilization of target transcripts (76, 81). The loss of the CIM, however, did not completely ablate the ability of TTP to promote mRNA decay, an observation that was further supported by the development of mice lacking the TTP-CIM, which exhibited an inflammatory phenotype significantly milder than that observed upon the complete loss of TTP (81). Separately, it was demonstrated that TTP has a second interaction with the CCR4-NOT complex via several conserved tryptophan residues that interact with the CNOT9 subunit (82). Mutation of those residues were also shown to stabilize TTP target transcripts. Furthermore, TTP is known to interact with the 4EHP-GYF2 translation repression complex and with decapping factors (32, 74, 115). However, the importance of these interactions for TTP's ability to activate mRNA decay in concert with the CCR4-NOT deadenylase complex remains less well understood.

TTP is a highly post-translationally regulated protein that has been shown to be a target of several kinase pathways. The most well-characterized of these is the p38 MAPK pathway, which is activated during the inflammatory response (119). A downstream kinase in the p38 MAPK pathway, MAPK-activated protein kinase 2 (MK2), targets TTP serine residues 52 and 178 (mouse numbering) whose phosphorylation leads to the stabilization of TTP target transcripts by inhibiting the recruitment of deadenylases (94, 98, 120, 121). Furthermore, MK2-mediated phosphorylation of TTP promotes the recruitment of 14-3-3 adaptor proteins, which have been speculated to inhibit degradation factor association, and affect both TTP localization and protein stability (83, 93, 116).

Another serine of TTP that undergoes phosphorylation is serine 316 (mouse numbering), a conserved serine of the CIM motif. Phosphorylation of this residue has been shown to inhibit association of TTP-family proteins with CNOT1, suggesting that the association of the major deadenylase complex is repressed by phosphorylation (76, 96, 97). However, a separate study using phosphomimetic mutations, suggested that phosphorylation of the CIM of the TTP homolog BRF1 promotes its association with decapping factors and accelerates mRNA decay (97). While several studies have identified the CIM as a target of MK2 (93, 96, 122), others have implicated the kinases RSK1 and PKA (96, 97). Thus, the importance of the highly conserved CIM and its phosphorylation in TTP regulation and function remains poorly defined.

In this chapter, to better understand the significance of TTP co-factor interactions in promoting activation of mRNA decay and how these are regulated by phosphorylation, I monitored the combinatorial effects of phosphorylation site and co-factor interaction motif disruptions on TTP function. My findings show that the CIM acts cooperatively with the conserved tryptophans of TTP to recruit the CCR4-NOT complex and activate mRNA decay, but upon mutation of these motifs, TTP remains unimpaired in its interaction with decapping factors and partially active. Phosphorylation of the TTP CIM reduces its ability to associate with the CCR4-NOT complex and promote mRNA deadenylation, and this phosphorylation event occurs with kinetics similar to that of the MK2-phosphorylated TTP serine 178 in stimulated mouse fibroblasts and macrophage cell lines. However, contrary to what has been previously reported, the CIM is not a target of the MK2 kinase, and TTP remains active in the presence of active MK2, primarily due to the activity of the CIM. Thus, TTP activates mRNA degradation through multiple co-activator complexes and the TTP CIM regulates TTP activity independently of the p38 MAPK-MK2 pathway.

2.3 Results

The TTP-CIM cooperates with other regions of TTP to promote mRNA decay

To establish a system for monitoring the interplay between the CIM and its phosphorylation with other known functional regions of TTP (Figure 2.1A), I utilized a previously established MS2-tethering pulse-chase decay assay (123) (Figure 2.1B) to first test the sufficiency and necessity of the conserved TTP-CIM motif for TTP-mediated mRNA degradation. A tetracycline-inducible β-globin mRNA containing MS2 coat protein binding sites in the 3'UTR was transiently co-expressed in human HeLa Tet-off cells with the MS2 coat protein fused to GFP and the TTP CIM. GFP served as a marker for transfection efficiency, and to stabilize an otherwise unstable MS2 coat protein. The MS2-GFP-CIM fusion protein promoted target mRNA degradation compared to the control MS2-GFP fusion protein alone (Figures 2.2A), which was expressed at a similar level (Figure 2.2B). An increase in mobility of the target mRNA through the gel was also observed over time in the presence of the MS2-GFP-CIM fusion protein over the MS2-GFP control (Figure 2.3A) consistent with the previously described function of the CIM in accelerating deadenylation (76). This conclusion was confirmed by oligo-dT and RNase H treatment to remove the poly-A tail, which resulted in the target mRNAs migrating at the same rate (Figure 2.3B). Co-immunoprecipitation (co-IP) assays for the MS2-GFP-CIM fusion protein confirmed CNOT1 association as compared with the control MS2-GFP protein (Figure 2.4). Thus, my MS2-coat protein tethering system recapitulates previously reported activities of the CIM (76), and the TTP-CIM is sufficient to accelerate mRNA deadenylation and decay.

Although the TTP-CIM can promote mRNA decay on its own, other regions of TTP have been implicated in mRNA decay as well. I was therefore interested in understanding the importance of the CIM in promoting mRNA degradation in conjunction with other functional motifs of TTP. I first deleted the CIM from full-length TTP and from the carboxy-terminal

domain (CTD) of TTP, each fused to the MS2 coat protein, and tested the effect on mRNA degradation. Consistent with previous reports (74), the target mRNA was rapidly degraded upon tethering of both the TTP-CTD and full-length TTP (Figures 2.5 and 2.6). Deletion of the CIM greatly stabilized target transcripts in the context of the CTD (Figure 2.5), while it only marginally impaired the activity of full-length TTP (Figure 2.6). This difference in the contribution of the CIM to mRNA decay promoted by the TTP-CTD and full-length TTP suggests a redundancy of the CIM with other regions of TTP, particularly outside of the CTD.

The TTP-CIM cooperates with conserved tryptophan residues to promote mRNA deadenylation and decay

TTP was previously reported to interact with another component of the CCR4-NOT complex, CNOT9, through its conserved tryptophan residues (Figure 2.1A) (82). Therefore, I was interested in understanding to what extent the CIM and tryptophan residues cooperate to activate mRNA decay. I generated alanine mutants for all conserved tryptophan residues of TTP and the TTP-CTD with the additional mutation of Proline 257, which was previously shown to also contribute to CNOT9 association (82) (Table 2.1). I performed tethered pulse-chase mRNA decay assays for these mutants with and without CIM deletion. The tryptophan to alanine (WA) mutation caused no significant reduction in activity in the context of the TTP-CTD with or without CIM deletion (Figure 2.5). However, for full-length TTP, further stabilization of the target mRNA was observed when the removal of the CIM was combined with mutations in the tryptophan motifs (Figure 2.6). This reduction in activity was accompanied by reduced association of TTP and the TTP CTD with CNOT1 and CNOT9 components of the CCR4-NOT complex upon mutation of CIM and tryptophan motifs (Figures 2.7 and 2.8). These observations demonstrate that the conserved tryptophan motifs and the CIM serve to cooperatively recruit the CCR4-NOT complex and activate mRNA

decay, likely via their previously reported interactions with different subunits of the CCR4-NOT complex.

Mutation of conserved tetraproline motifs does not significantly affect TTP-mediated mRNA decay rates

Other regions of TTP that interact with mRNA repression factors are the tetraproline motifs, which are conserved among TTP orthologs and promote the association with the 4EHP-GYF2 translation repression complex (115, 124). Mutations in these motifs, and depletion of 4EHP, were previously found to cause increased protein production from TTP target transcripts. Given the interconnected roles of translation repression and mRNA decay, I next performed tethered mRNA decay assays for TTP tetraproline mutants. I found that mutation of TTP tetraproline motifs (PS) did not increase the stability of the tethered target mRNA (Figure 2.9). To address whether the tetraproline motifs act cooperatively with the CNOT1 and CNOT9 interaction motifs, I established double and triple mutant TTP proteins. Comparing TTP mutants with and without tetraproline motif mutations revealed no stabilization of the target mRNA attributed to the tetraproline mutations (PS) when combined with the tryptophan mutations (WA) and/or CIM deletion (DCIM) (Figure 2.10), despite loss of association with CCR4-NOT and GYF2-4EHP complexes as monitored by co-immunoprecitation assays for CNOT1, CNOT9 and GYF2 (Figure 2.11). Interestingly, the TTP triple mutant protein defective in both CCR4-NOT and GYF2-4EHP complex association maintained undisrupted association with DDX6 and EDC4 of the decapping complex (Figure 2.11), suggesting that additional functional motifs exist in TTP that may explain the partial activity of this triple mutant.

TTP is transiently phosphorylated at the conserved CIM serine residue

Having established the degree of cooperativity between the TTP CIM and other known functional motifs of TTP, I next turned to the significance of CIM phosphorylation. I generated and validated a phospho-specific antibody raised against the phosphorylated serine 316 residue of mouse TTP (Figure 2.12). Consistent with a recent report (96), induction of the inflammatory response by serum shock of mouse NIH3T3 fibroblasts (Figure 2.13A), or treatment with lipopolysaccharide (LPS) of mouse RAW264.7 macrophages (Figure 2.13B), both caused rapid upregulation of TTP accompanied by phosphorylation at TTP serine 316, with kinetics similar to what has been described previously for TTP serine 178 phosphorylation (93, 121).

The TTP-CIM is phosphorylated in a p38 MAPK-MK2-independent manner

The TTP-CIM has been reported as a target of several kinase pathways (93, 96, 97, 122), including the p38 MAPK-MK2 pathway, which also targets TTP serines 52 and 178 (93, 121). HeLa cells transiently expressing TTP show detectable levels of phosphorylation of both serines 178 and 316 of TTP (Figure 2.14A). Treatment with the p38 MAPK inhibitor SB203580 (125) decreased serine 178 phosphorylation, as expected, while surprisingly serine 316 phosphorylation remained unaffected (Figure 2.14A). Consistent with this observation, co-expression of TTP or the TTP-CIM in HEK293 cells with constitutive active MK2 (83, 121) resulted in phosphorylation of TTP serine 178 but not serine 316 (Figures 2.14B).

Other kinases that have been observed to phosphorylate the CIM of TTP-family proteins include p90 ribosomal S6 kinase 1 (RSK1) and Protein Kinase A (PKA) (96, 97, 108). Another kinase predicted to phosphorylate TTP serine 316 in a kinase prediction

algorithm (126) is Protein Kinase C-alpha (PKCα). Treatment of HeLa cells with a PKC inhibitor, Gö6983 (127), decreased TTP Serine 316 phosphorylation while Serine 178 phosphorylation remained unaffected (Figure 2.14A). Moreover, constitutive active PKCα increased Serine 316 phosphorylation both in the context of full-length TTP (Figure 2.14B) and the TTP-CIM (Figures 2.15). I also observed an increase in TTP serine 178 phosphorylation in the presence of active PKCα (Figure 2.14B), which is likely due to reported activation by PKCα of the p38 MAPK pathway (128). Thus, serine 316 of the CIM can be phosphorylated by kinases including PKCa, but unlike serines 52 and 178, is not a target of MK2.

MK2-phosphorylated TTP promotes mRNA decay via the CIM

TTP activity has been previously reported to be inhibited by MK2 phosphorylation on serine residues 52 and 178, correlating with decreased association with deadenylation factors as well as the recruitment of 14-3-3 adaptor proteins (83, 93, 116, 129). My observation that the CIM is not a target of MK2 phosphorylation raised the possibility that the CIM continues to promote deadenylation and decay in the presence of active MK2. To test whether the CIM indeed acts independently of MK2 phosphorylation, I performed tethered mRNA decay assays comparing the effect of MK2 on wild-type TTP and TTP deleted of the CIM. Consistent with previous reports (83, 121), constitutive active MK2 (MK2A) stabilized the TTP target transcript, as compared to catalytic dead MK2 (MK2D), although this effect was relatively small (Figure 2.16). However, removal of the CIM from TTP, while having only a minor effect on TTP activity in the presence of inactive MK2, dramatically stabilized the target mRNA in the presence of active MK2 (Figure 2.16). This stabilization was dependent on the two serines, serines 52 and 178, targeted by MK2 as mutating them to alanines (TTP-2A) restored the activity of TTP deleted of the CIM in the presence of active MK2 (Figure

2.17). Consistent with these observations, treatment of TTP with the phosphatase inhibitor okadaic acid, which causes general upregulation of TTP phosphorylation, caused a reduction in association of TTP with CNOT1, which was exacerbated when the CIM was deleted (Figure 2.18). I observed similar strong dependence on the CIM of TTP activity in the presence of active MK2 when the activity of the $TTP_{PS;WA;\Delta CIM}$ triple mutant was compared to $TTP_{PS;WA}$ and when wild-type TTP was compared to TTP mutated at a phenylalanine residue within the CIM critical for association with CNOT1 (Figures 2.19 and 2.20).

The TTP-CIM is regulated by phosphorylation independently of MK2

Phosphorylation of the TTP CIM has been previously observed to inhibit association with CNOT1 (76), while another report focusing on BRF1 observed increased association with a decapping factor (97). I therefore wished to test whether CIM phosphorylation regulates TTP activity independently of MK2. To first test the importance of the phosphorylated serine 316 residue in mRNA decay activated by the TTP-CIM alone, I mutated this residue to an alanine, which prevented CIM phosphorylation (Figure 2.2B). MS2-tethered pulse-chase decay assays showed an increase in the degradation rate as a result of the serine to alanine mutation (Figure 2.2A), and an apparent corresponding increase in deadenylation (Figure 2.3A), although the latter did not reach a level of statistical significance. Expression of PKCa caused an acceleration of mRNA degradation that was independent of TTP-CIM phosphorylation (Figure 2.21) and could therefore not be used as a means to test the effect of TTP-CIM phosphorylation. I next tested the importance of CIM phosphorylation in the context of full-length TTP. Mutating serine 316 to an alanine, which prevented phosphorylation of the CIM (Figure 2.22), resulted in a minor increase in the rate of degradation by TTP in the presence of inactive MK2. This effect of the serine 316 to an alanine mutation was further exacerbated in the presence of active MK2 (Figure 2.22)

consistent with TTP relying on an unphosphorylated CIM to activate mRNA decay in the presence of active MK2. In addition, although serine 316 point mutations did not show and increase in CNOT1 association by pull-down assays (Figure 2.23), there was a decrease in 14-3-3 adaptor protein association which have been previously reported to inhibit TTP function (83). Interestingly, treatment with okadaic acid saw an increase in 14-3-3 association that decreased upon combined mutations of serines 52, 178, and 316 (Figure 3.23). Altogether, these findings demonstrate that the TTP CIM activates mRNA decay unregulated by the p38 MAPK-MK2 pathway and that the two separate events of MK2-mediated phosphorylation and phosphorylation of the CIM acts cooperatively to regulate TTP activity.

2.4 Discussion

The regulation of TTP by the p38 MAPK-MK2 pathway during the inflammatory response is a well-established paradigm for the regulation of mRNA decay by signaling. In this study, we demonstrate that the highly conserved C-terminal CIM motif of TTP, which plays a key role in connecting TTP family proteins with the CCR4-NOT deadenylase complex central to mRNA decay, is regulated independently of the p38 MAPK-MK2 pathway. This conclusion is supported by our observations that, unlike TTP serine 178, the TTP CIM serine 316 remained phosphorylated in the presence of a p38 MAPK inhibitor and was not phosphorylated by constitutive active MK2 (Figure 2.14 and 2.15). Moreover, TTP remained partially active in the presence of constitutive active MK2, largely due to the activity of the CIM (Figure 2.16). The CIM, in turn, is regulated by other kinases, such as PKCα (Figure 2.14 and 2.15), RSK1 (96, 108), and PKA (97), whose phosphorylation of the CIM results in impaired association with CNOT1 of the CCR4-NOT complex and reduced decay activity (Figure 2.18 and 2.22) (76, 122). The TTP CIM recruits the CCR4-NOT complex, and activates deadenylation and decay, in cooperation with conserved tryptophans of TTP

(Figures 2.5 and 2.6), which had previously been found to interact with CNOT9 (82). By contrast, association of TTP with the 4EHP-GYF2 complex via TTP tetraproline motifs was not rate-limiting for TTP-mediated mRNA decay (Figure 2.10).

My finding that TTP remains highly active even when deletion of the TTP CIM and mutations in conserved tryptophans and tetraproline motifs disrupt associations with CCR4-NOT and 4EHP-GYF2 complexes (Figures 2.7, 2.8, and 2.11), suggests that TTP promotes degradation via additional interactions with cellular RNA decay machinery. This residual activity of TTP may in part be explained by its undisrupted association with decapping factors (Figure 2.11). With the exception of its conserved RNA binding zinc-finger domain, TTP is composed of mostly predicted intrinsically disordered regions (81). These types of domains have been implicated in the association with decapping factors and p-bodies and therefore may contribute to the activity of TTP (73, 85, 130). It is also possible that additional regions of TTP contribute to the association with the CCR4-NOT complex or other, yet to be determined, mRNA decay factors. My mutational studies found no rate-limiting role for the 4EHP-GYF2 complex in mRNA decay by tethered TTP. 4EHP-GYF2 may specifically promote translation repression (32, 115, 124). The knockout of 4EHP in mouse embryonic fibroblasts caused upregulation of TTP target mRNAs in addition to their encoded proteins (Fu et al. 2016), which could be an indirect effect of interfering with TTP-mediated translation repression during inflammation. An important goal for future studies will be to identify the complete interaction network of TTP with mRNA decay and translation repression machinery.

The most surprising finding of this study was that the TTP CIM remains active and capable of promoting mRNA decay in the presence of active MK2, despite the p38 MAPK-MK2 pathway having been previously implicated in TTP CIM phosphorylation and inhibition of TTP deadenylase association (96, 121, 122, 125, 131, 132). This observation suggests that activation of the p38 MAPK-MK2 pathway is insufficient to fully inactivate TTP and

cooperativity with one or more additional kinase pathways is required. This has important implications for how TTP activity is repressed in physiological conditions, for example during the inflammatory response when TTP repression allows accumulation of ARE-mRNAs expressing pro-inflammatory cytokines (52, 59, 88, 117). The observation that TTP associates with the CCR4-NOT complex via additional interactions beyond the CIM (82) (Figure 2) may explain how phosphorylation by MK2 of residues outside of the CIM impairs CCR4-NOT association (96, 97, 120, 121). The CIM and its phosphorylated serine is a highly conserved motif shared by all members of the ZFP36 family. ZFP36 paralogs have both overlapping as well as unique roles in mRNA decay. Thus, certain kinase pathways may regulate all members of the ZFP36 family, for example via phosphorylation of the conserved CIM, whereas other kinase pathways may specifically regulate a subset of ZFP36 family members. This may provide specificity to how ARE-mRNA decay is regulated in different cell types and under different conditions.

2.5 Figures

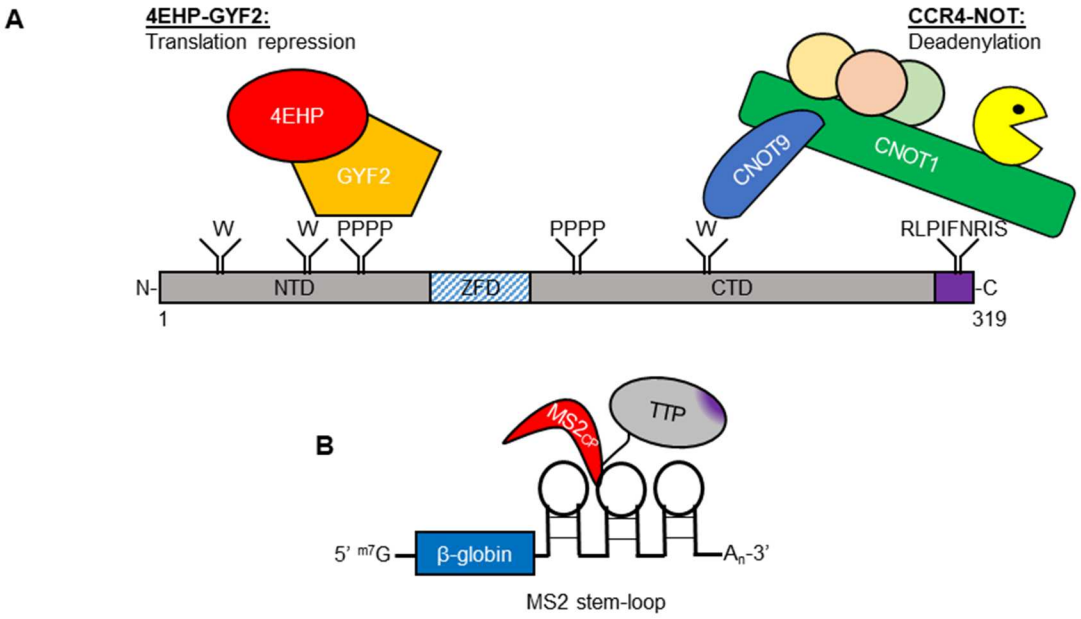

Figure 2.1 TTP promotes mRNA decay cooperatively with other regions of the TTP protein. (A) Schematic of mouse TTP, highlighting conserved tryptophan residues (W) interacting with CNOT9, tetraproline motifs (PPPP) interacting with the 4EHP-GYF2 translation repression complex, and the CNOT1-interacting motif (CIM), shown in purple. NTD: N-terminal domain, ZFD: Zinc-Finger Domain, CTD: C-terminal domain. (B) Schematic of the tethered mRNA decay assay. A tetracycline-regulated β-globin mRNA containing MS2 coat protein (MS2cp) stem-loop binding sites in the 3'UTR is targeted by MS2-TTP fusion proteins.

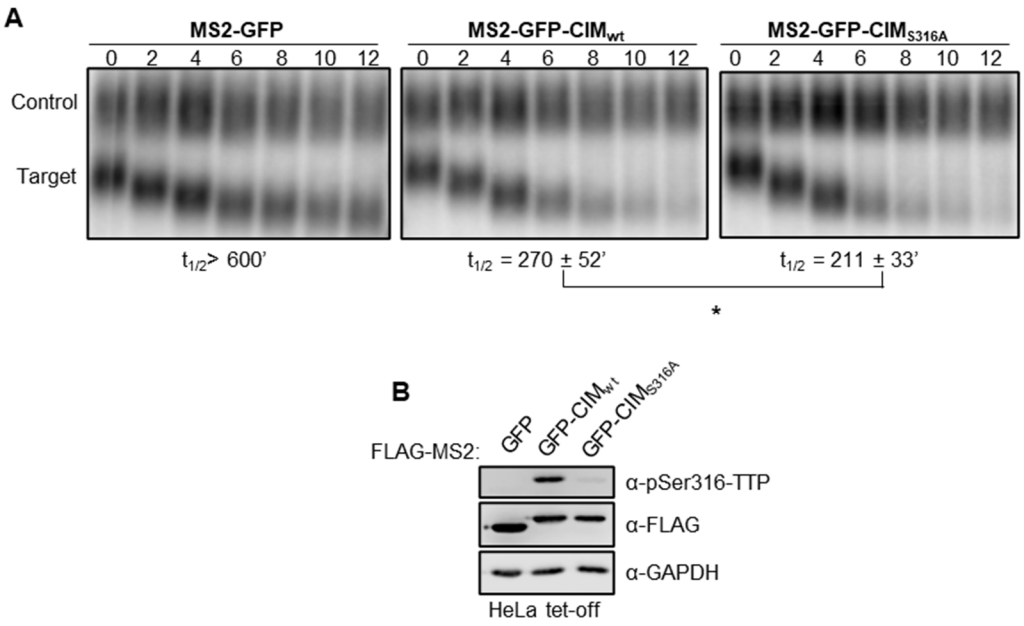

Figure 2.2 The TTP CIM promotes mRNA decay. (A) Northern blot monitoring the degradation in HeLa Tet-off cells over time after transcriptional shut-off by addition of tetracycline of β-globin mRNA (Target) tethered to MS2-GFP (left), MS2-GFP-CIM (middle), or MS2-GFP-CIM$_{S316A}$ (right) fusion proteins. An extended β-globin mRNA that lacks MS2-coat protein binding sites and whose transcription is not regulated by tetracycline served as an internal control (Control). The half-life of the target mRNA calculated after normalization to the internal control is shown below each panel with standard deviation from four independent experiments. Calculated half-lives are given with standard deviation. *: $p<0.05$; student's two-tailed t-test. (B) Western blots monitoring expression levels and phosphorylation of indicated FLAG-MS2-GFP fusion proteins in HeLa Tet-off cells.

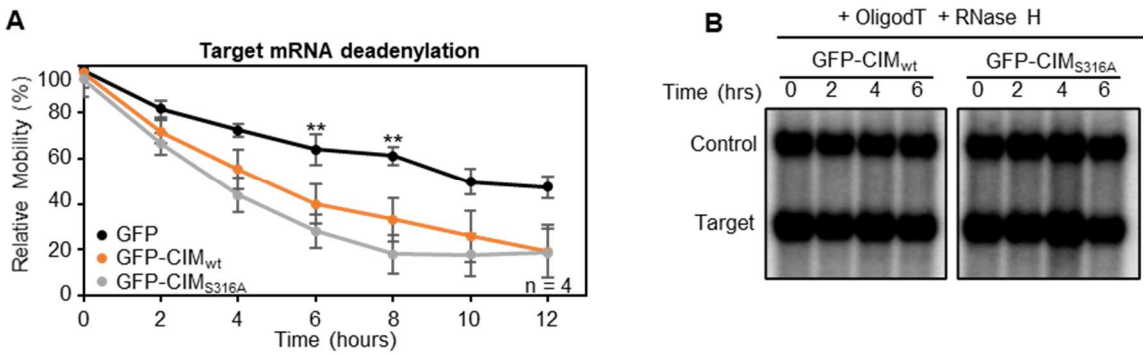

Figure 2.3 The TTP CIM promotes mRNA deadenylation cooperatively with other regions of the TTP protein. (A) Graph showing relative band mobilities as a measure of mRNA deadenylation from the experiments in figure 2.2. Dots represent mobility of the target mRNA relative to the control mRNA, with the mobility at time 0 set to 100% and the mobility of a deadenylated target mRNA, generated by treatment with oligo-dT and RNase H, set as 0%. Error bars represent standard deviation. *: $p<0.05$, **: $p<0.01$ (two-tailed student's t-test, comparing band mobility at each time point). (B) Northern blot monitoring β-globin mRNA tethered to indicated MS2-GFP fusion proteins in HeLa tet-off cells and treated with oligo-dT and RNase H.

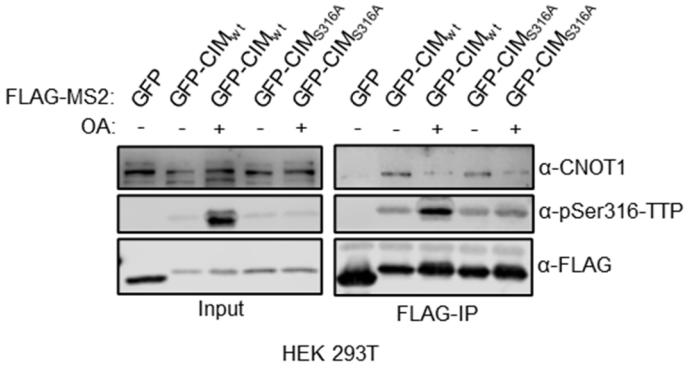

Figure 2.4 The TTP CIM phosphorylation reduces CNOT1 association. Western blots showing proteins co-immunoprecipitating (IP, right panels) with indicated FLAG-MS2-GFP fusion proteins from HEK293T cells treated with or without okadaic acid. Input samples corresponding to 2.5% of IPs are shown on the left

Table 2.1 FLAG-MS2-TTP mutant constructs.

FLAG-MS2:	TTP mutation(s):
CTD_{WA}	Δ1-166; W255A,P257A
$CTD_{WA;\Delta CIM}$	Δ1-166; W255A,P257A; Δ304-319
TTP_{WA}	W31A,W61A,W255A,P257A
TTP_{PS}	P64-66S; P191-193S
$TTP_{WA;\Delta CIM}$	W31A,W61A,W255A,P257A; Δ304-319
$TTP_{PS;\Delta CIM}$	P64-66S; P191-193S; Δ304-319
$TTP_{PS;WA;\Delta CIM}$	P64-66S; P191-193S; W31A,W61A,W255A,P257A; Δ304-319
TTP_{S316A}	S316A
TTP_{2A}	S52A,S178A

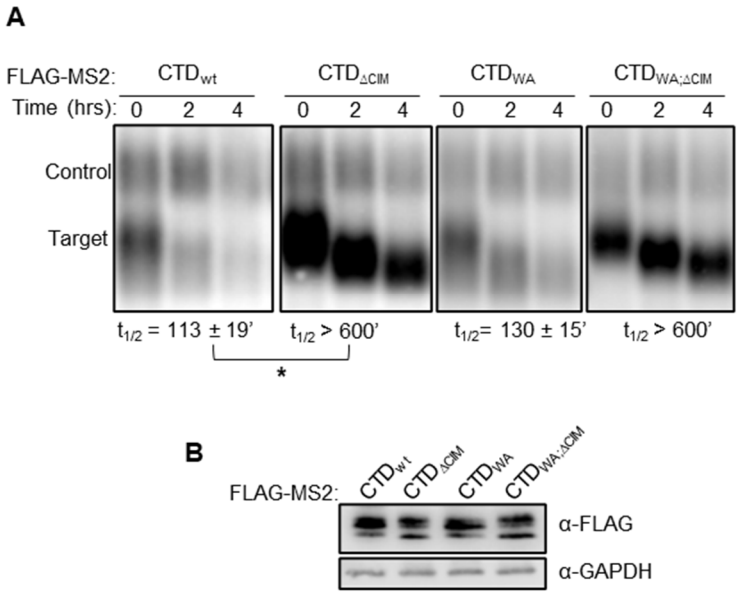

Figure 2.5 Cooperative activation of deadenylation by the TTP CIM and conserved tryptophans. (A) Representative Northern blots monitoring the degradation of β-globin mRNA tethered to TTP-CTD wild-type (wt) or mutant proteins with the CIM deleted (DCIM), conserved tryptophans mutated to alanines (WA), or both (WA,DCIM). *: $p<0.05$; student's two-tailed t-test. (B) Western blots monitoring expression levels of fusion proteins.

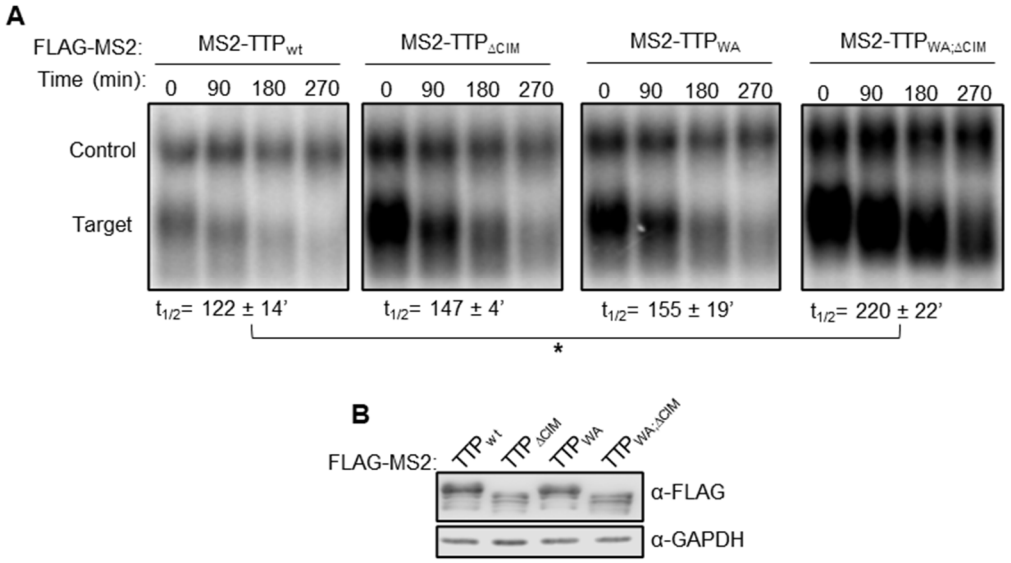

Figure 2.6 Cooperative activation of deadenylation by the TTP CIM and conserved tryptophans. (A) Representative Northern blots monitoring the degradation of β-globin mRNA tethered to MS2-TTP wild-type (wt) or mutant proteins with the CIM deleted (DCIM), conserved tryptophans mutated to alanines (WA), or both (WA,DCIM). *: $p<0.05$; student's two-tailed t-test. (B) Western blots monitoring expression levels of fusion proteins.

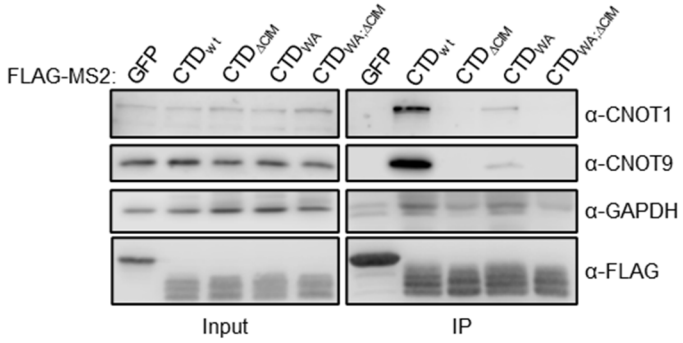

Figure 2.7 Cooperative recruitment of deadenylases by the TTP CIM and conserved tryptophans. Western blots showing proteins co-immunoprecipitating (IP, right panels) with the indicated FLAG-tagged MS2-CTD fusion proteins from HEK293T cells after treatment with RNase A, as compared with input samples (left). IP samples correspond to 2.5% of the input.

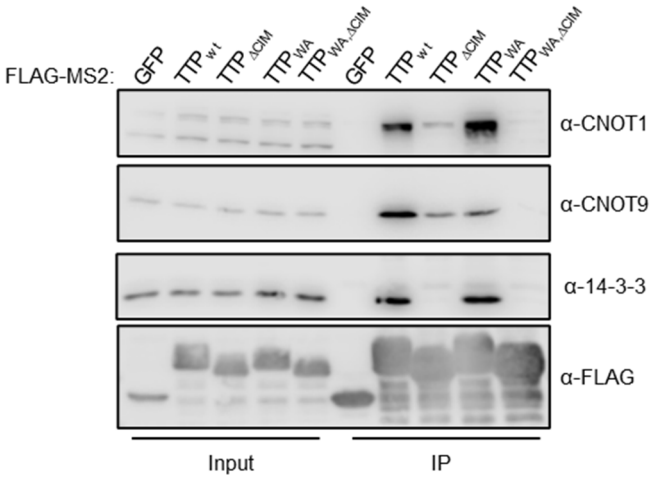

Figure 2.8 Cooperative recruitment of deadenylases by the TTP CIM and conserved tryptophans. Western blots showing proteins co-immunoprecipitating (IP, right panels) with the indicated FLAG-tagged MS2-TTP fusion proteins from HEK293T cells after treatment with RNase A, as compared with input samples (left). IP samples correspond to 2.5% of the input.

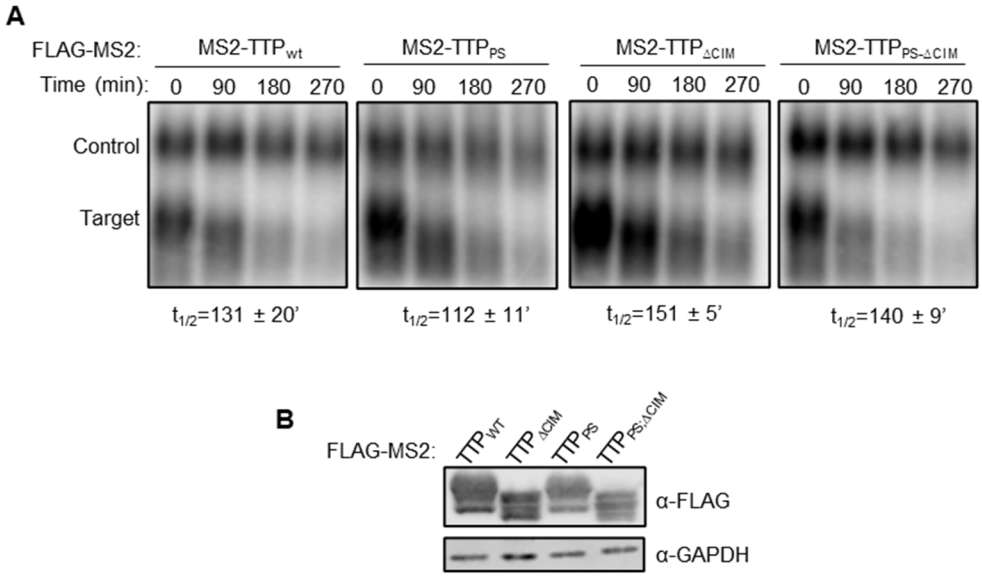

Figure 2.9 TTP tetraproline motifs are not rate-limiting for mRNA decay. (A) Representative northern blots monitoring the degradation of β-globin mRNA tethered to indicated MS2-TTP wild-type (wt) or mutant proteins with the tetraproline motifs mutated to serines (PS), the CIM deleted (DCIM), or both (PS,DCIM). n.s: p>0.05 (student's two-tailed t-test). (B) Western blots monitoring expression levels of fusion proteins.

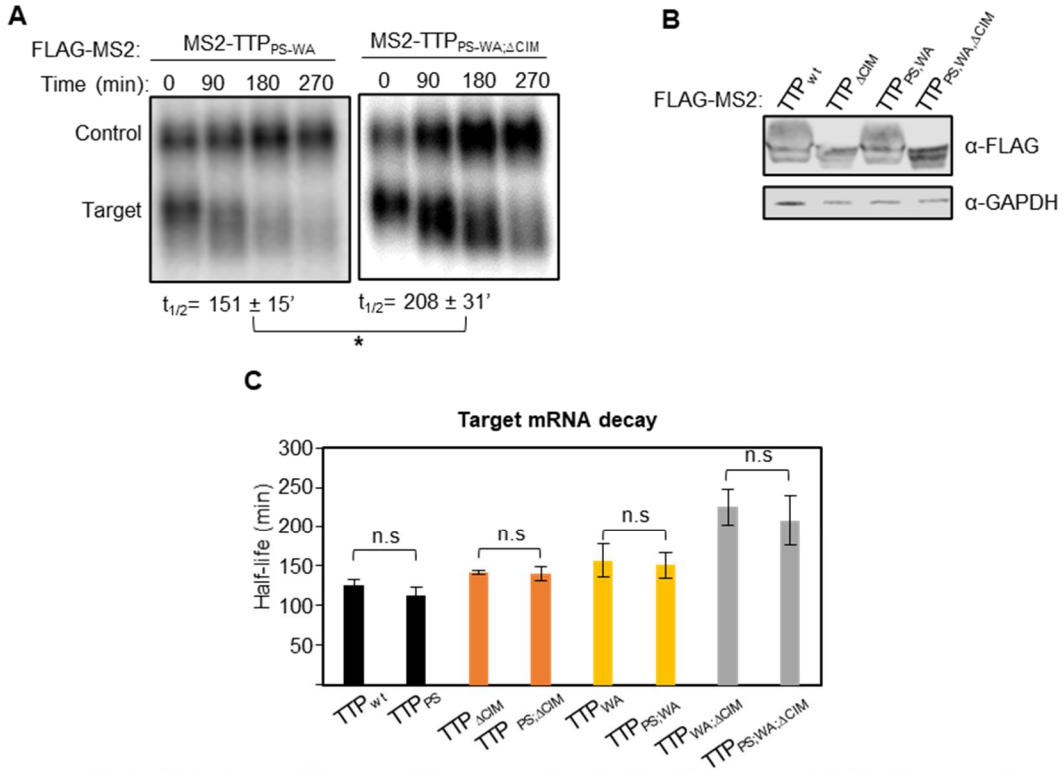

Figure 2.10 TTP tetraproline motifs are not rate-limiting for mRNA decay. (A) Representative northern blots monitoring the degradation of β-globin mRNA tethered with indicated mutant MS2-TTP fusion proteins with tetraproline motifs mutated to serines and conserved tryptophans to alanines (PS,WA), or additional deletion of the CIM (PS,WA,DCIM). *: $p<0.05$; student's two-tailed t-test. (B) Western blots monitoring expression levels of fusion proteins. (C) Bar-graph comparing half-lives of b-globin mRNA tethered to the indicated MS2-TTP fusion proteins with or without mutation in tetraproline motifs (PS). n.s: $p>0.05$ (student's two-tailed t-test).

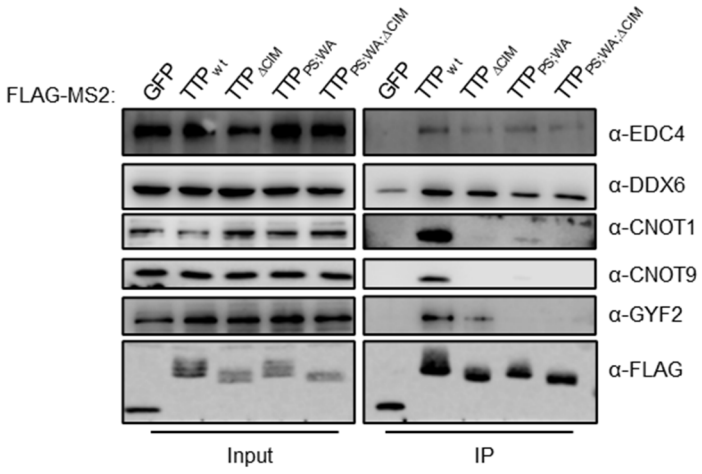

Figure 2.11 TTP mutants maintain associations with decapping factors. Western blots showing proteins co-immunoprecipitating (IP, right panels) with indicated FLAG-tagged MS2-TTP fusion proteins from HEK293T cells after treatment with RNase A, as compared with input samples (left). IP samples correspond to 2.5% of the input.

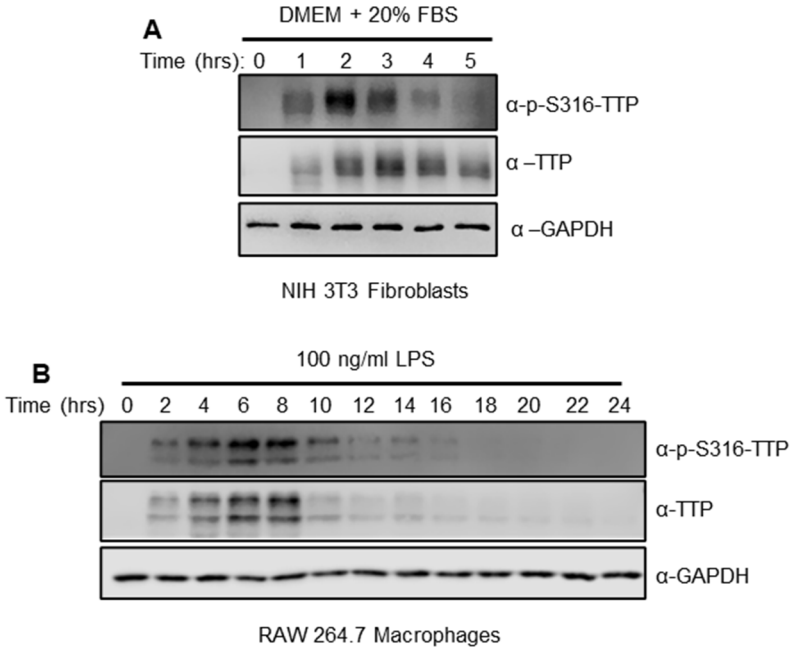

Figure 2.12 TTP serine 316 is phosphorylated during TTP induction. (A) Western blots monitoring levels of TTP and its phosphorylation at serine 316 (p-S316-TTP) in serum-shocked mouse NIH 3T3 cells. GAPDH serves as a loading control. (B) Same as panel *A*, but monitoring TTP in LPS-induced RAW 264.7 mouse macrophage cells.

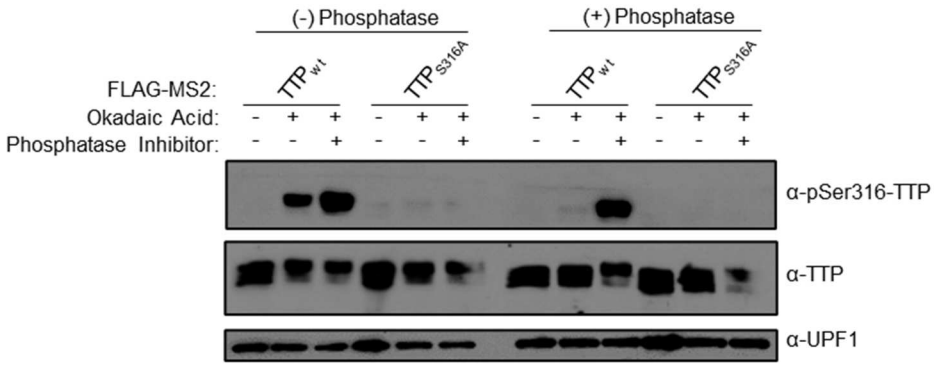

Figure 2.13 Validation of the anti-p-S316 TTP antibody. Western blot of indicated FLAG-MS2-TTP fusion proteins expressed in HEK293T cells incubated with or without okadaic acid (OA). Following cell lysis, samples were treated without (-, left panels) or with (+, right panels) calf-alkaline phosphatase in the presence or absence of phosphatase inhibitors (PhosphataseArrest I), prior to Western blotting using the anti-p-S316-TTP antibody as compared with TTP and UPF1 controls.

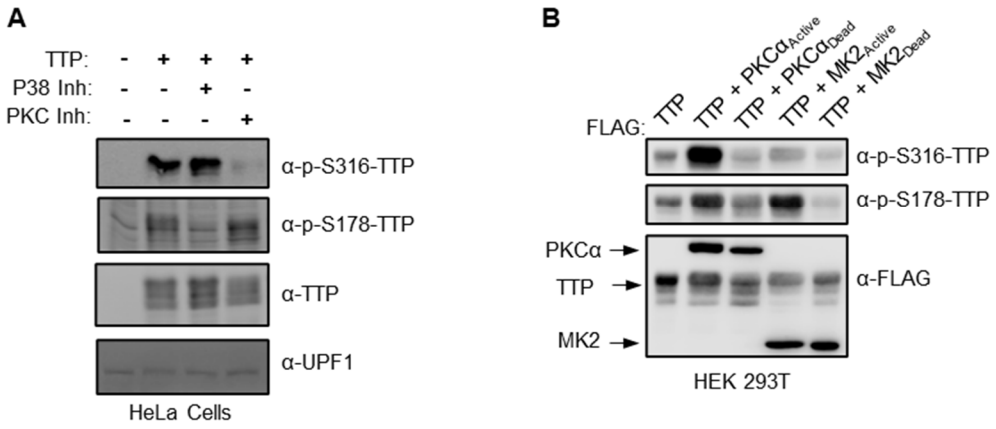

Figure 2.14 TTP serine 316 is phosphorylated by kinase(s) other than MK2. (A) Western blots monitoring TTP and its phosphorylation at serine 316 (p-S316-TTP) or serine 178 (p-S178-TTP), exogenously expressed in HeLa cells incubated with inhibitors of p38 (SB203580) or PKC (Gö 6983) kinases. The left lane is a control sample from HeLa cells not expressing TTP. UPF1 served as a loading control. (B) Western blots monitoring phosphorylation of exogenous FLAG-tagged TTP co-expressed with FLAG-tagged, constitutive active or catalytic dead, MK2 or PKCa kinases in HEK293T cells.

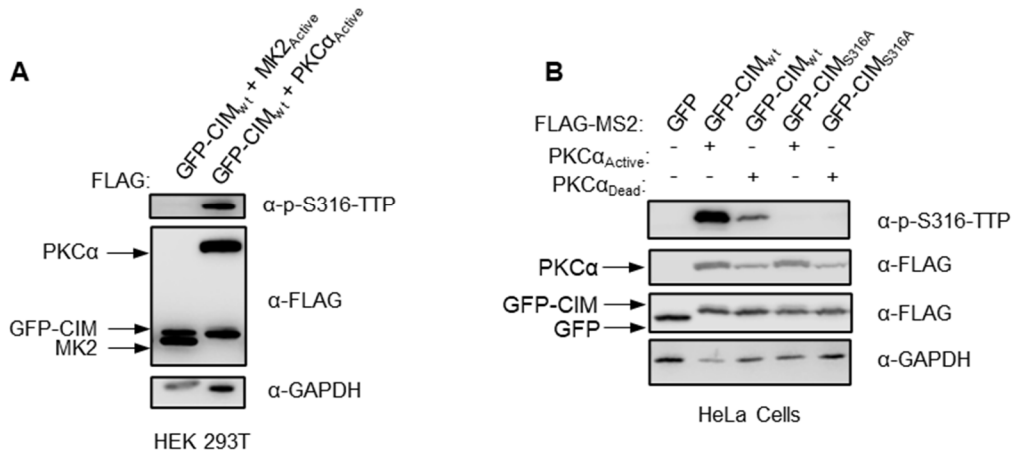

Figure 2.15 TTP serine 316 is phosphorylated by kinase(s) other than MK2. (A) Western blots monitoring phosphorylation of FLAG-tagged GFP-CIM fusion protein co-expressed with indicated constitutive active kinases in HEK293T cells. (B) Western blots monitoring phosphorylation of FLAG-tagged GFP-CIM and GFP-CIM S316A mutant fusion proteins co-expressed with constitutive active or catalytic dead PKCa kinase in HeLa cells.

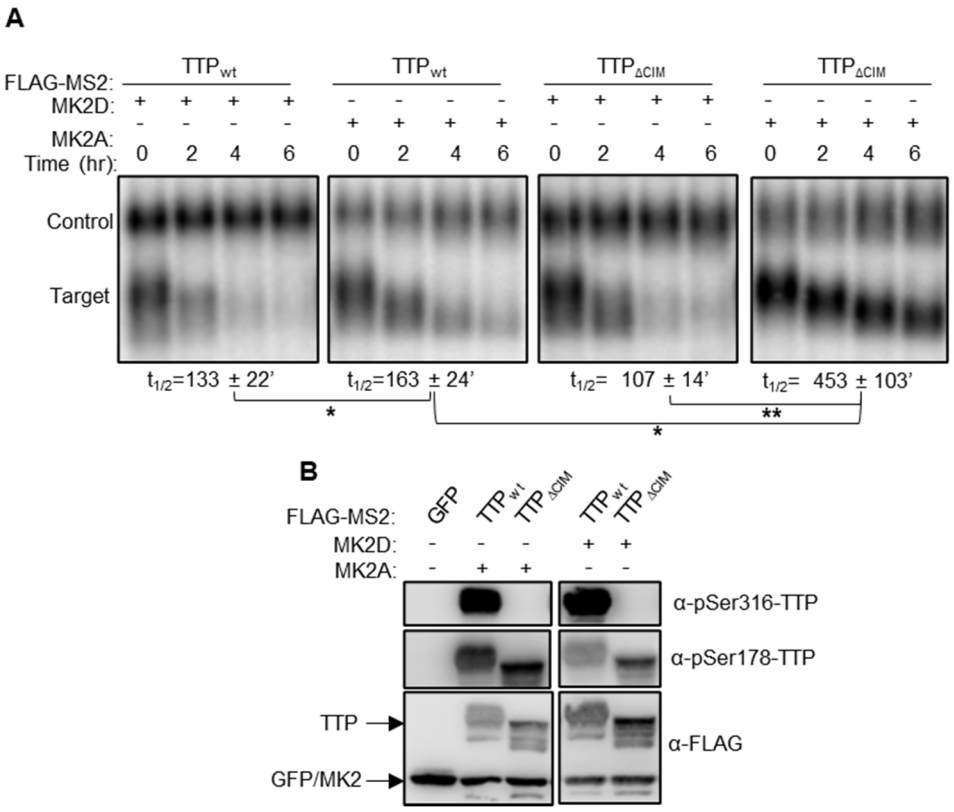

Figure 2.16 The TTP-CIM remains active in the presence of active MK2.
(A) Representative Northern blots monitoring degradation of β-globin mRNA tethered to indicated MS2-TTP wild-type (wt) or ΔCIM proteins, co-expressed with constitutive active (MK2A) or catalytic dead (MK2D). *: $p<0.05$, **: $p<0.01$; student's two-tailed t-test.
(B) Western blots monitoring FLAG-MS2-TTP fusion protein phosphorylation and levels.

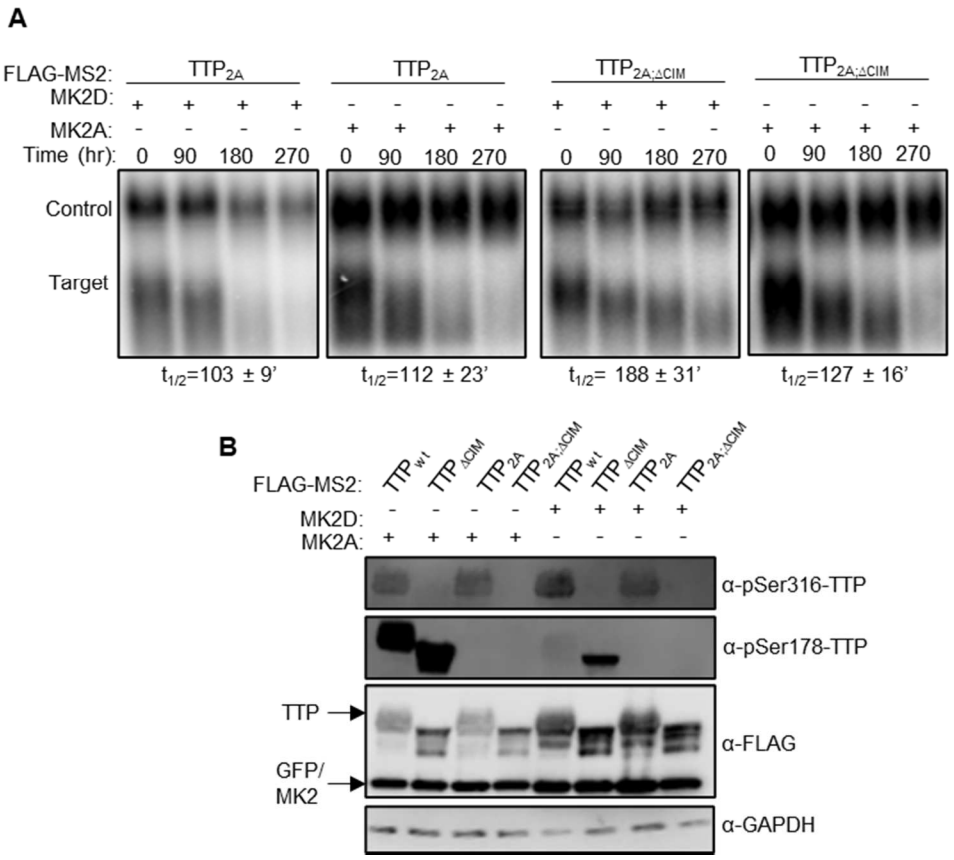

Figure 2.17 The TTP-CIM remains active in the presence of active MK2.
(A) Representative Northern blots monitoring degradation of β-globin mRNA tethered to indicated MS2-TTP serine 52 and 178 alanine mutants with (2A) or without the CIM (2A; ΔCIM), co-expressed with constitutive active (MK2A) or catalytic dead (MK2D). *: $p<0.05$, **: $p<0.01$; student's two-tailed t-test. (B) Western blots monitoring FLAG-MS2-TTP fusion protein phosphorylation and levels.

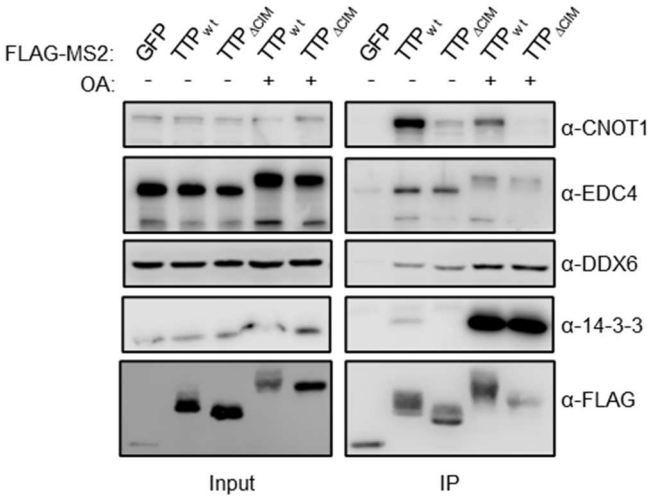

Figure 2.18 Hyperphosphorylated TTP associates with decapping factors. Western blot showing proteins co-immunoprecipitating (IP, right panels) with indicated FLAG-tagged TTP proteins expressed in HEK293T cells treated with or without okadaic acid. Input samples corresponding to 2.5% of IPs are shown on the left.

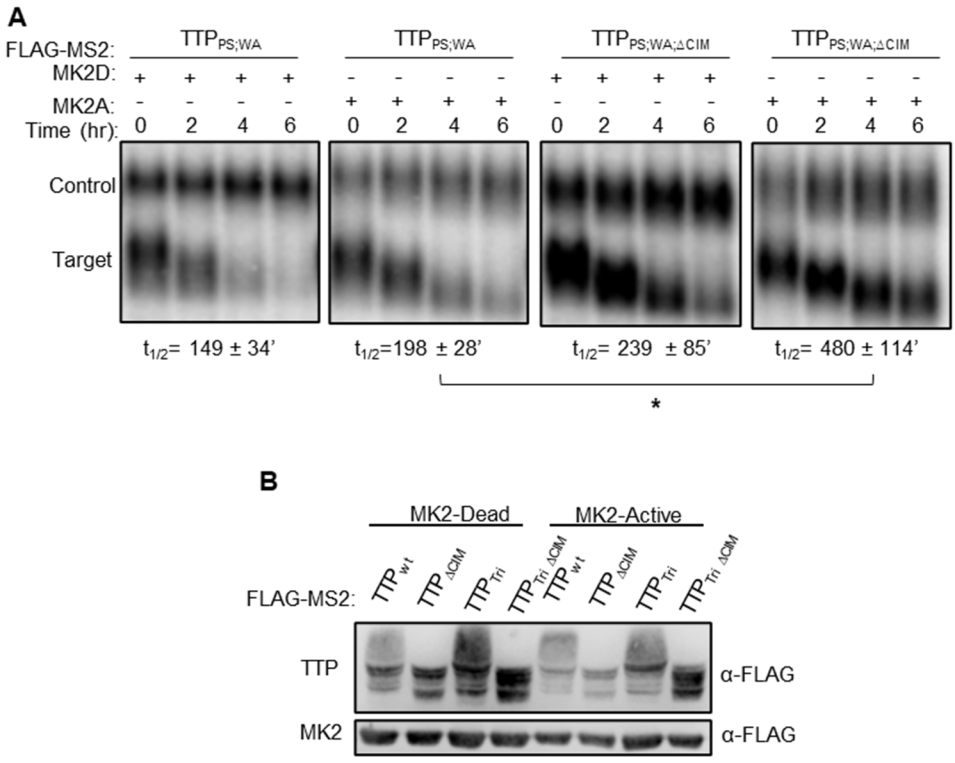

Figure 2.19 The TTP-CIM remains active in the presence of active MK2.
(A) Representative Northern blots monitoring degradation of β-globin mRNA tethered to indicated MS2-TTP tryptophan and proline mutants with (PS; WA) or without the CIM (PS; WA; ΔCIM), co-expressed with constitutive active (MK2A) or catalytic dead (MK2D). *: $p<0.05$, **: $p<0.01$; student's two-tailed t-test. (B) Western blots monitoring FLAG-MS2-TTP fusion protein phosphorylation and levels.

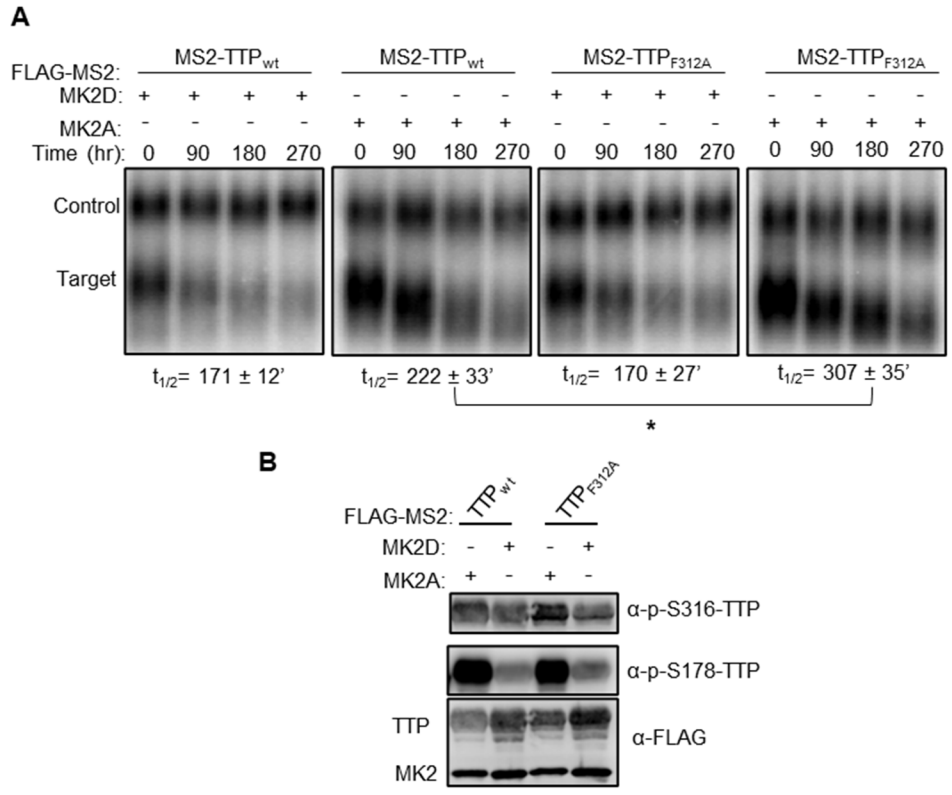

Figure 2.20 The TTP-CIM remains active in the presence of active MK2.
(A) Representative Northern blots monitoring degradation of β-globin mRNA tethered to indicated MS2-TTP wild-type (wt) or phenylalanine mutant proteins (F312A), co-expressed with constitutive active (MK2A) or catalytic dead (MK2D). *: $p<0.05$, **: $p<0.01$; student's two-tailed t-test. (B) Western blots monitoring FLAG-MS2-TTP fusion protein phosphorylation and levels.

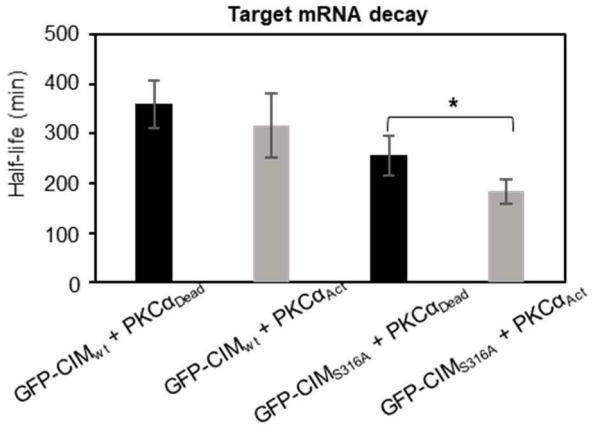

Figure 2.21 PKCα accelerates mRNA decay in tethering decay assays.
Bar graph showing calculated half-lives for β-globin mRNA tethered to MS2-GFP-CIM or MS2-GFP-CIM-S316A in the presence of co-expressed catalytic inactive (Dead) or constitutive active (Act) PKCa. *: $p<0.05$ (Student's two-tailed t-test) (n=4).

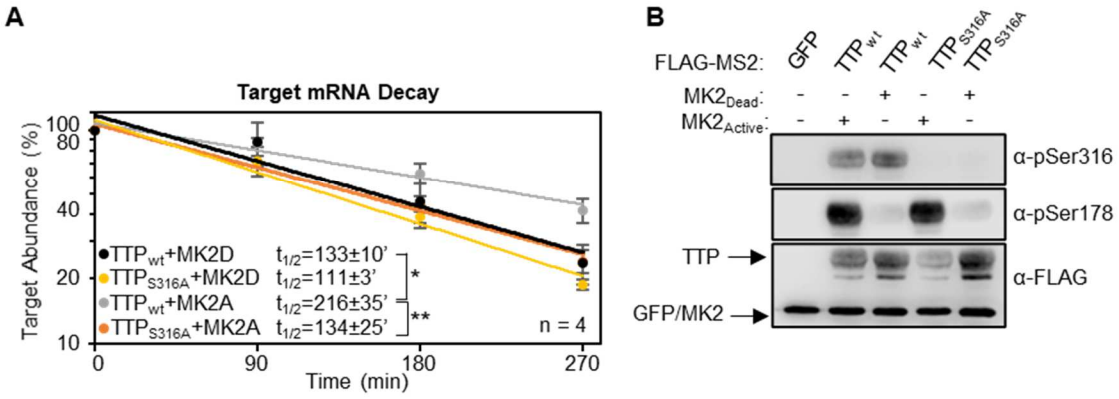

Figure 2.22 TTP-CIM activity is regulated by phosphorylation independently of MK2. A) mRNA decay assays for β-globin mRNA tethered to MS2-TTP proteins co-expressed with MK2 kinases described in panel *C*. *: $p<0.05$, **: $p<0.01$; student's two-tailed t-test. (B) Western blots monitoring phosphorylation of MS2-TTP wild-type (wt) or S316A mutant fusion proteins in the presence of constitutive active (MK2A) or catalytic dead (MK2D) MK2 kinase in HeLa Tet-off cells. (C) Bar graph showing calculated half-lives for β-globin mRNA tethered to MS2-GFP-CIM or MS2-GFP-CIM-S316A in the presence of co-expressed catalytic inactive (Dead) or constitutive active (Act) PKCa. *: $p<0.05$ (Student's two-tailed t-test) (n=4).

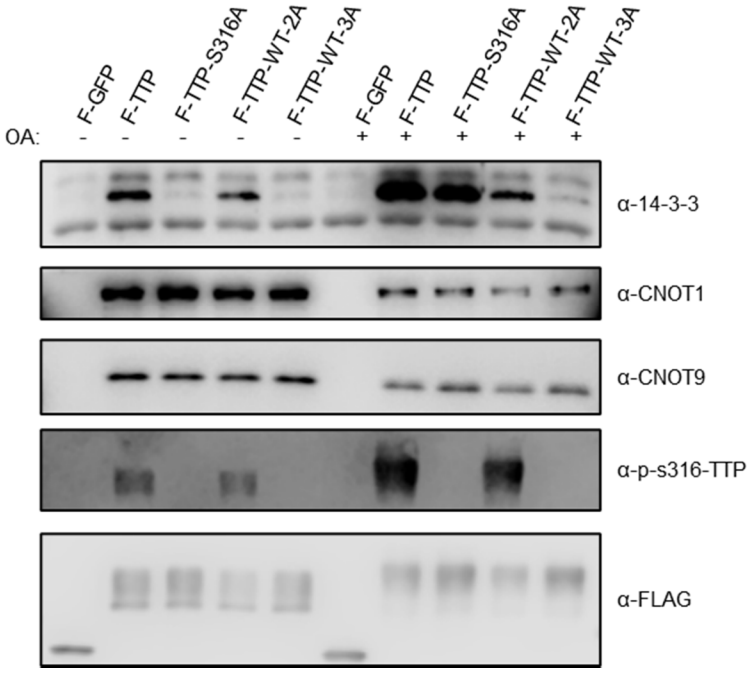

Figure 2.23 TTP serine residues recruit 14-3-3 adaptor proteins. Western blot showing proteins co-immunoprecipitating (IP, right panels) with indicated FLAG-tagged TTP proteins expressed in HEK293T cells treated with or without okadaic acid. Input samples corresponding to 2.5% of IPs are shown on the left.

2.6 Materials and Methods

Plasmids

pcDNA3-FLAG-MS2 plasmids expressing FLAG-MS2-tagged TTP mutant proteins (Table 2.1) were generated from previously described pcDNA3-FLAG-MS2-TTP plasmids (121) using site-directed mutagenesis according to manufacturer's protocol (New England Biolabs). Expression plasmids for FLAG-tagged constitutive active and catalytically dead MK2 kinases were previously described (83, 121). Similarly, expression plasmids for the control β-globin mRNA containing a 3'UTR sequence from GAPDH mRNA and the target tetracycline-regulated β-globin mRNA containing a 3'UTR with six MS2 coat protein stem-loop binding sites were previously described (123). The pcDNA3-FLAG-MS2-GFP-CIM constructs were generated by first generating a pcDNA3-FLAG-MS2-CIM plasmid by inserting the sequence corresponding to mouse TTP residues 304-319 into the pcDNA3-FLAG-MS2 plasmid (74) between restriction sites *Bam*HI and *Not*I. Gibson Assembly (New England Biolabs (NEB)) was subsequently performed to insert the GFP coding region from pSpCas9(BB)-2A-GFP (PX458) into the pcDNA3-FLAG-MS2-CIM vector between the MS2 coat protein and the CIM. pcDNA3-FLAG-PKCa constructs expressing FLAG-tagged PKCa were generated by amplifying the coding region of PKCα from HeLa Tet-off cell total RNA and inserting it into pcDNA3-FLAG (133) immediately downstream of the FLAG peptide sequence using Gibson Assembly (NEB). Constitutive active PKCa-AE was generated by mutating alanine 25 into glutamic acid. Catalytic dead PKCa-KR was generated by mutating lysine 368 into arginine.

Cell Culture

HeLa Tet-off, HEK293T, RAW264.7, and NIH3T3 cells were cultured in Dulbecco's modified Eagle's medium (DMEM; Gibco) with 10% fetal bovine serum (FBS) and 1% Penicillin-Streptomycin. For experiments shown in Figure 4A, NIH3T3 cells were washed with phosphate-buffered saline (PBS) and grown in DMEM containing 0.5% FBS for 24 hours. Cells were subsequently treated with DMEM containing 20% FBS for the indicated amount of time and collected in Laemmli sample lysis buffer (2% SDS, 10% Glycerol, 60 mM Tris-HCl pH 6.8, 5% β-Mercaptoethanol). For experiments shown in Figure 4B, RAW264.7 cells were treated with DMEM containing 100 ng/mL lipopolysaccharide (LPS) for the indicated times and collected in sample lysis buffer.

Antibodies

Rabbit polyclonal anti-pS316-TTP antibody was generated with the synthesized oligo peptide PRRLPIFNRI(p)SVSE (Pocono Rabbit Farm & Laboratory, USA). The antiserum was purified by affinity chromatography by first collecting antibody binding to a PRRLPIFNRI(p)SVSE-peptide column, and, after elution, collecting the flow-through from a subsequent unphosphorylated PRRLPIFNRISVSE-peptide column. Western blots were probed with the following antibodies at the indicated concentrations: rabbit polyclonal anti-FLAG (Millipore Sigma, F7425; 1:1,000), mouse monoclonal anti-FLAG M2 (Millipore Sigma, F1804; 1:1000), rabbit polyclonal anti-DDX6 (Bethyl, A300-461A; 1:1,000), rabbit polyclonal anti-GIGYF2 (Santa Cruz Biotechnology, sc-134708; 1:50), mouse monoclonal anti-14-3-3 (Santa Cruz Biotechnology, sc-1657; 1:1,000), rabbit polyclonal anti-TTP (Sigma-Aldrich, T5327; 1:500), rabbit polyclonal anti-CNOT1 (Proteintech, 14276-1-AP; 1:200), rabbit polyclonal anti-CNOT9 (Proteintech, 22503-1-AP, 1:500), mouse monoclonal anti-GAPDH (Cell Signaling Technology, 97166, 1:1,000), rabbit polyclonal anti-EDC4 ((73); 1:200) rabbit polyclonal anti-pSer178-TTP ((116) a generous gift from Dr. Georg Stoecklin, Heidelberg University; 1:500).

Co-Immunoprecipitation assays

Co-immunoprecipitation assays were performed as previously described (115). Briefly, confluent HEK 293T cells were split at 1:10 onto 10-cm plates. The following day, samples were transfected with 5 µg of the indicated FLAG-tagged TTP wild-type or mutant expression plasmids using TransIT 293 reagent according to the manufacturer's protocol (Mirus). 48 hours after transfection, samples were washed in PBS, pelleted by centrifugation, and collected in hypotonic lysis buffer (10 mM Tris-HCl pH 7.5, 10 mM NaCl, 2 mM EDTA, 0.5% triton X-100, 1 mM PMSF, 1 µM aprotinin, and 1 µM leupeptin) for 10 minutes on ice. NaCl concentrations were increased to 150 mM and samples were treated with 50 µg/mL RNase A for 10 minutes. Samples were centrifuged at 21,130*g* for 15 minutes at 4^{o}C and supernatants were added to 50 µl of M2 anti-FLAG-agarose beads (Sigma). Beads were washed 4 times with NET-2 (50 mM Tris-HCl pH 7.5, 150 mM NaCl, 0.05% Triton-X100) and resuspended in 50 µl of 2x Laemmli sample lysis buffer (4% SDS, 20% Glycerol, 120 mM Tris-HCl pH 6.8, 10% β-Mercaptoethanol). Samples were separated by SDS-polyacrylamide gel electrophoresis (SDS-PAGE) and analyzed by western blot. 0.5% of whole cell extracts and 20% of pull-down elutions were loaded for analyses.

Pulse-chase mRNA decay assays

Tethered mRNA decay assays were performed as previously reported (121, 123). Briefly, confluent HeLa Tet-off cells (Takarabio) in 10-cm plates were split into 12-well plates at between 1:15 to 1:20. Two days later, cells were transfected with β-globin control (25 ng) and reporter constructs containing MS2 binding sites (250 ng) and FLAG-MS2-TTP constructs (100 ng), or MS2-GFP constructs as a control, using TransIT-HeLaMONSTER transfection

kit according to the manufacturer's protocol (Mirus). Cells were subsequently incubated in the presence of 50 ng/ml tetracycline to inhibit expression of the target mRNA. 24 hours post-transfection, transcription of the reporter transcripts was pulsed with the addition of fresh media lacking tetracycline for 4-6 hours and then treated with 1 µg/ml tetracycline to shut off transcription. Total RNA was harvested at indicated times after transcription shut-off by extraction with Trizol following the manufacturer's protocol (Thermo Fisher) and analyzed by Northern blotting as previously described (121). Deadenylated samples were generated by resuspending total RNA in 9 µl water and incubating the samples with 1 µl of 1 mM oligo-dT_{20} at 80°C for 2 minutes followed by annealing at room temperature for 5 minutes. 7 µl of water, 2 µl of 10x RNAse H Buffer (500 mM Tris-HCl, 750mM KCl, 30mM MgCl2, 100mM DTT, pH 8.3; NEB) and 1 µl of 5 units/µl RNase H (NEB) were added and samples were incubated at 37°C for 30 minutes. RNA samples were extracted with phenol:chloroform (1:1), followed by ethanol precipitation, and analyzed by Northern blotting. Half-lives were determined as previously described (123). Briefly, target signal was normalized against control for the corresponding time and plotted on a graph. Slopes of exponential regressions were used to determine the first order decay kinetics to determine mRNA half-lives. Band mobility was determined by plotting signal intensity against migration distance and measuring the mobility of the peak of the target mRNA relative to the peak of the internal control mRNA, with mobility of the target mRNA at the zero-hour time point set to 100 and mobility of the target mRNA after treatment with RNase H and oligo-dT to remove the poly(A)-tail set to 0.

2.7 Acknowledgements

We thank members of the Lykke-Andersen lab, Tim Nicholson-Shaw, Cody Ocheltree, and Tiantai Ma for input on the manuscript. We thank Georg Stoecklin (Heidelberg University) for sharing the anti-p-Ser178-TTP antibody. This work was supported by National Institutes of Health (NIH) fellowship F32 GM128320-03 to A.C. and National Institutes of Health (NIH) grant R35 GM118069 to J. L.-A.

Chapter 2, in full, has been submitted for publication of the material. Carreño, Alberto; Lykke-Andersen, Jens. The dissertation author was the primary investigator and author of this material.

Chapter 3: Generation of endogenous TTP mutant RAW 264.7 macrophage cells.

3.1 Abstract

The induction of the inflammatory response is a dynamic process that involves the activation of various signaling cascades and expression of pro-inflammatory transcripts. Tristetraprolin is a rapidly induced mRNA destabilizing factor whose activity, stability, and localization are regulated by post-translational modifications. Mechanistic studies of TTP function have been carried out in large part through overexpression in non-native or immune-relevant cells; however, these conditions do not recapture the endogenous environment and expression levels in which TTP normally exists. In this chapter, I report on my efforts at generating TTP mutants in the mouse macrophage cell line RAW 264.7. I generated TTP knockout cells using CRISPR-Cas9 targeting of the endogenous TTP locus. Lentiviral addbacks within these $TTP^{-/-}$ cells were generated but were found to insufficiently express TTP. Furthermore, I report on my attempts to generate a $TTP^{S316A/S316A}$ RAW 264.7 mutant cell line.

3.2 Introduction

In order to properly recreate the native environment of the inflammatory response, it is important to recreate similar gene expression patterns. In uninduced macrophage cells, TTP is observed to localize to the nucleus and is expressed at low levels (51, 134). Upon induction of the inflammatory response, TTP expression experiences a transient burst, with expression patterns similar to immediate early-genes, and the protein levels of TTP are seen to increase within the first two hours of induction. In addition, the activation of signaling pathways such as p38 MAPK and p42 ERK signaling are seen to phosphorylate TTP and this is correlated with localization of TTP to the cytoplasm (94). TTP binds to and facilitates the degradation of pro-inflammatory transcripts that contain AU-rich elements (AREs) in their

3’ untranslated regions (UTRs). Interestingly, the TTP transcript contains AREs in its 3’UTR and TTP has been demonstrated to target its own mRNA. TTP is seen to undergo bi-phasic expression where it has been observed that hours after its initial burst of expression, the TTP gene undergoes a latent and longer lasting time-course of mRNA expression (54).

A considerable number of studies of TTP function have been performed in exogenous systems such as HEK 293 cells, A549 adenocarcinoma lung cells, or HeLa cells, which do not normally express TTP. Although these cells are easy to manipulate, TTP is expressed in a non-native environment and therefore does not accurately represent the global effect that TTP may have in immune-relevant cells. Overexpression experiments have been previously performed in mouse RAW 264.7 macrophage cells, which at least place TTP in a native environment. The limitation of these experiments however is that TTP is constitutively expressed from a non-native promoter, which contains its own unique limitations. First, the expression of TTP is not accurately represented in uninduced cells which normally cause TTP to be expressed at low levels. Secondly, the induction patterns of TTP are not similar to those found in endogenously expressed system where TTP is expressed in a bi-phasic manner. Another method that has been used to express TTP in a native setting employed the strategy of placing TTP behind the expression of an inducible promoter (135). However, this approach also suffers drawbacks in the difficulty to accurately mimic native TTP expression patterns.

In this chapter, I describe my efforts in generating RAW 264.7 macrophage cell lines in which TTP function can be manipulated in a native setting. Using CRISPR-Cas9 targeting of exon 2 of the TTP gene, I generated $TTP^{-/-}$ RAW 264.7 macrophage cells. These $TTP^{-/-}$ cells were subsequently used for lentiviral addbacks of TTP driven by the endogenous TTP promoter or the TNFα promoter. Furthermore, I demonstrate different strategies and efforts at generating $TTP^{S316A/S316A}$ RAW 264.7 macrophage cells by targeting the endogenous TTP locus using CRISPR-Cas9 mediated gene editing.

3.3 Results

Generation of TTP knockout RAW 264.7 macrophages

To generate a background in which to study TTP mutation in an immortalized immune-relevant cell line, I first established a TTP$^{-/-}$ RAW 264.7 cell line. To do this, I utilized the CRISPR-Cas9 system using a guide RNA that targeted the upstream region of exon 2 of the TTP gene (Figure 3.1). Plasmid constructs expressing GFP-tagged Cas9 were transfected into RAW 264.7 cells and single-cell sorted by fluorescence activated cell sorting (FACS). Colonies were expanded and tested for knockout of TTP by induction of the inflammatory response with LPS and probing for TTP by Western blotting (Figure 3.2). As a control, I treated wild-type RAW 264.7 cells under similar conditions. Probing for TTP reveals signal for endogenous TTP expression that is low in uninduced macrophages but is readily detectable two hours after induction and beyond. Probing for TTP in the CRISPR-Cas9 transfected cell clones showed no detectable levels of TTP protein expression throughout the time course. Because the TTP antibody used in these experiments is raised against the N-terminal domain of TTP, I also tested for the C-terminal domain of TTP by probing for phosphorylation of the highly conserved serine residue, serine 316 (mouse numbering). No signal was detected in the CRISPR-Cas9-generated clones, while signal was readily detectable in the wild-type RAW 264.7 cells after two hours of induction.

Previous work has shown that stabilization of TNF-α mRNA significantly contributes to the chronic inflammatory phenotype seen in TTP KO mice (117). To test the effect on TNF-α mRNA expression in my TTP$^{-/-}$ RAW 264.7 cells, I induced the inflammatory response using LPS and treated cells with actinomycin D to shut off transcription and measured TNF-α mRNA decay rates by RT-qPCR (Figure 3.3). As previously shown, TTP $^{-/-}$ conditions considerably increased TNF-α mRNA stability. These results demonstrate that our TTP $^{-/-}$ RAW 264.7 cells recreate conditions previously shown to occur upon depletion of TTP.

Lentiviral-mediated add-backs of TTP in TTP$^{-/-}$ RAW 264.7 Macrophages using native promoters

To better understand the role TTP post-translational modifications on the inflammatory response requires the introduction of TTP mutants into immune-relevant cells. Previous work examining the effect of TTP in native settings have utilized overexpression systems that do not adequately recapitulate the pre-inflammatory environment. To accurately recreate the inflammatory response requires that TTP expression follows a more endogenous pattern as seen in immediate early genes. To recreate an endogenous TTP expression system in RAW 264.7 macrophage cells I used a lentiviral delivery system to insert the TTP gene with its native promoter region into the genome of my TTP$^{-/-}$ RAW 264.7 cells. A schematic of the used lentiviral construct is shown in Figure 3.4, with the long-terminal repeats of HIV-1 flanking a 4.6 kb genomic region containing the TTP gene exons, intron, and intergenic regions. TTP contains several promoter elements upstream of the transcription start site (54, 55), including an NF-κB binding element (5'-GGRNNYYCC-3', where R is a purine, Y is a pyrimidine, and N is any nucleotide) 1,859 base pairs (bps) upstream of the transcription start site. To accommodate for this distal transcription element, I included the genomic region of the TTP gene from 2,092 bps upstream of the transcription start site (Fig 3.4.A). In addition, 150 bps of the region downstream of the poly-A site of exon 2 of the TTP gene was included.

Five clonal cell lines isolated after blasticidin selection were treated with LPS and analyzed by Western blotting for TTP (Figure 3.5). Signal for TTP was detected in samples treated with LPS for three hours while little signal was detected in uninduced conditions, suggesting that the endogenous promoter elements were responsive to LPS stimulation. However, comparing the signal intensity from one of the clones (C-4) to that observed from wild-type RAW 264.7 cells showed much lower TTP expression (Figure 3.6). Parallel

experiments with a similarly constructed lentiviral TTP-S316A add-back construct produced similar expression results.

TTP protein levels were similar for all clones analyzed (Figure 3.5), suggesting that the promoter region used was insufficient to promote an appropriate LPS-driven response. By further analyzing of the TTP gene region I found an additional predicted NF-κB binding element 2,826 bp upstream of the transcriptional start site, which encouraged the design of a new delivery vector containing a 4.0 kbp promoter region upstream of the TTP transcription start site (Figure 3.4 B). Viral transduction was performed in the $TTP^{-/-}$ RAW 264.7 macrophages and basticidin-selected clones were tested for TTP protein expression upon LPS induction (Figure 3.7). Despite extension of the promoter region containing the additional NF-κB binding element, I did not observe TTP expression levels that approached those of wild-type RAW 264.7 cells.

Lentiviral-mediated add-backs of TTP mutants in $TTP^{-/-}$ RAW 264.7 macrophages using the TNF-α promoter

As an immediate early gene, TNF-α expression is rapidly induced upon treatment with LPS. Unable to produce a robust expression of TTP protein using its native promoter, I generated an additional lentiviral add-back construct where TTP expression was regulated by the TNF-α promoter (Figure 3.4C). The promoter region of TTP was replaced with the entire genomic region upstream of the TNF-α gene, which spanned 1.2 kbp, beginning at the terminal exon of the upstream TNF-β gene. Following clonal selection and expansion of virally transduced $TTP^{-/-}$ RAW 264.7 cells, isolated clones were treated with LPS and probed for TTP protein expression by Western blotting (Figure 3.8). Signal for TTP in these $TNF\alpha_{prom}$: TTP clones was readily detected in conditions where cells were incubated with LPS and, importantly, low signal was detected in uninduced conditions. Similar to previous

attempts however, TTP expression was markedly higher in wild-type RAW 264.7 cells as compared to cells where TTP expression was induced from the TNF-α promoter.

CRISPR-Cas9 mediated gene editing of the TTP locus in RAW 264.7 cells

Observing that stable lentiviral add-backs of TTP in TTP knock-out cell lines was unable to produce robust TTP protein expression, I attempted to generate mutations in the endogenous TTP locus in RAW 264.7 cells using CRISPR-Cas9 gene editing strategies. With the goal of generating $TTP^{S316A/S316A}$ mutants in RAW 264.7 cells I developed a guide RNA that targeted the TTP-CIM genomic region (Figure 3.9A). RAW 264.7 cells were transfected, and single cell sorting for GFP expression from the Cas9 plasmid was performed. A single-stranded oligodeoxynucleotide (ssODN) was co-transfected to promote homology-directed repair of Cas9 cleaved cells to generate TTP-S316A mutants. To prevent the re-cleavage of successful mutations, ssODNs were engineered with a silent mutation that would mutate the protospacer adjacent motif (PAM) critical for Cas9 cleavage. Colonies were expanded and the presence of mutations was analyzed by PCR followed by restriction digest using *Bsm*BI, where mutants generated from homology directed repair (HDR) from the ssODN would also contain a silent mutation that mutated a *Bsm*BI cleavage site (Fig 3.9B). As shown in Figure 3.10, based on *Bsm*BI cleavage patterns, CRISPR-Cas9 targeted cells produced clones that appeared to display heterozygous and homozygous mutations. However, sequencing of the homozygous mutants revealed the occurrence of clones that had undergone deletion in the TTP locus by non-homologous end joining.

One unintended, but predictable, consequence of targeting the TTP-CIM was the generation of TTP mutants that contained an ablated C-terminal end through non-homologous end joining. The generation of these clones allowed for a robust expression of $TTP_{\Delta CIM}$ (Figure 3.11). Preliminary results (n=1) suggest that expression of $TTP_{\Delta CIM}$ causes

slight upregulation of TNFα transcripts and protein (Figure 3.12). The generation of these $TTP^{\Delta CIM/\Delta CIM}$ RAW 264.7 cells could be used for downstream analysis in future studies.

To limit unintended pleiotropic effects, no selectable markers or tags were utilized in the donor repair templates described above. These initial decisions made it difficult to select for clones in a high-throughput manner with confidence. Furthermore, the *Bsm*BI site used as a marker could become disrupted by DNA repair mechanisms, such as non-homologous end joining, which gave the appearance of false positives in restriction digest experiments. To alleviate these technical challenges, I developed a plasmid construct containing a blasticidin-resistance gene downstream of TTP (Figure 3.13). The plasmid contains desired TTP mutations along with silent mutations that remove the PAM sequence to prevent cleavage by Cas9. Following transfection of wild-type RAW 264.7 cells, clones were expanded and genomic DNA was isolated. PCR amplification using primers for TTP exon 1, which was not present in the transfected repair template, and downstream of the selectable marker, reveals a slower migrating band in an agarose gel (Figure 3.14). As shown in Figure 3.15, two selected clones that contained the proper insertion were induced with LPS and analyzed by Western blotting. These clones appeared to express TTP at similar levels to the wild-type cells and no signal was apparent using the phospho-TTP-S316 antibody. Some signal, albeit at a lower level, was detected using an antibody with affinity for the non-phosphorylated CIM. This suggests that I successfully generated $TTP^{S316A/S316A}$ mutant RAW 264.7 cell lines. However, these cell lines need to be further characterized, including by sequencing, before being used to study TTP function.

3.4 Discussion

In this work I demonstrate that lentiviral integration of the TTP gene with its native promoter does not recapitulate the endogenous protein expression seen in wild-type

conditions. Using the CRISPR-Cas9 system, I generated $TTP^{-/-}$ RAW 264.7 macrophages which showed no detectable TTP protein expression (Figure 3.2). The TTP genomic locus was re-integrated into $TTP^{-/-}$ RAW 264.7 macrophages using the pHAGE lentiviral transduction system where 2.0 kbp of the TTP promoter region was sufficient to induce TTP expression upon treatment with LPS, albeit at a lower level than seen in wild-type cells (Figures 3.5 and 3.6). Viral transduction of TTP containing an extended 4.0 kbp promoter sequence was also unable to produce TTP expression similar to endogenous TTP (Figure 3.7). Furthermore, placing the TTP gene under the expression of the entire TNF-α promoter region of ~1.2 kbp also generated weakly inducible TTP expression in stably virally transduced $TTP^{-/-}$ RAW 264.7 cells (Figure 3.8). Initial attempts at generating CRISPR-Cas9-mediated $TTP^{S316A/S316A}$ clones using ssODNs were unsuccessful; however, these experiments generated cell lines whose conserved TTP CIM motif was deleted by non-homologous end joining. Using larger repair templates containing selectable markers in the TTP intergenic region allowed for selection of clones with desired insertions at the proper genomic locus (Figure 3.14).

Analysis of my RAW 264.7 $TTP^{-/-}$ clones that have been targeted by Cas9 directed to the upstream region of exon 2 of the TTP gene revealed no detectable expression of TTP. Additional preliminary analyses indicate that compared to wild-type RAW 264.7 cells, my $TTP^{-/-}$ clones exhibited an increase in the stability of TNF-α mRNA during LPS induction (Figure 3.3). These observations agree with previous findings and suggest that the functional effect of removing TTP is recapitulated in RAW 264.7 cells. Further validation of these knockout clones needs to be performed. I have not yet analyzed what genomic aberrations have occurred such that TTP protein levels are no longer detected by Western blotting. In addition, analysis of TTP mRNA expression by RT-qPCR remains to be done. Generating $TTP^{-/-}$ RAW 264.7 macrophage cells is a critical step in setting up the proper controls with

which to test future endogenously expressed TTP mutants. In addition, the generation of $TTP^{-/-}$ clones allows us to study the role of nuclear localized TTP by comparing gene expression profile changes with uninduced wild-type macrophages. Previous work suggests a nuclear role for TTP involved in alternative splicing (136) as well as alternative polyadenylation (Boris Reznik, unpublished work).

Lentiviral transduction is an effective technique for integrating constructs into a variety of different cell lines. The third generation pHAGE lentiviral system used here was effective at reintroducing the TTP locus composed of approximately 2.5 kbp with an additional 2.0 kbp of its native promoter upstream of the transcription start site. TTP expression in clones was detected upon LPS stimulation and, importantly, little signal was detected in uninduced cells (Figures 3.5-3.8). Despite transduction with its native promoter, TTP protein expression in these clones was observed to be substantially lower than endogenous TTP levels. Furthermore, TTP constructs containing a 4.0 kbp promoter did not elevate the expression of TTP protein to levels seen in wild-type cells. In addition, placing TTP under the TNF-α promoter also generated clones that did not be express TTP at endogenous levels. With only 150 bp downstream of the TTP gene present in the add-back vectors used here, it is possible that the process of cleavage and polyadenylation (CPA) is inefficient, although there is also a bGH polyadenylation signal sequence downstream of the genomic insert which could also promote CPA. Another possibility could be that proper TTP gene expression depends on distal enhancer regions downstream of TTP where an intergenic region of 3 kb is present before the next downstream gene, or that the efficient expression of TTP relies on even more distal enhancer elements beyond the TTP gene locus.

CRISPR-Cas9 targeting of the TTP-CIM region serendipitously led to the generation of $TTP^{\Delta CIM/\Delta CIM}$ RAW 264.7 cells due to non-homologous end joining. As described in Chapter 2, the CIM has been demonstrated to remain active in conditions where the downstream kinase of the p38 MAPK pathway, MK2, targets TTP at serines 52 and 178 (mouse

numbering). These clones could be used in the future to probe the effect that $TTP_{\Delta CIM}$ protein expression has on the inflammatory response.

My preliminary work using CRISPR-Cas9 mediated gene editing using a repair template containing a selectable marker downstream of the TTP locus appears promising. Stable integration of the blasticidin resistance gene simplifies the gene editing protocol by selecting clones without requiring the use of FACS sorting. Although, placing the selectable marker downstream of TTP did not appear to limit the expression of TTP (Figure 3.15), the blasticidin-selectable marker used in this construct is integrated within the unstranslated exon 1 of variant X1 of the *Paf1* gene which is expressed anti-sense to the TTP locus. Future work should investigate whether this insertion is deleterious to the expression of this RNA polymerase II complex component.

Preliminary work with this mutagenesis approach appears to yield a rate of successful integration, as seen by PCR tests (Figure 3.14), at around five percent. Although the role of TTP-serine 316 was recently characterized in RAW 264.7 macrophage cells (96), this method of clonal selection and screen should be implemented in future experiments. In particular, the work from Chapter 2 reveals that the TTP-CIM contributes to TTP-mediated mRNA decay independently of the MK2 pathway in an exogenously expressed system. To examine the endogenous effects of the CIM would require the generation of RAW 264.7 cells expressing a bona-fide $TTP_{\Delta CIM}$ protein, containing a stop codon prior to the CIM motif. The method described here could generate such a mutant, by editing a repair template such that the endogenous CIM is removed while preserving the TTP 3'UTR. Furthermore, the generation of the various serine to alanine mutations would allow us to investigate the role of various post-translational modifications on TTP-mediated decay, studied in an exogenous system in Chapter 2. Future attempts to modify and improve on the system shown here should include the addition of an additional gRNA targeting the downstream intergenic region of TTP in addition to optimizing gRNA sequences to reduce potential off-target effects.

3.5 Figures

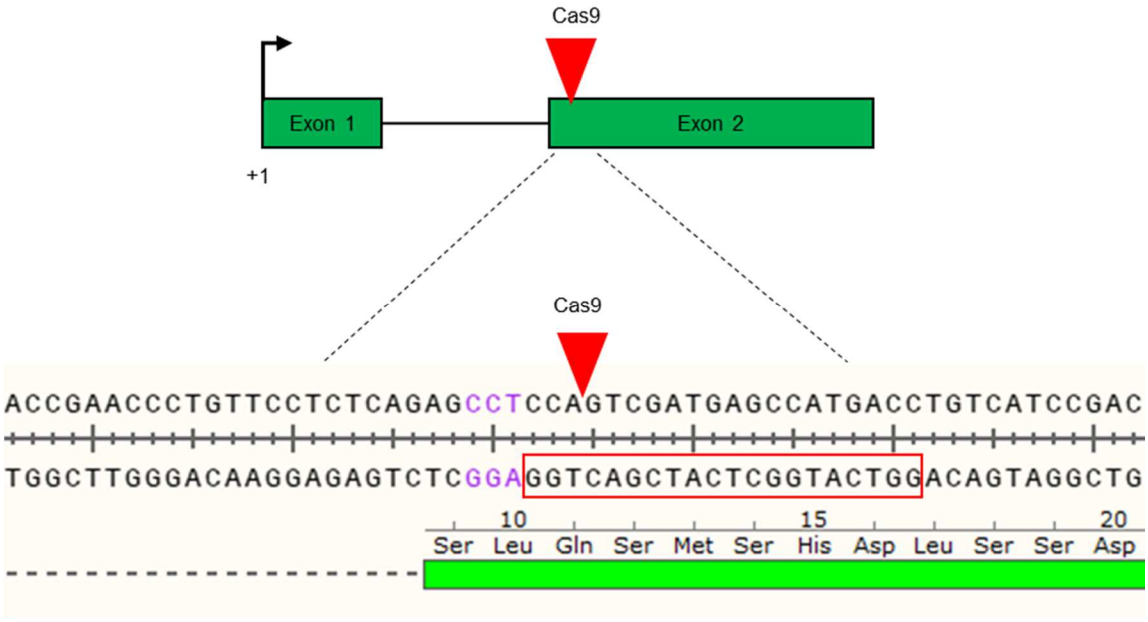

Figure 3.1. Strategy to generate TTP knockout RAW 264.7 macrophage cells. Schematic of CRISPR-Cas9 targeting TTP-exon2. Insert represents site of Cas9 targeting where the sequence within the red box indicates the gRNA sequence. Purple nucleotides illustrate the PAM sequence. Red triangle indicates site of cleavage by Cas9.

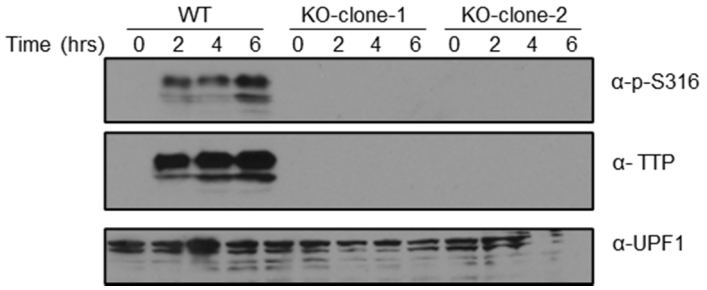

Figure 3.2. Validation of TTP$^{-/-}$ RAW 264.7 cells. Western blot monitoring levels of TTP and its phosphorylation in LPS induced RAW 264.7 macrophage cells. UPF1 served as a loading control.

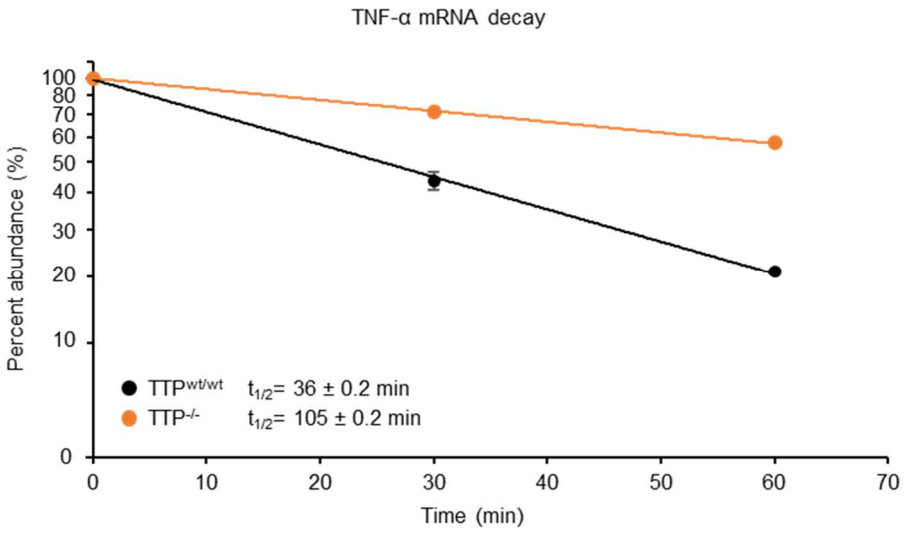

Figure 3.3. LPS-induced TTP$^{-/-}$ RAW 264.7 cells stabilize TNF-α transcripts. Measurement of mRNA decay rates for TNF-α using actinomycin D treatment on RAW 264.7 mouse macrophage cells after three hours of LPS induction. Dots represent mRNA abundance relative to time 0 for each condition with standard deviations from two independent experiments. Calculated half-lives are given with standard deviation.

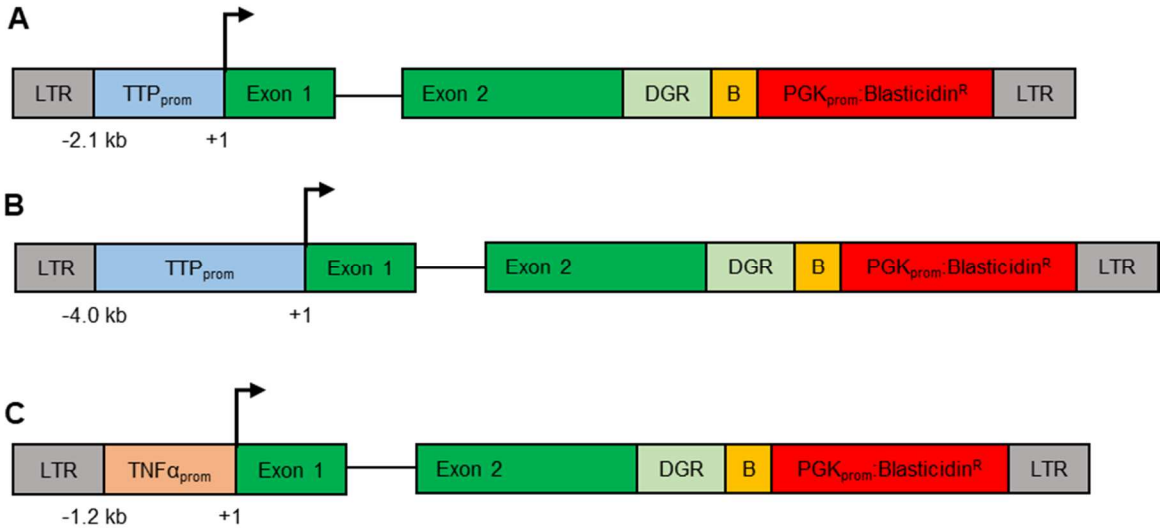

Figure 3.4. Schematics of lentiviral add-back constructs. Diagrams illustrating design of lentiviral addback constructs flanked by HIV-1 LTR sequence (grey box). (A) Schematic of TTP genomic region containing exons 1 and 2 (dark green) with the black arrow indicating transcription start site and the corresponding TTP promoter region shown in blue. The downstream genomic region, DGR, (light green) of 150 bps is followed by a bGH polyadenylation signal sequence (labelled as “B”, gold). Downstream of the TTP locus is the blasticidin resistance gene under a PGK promoter (red). (B) same as A but with a 4.0 kb endogenous promoter sequence. (C) Same as *A* and *B* but with the endogenous TTP promoter region swapped for the TNF-α promoter (light red).

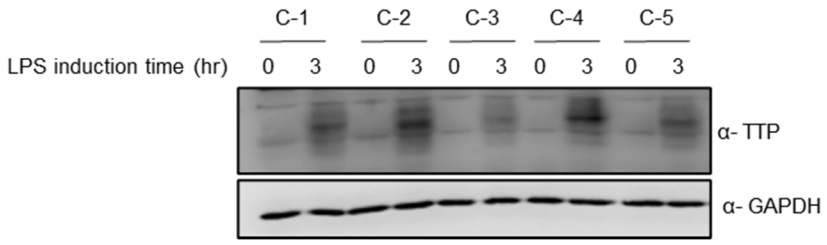

Figure 3.5. Validation of LPS-inducible $TTP_{2K\ prom}$:TTP protein expression. Western blot monitoring levels of TTP in lentiviral addback RAW 264.7 clones (labelled C-1 through C-5) under LPS induction for times indicated. GAPDH served as a loading control.

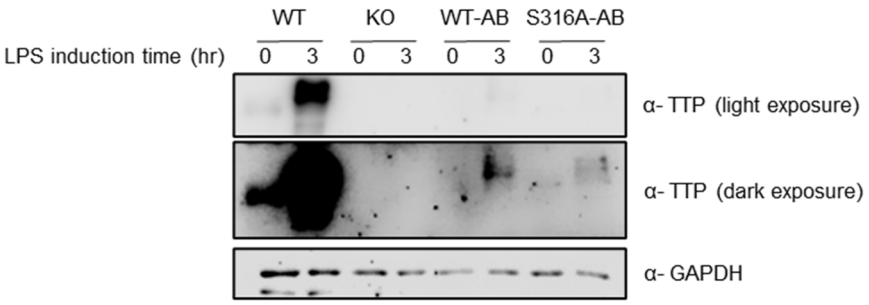

Figure 3.6. Analysis of $TTP_{2K\ prom}$:TTP expression levels. Western blot monitoring levels of TTP in wild type (WT), TTP-knockout (KO), and lentiviral addback RAW 264.7 clones expressing a wild-type (WT-AB;C-4 from Figure 3.5) and a S316A mutant TTP (S316A-AB). GAPDH served as a loading control.

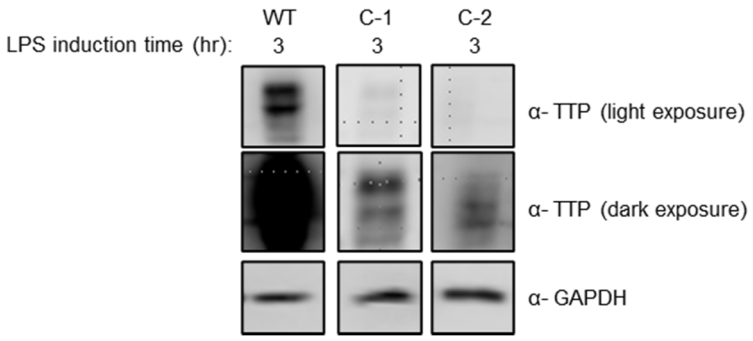

Figure 3.7. Validation and analysis of LPS-Inducible $TTP_{4K\ prom}$:TTP expression: Western blot monitoring levels of TTP in lentiviral addback RAW 264.7 clones (labelled C-1 and C-2) compared to wild-type (WT) cells under LPS induction for times indicated. GAPDH served as a loading control. Cutouts are all from the same blot and exposure.

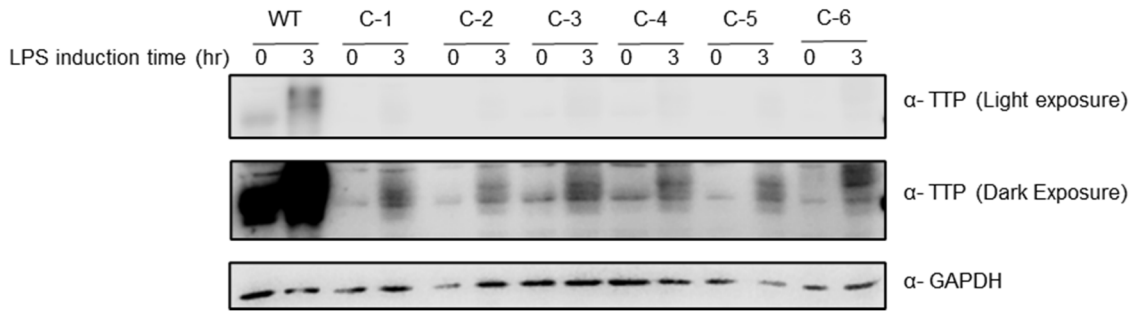

Figure 3.8. Validation and analysis of LPS-Inducible TNF-α $_{prom}$:TTP expression. Western blot monitoring levels of TTP in lentiviral addback RAW 264.7 clones (labelled C-1 through C-6) compared to wild-type (WT) cells under LPS induction for times indicated. GAPDH served as a loading control.

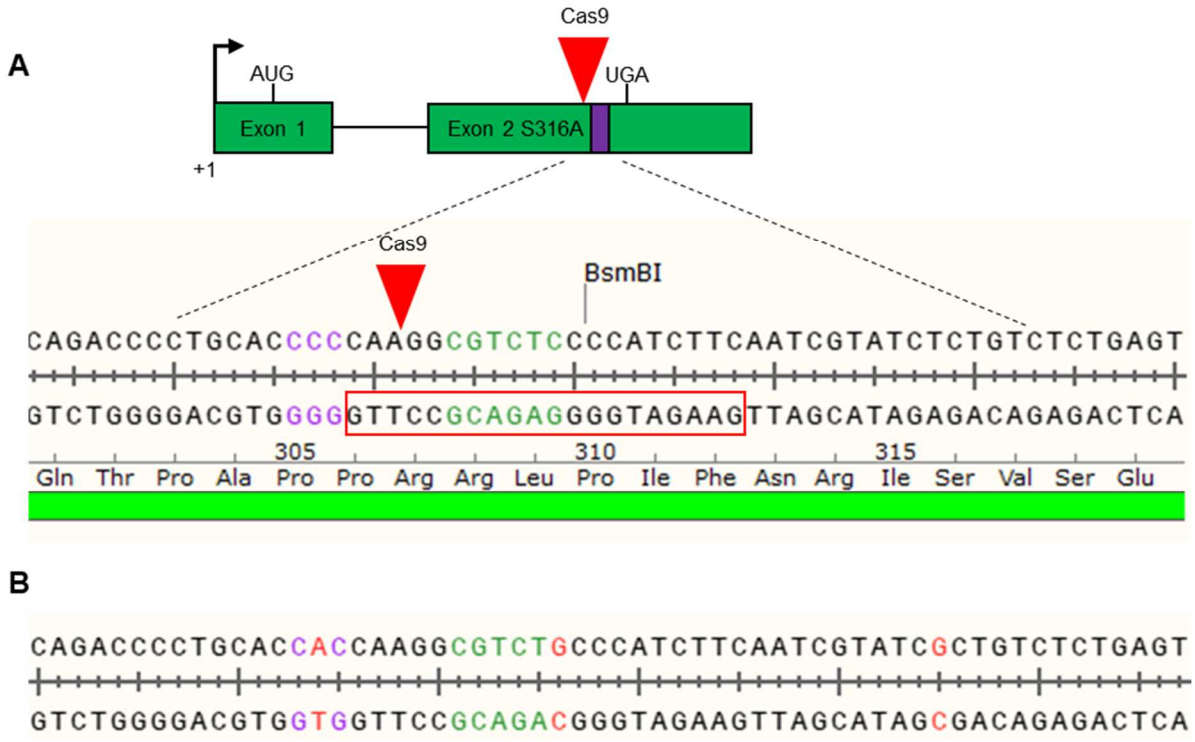

Figure 3.9. Strategy to generate homozygous TTP S316A RAW 264.7 macrophage cells. (A) Schematic of CRISPR-Cas9 targeting the TTP-CIM (purple rectangle). Insert represents site of Cas9 targeting where sequences within red box indicate gRNA sequence. Purple nucleotides illustrate the PAM sequence. Red triangle indicates site of cleavage by Cas9. Green sequences highlight the *BsmBI* restriction enzyme recognition sequence. (B) same as in A but the red nucleotides illustrate the nucleotide mutations contained within repair templates used.

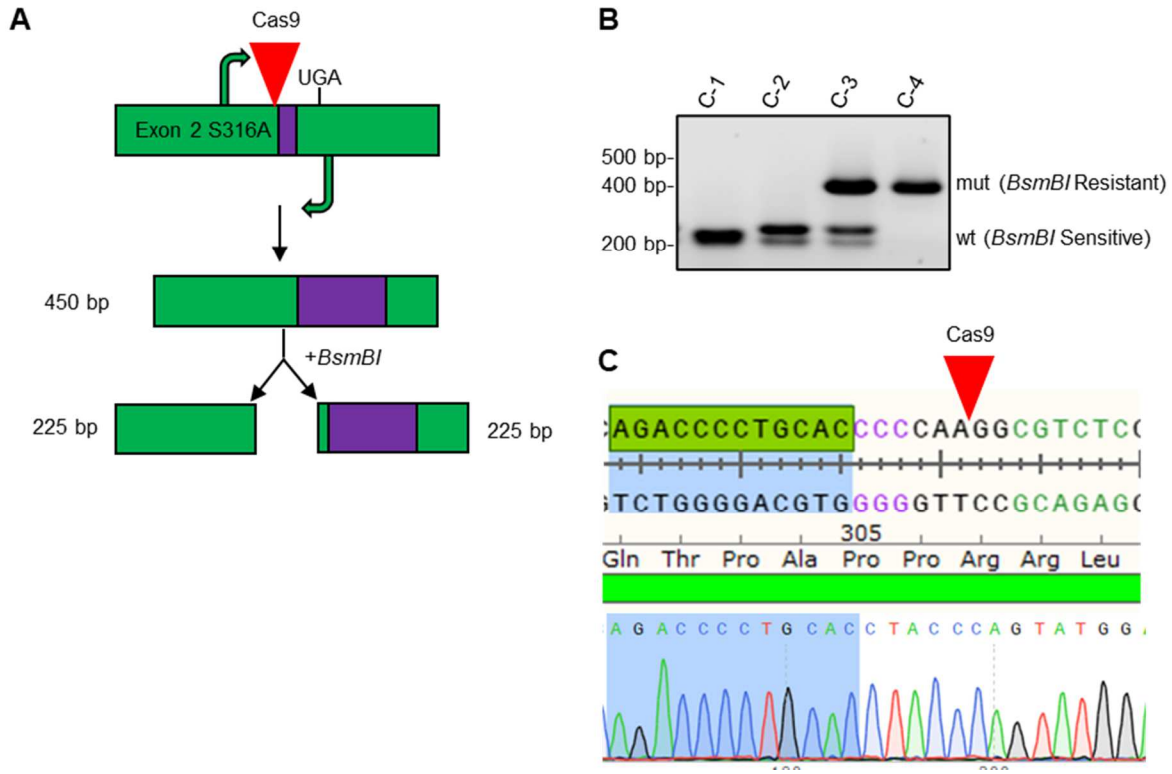

Figure 3.10. Restriction digest and sequencing of the targeted TTP-CIM region. (A) Schematic of *BsmB*I mediated validation of CRISPR-Cas9 mediated gene editing green arrows indicate primer directionality. 450 bp amplicon of TTP genomic locus was treated with *BsmBI* to generate two 225 bp fragments. (B) Agarose gel of *BsmBI* treated amplicons for CRISPR-Cas9 generated clones (C-1 through C-4). (C) Representative sequencing result of CRISPR-Cas9 generated clone revealing a 59 bp deletion generated by NHEJ. Regions highlighted in blue indicate correctly aligned regions.

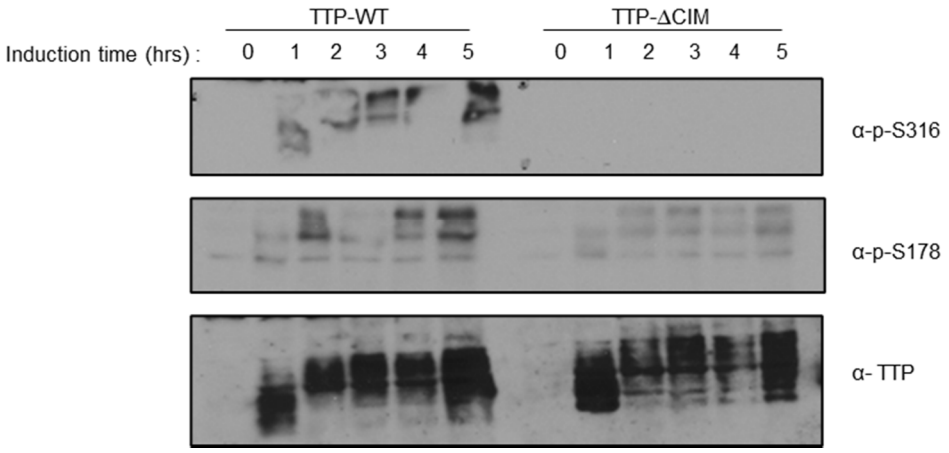

Figure 3.11. Validation of TTP-ΔCIM expression in RAW 264.7 cells. Western blot monitoring levels of TTP and its phosphorylation in LPS induced RAW 264.7 macrophage cells. TTP-ΔCIM refers to truncation mutations as seen in Figure 3.10C

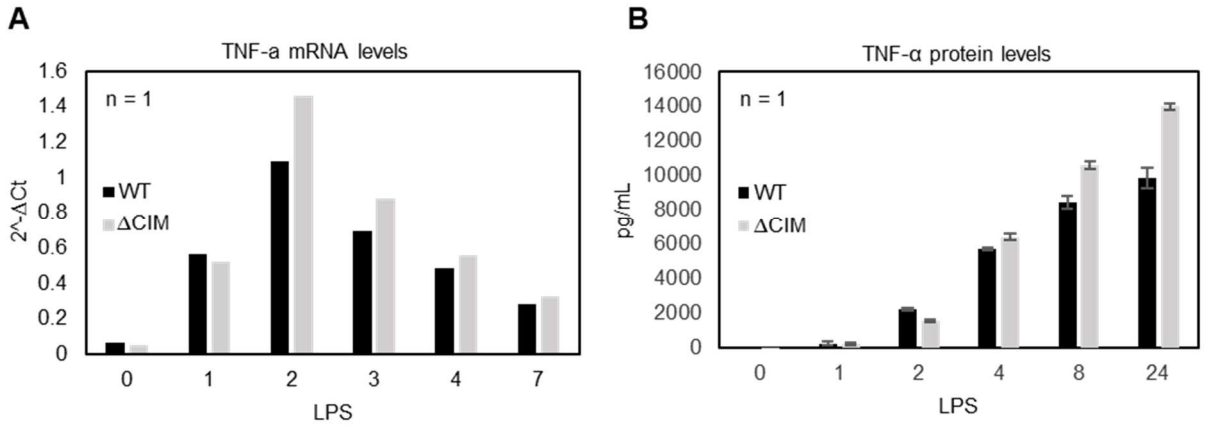

Figure 3.12. Analysis of TTP-ΔCIM–mediated effects on TNF-α expression in RAW 264.7 cells. (A) RT-qPCR monitoring TNF-α mRNA levels in LPS induced RAW 264.7 macrophage cells. Samples were run with technical triplicates. (B) ELISA for TNF-α protein levels in LPS induced RAW 264.7 cells. Standard deviations were measured from three technical replicates.

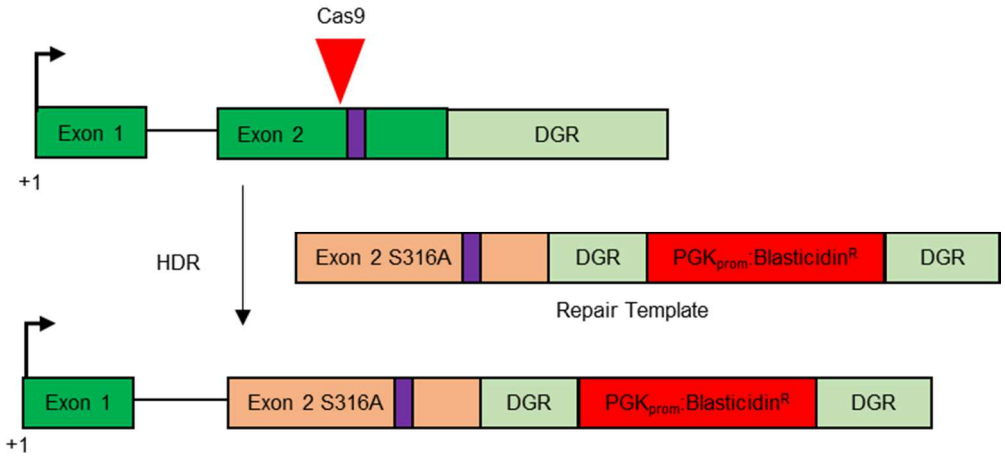

Figure 3.13. Strategy to generate homozygous TTP-S316A RAW264.7 cells.
Schematic of the TTP-Blasticidin resistance repair template used for homology-directed repair. TTP genomic region containing both exon 1 and 2 (dark green) with black arrow indicating transcription start site and the corresponding TTP-CIM (purple). The downstream genomic region (DGR) of TTP is shown in light green. A repair template containing desired mutations removing the PAM sequence and mutating S316A (light red) contains a blasticidin resistance gene under a PGK promoter (red) that is flanked upstream by 500 bp and downstream by 900 bps of the TTP downstream genomic region (DGR).

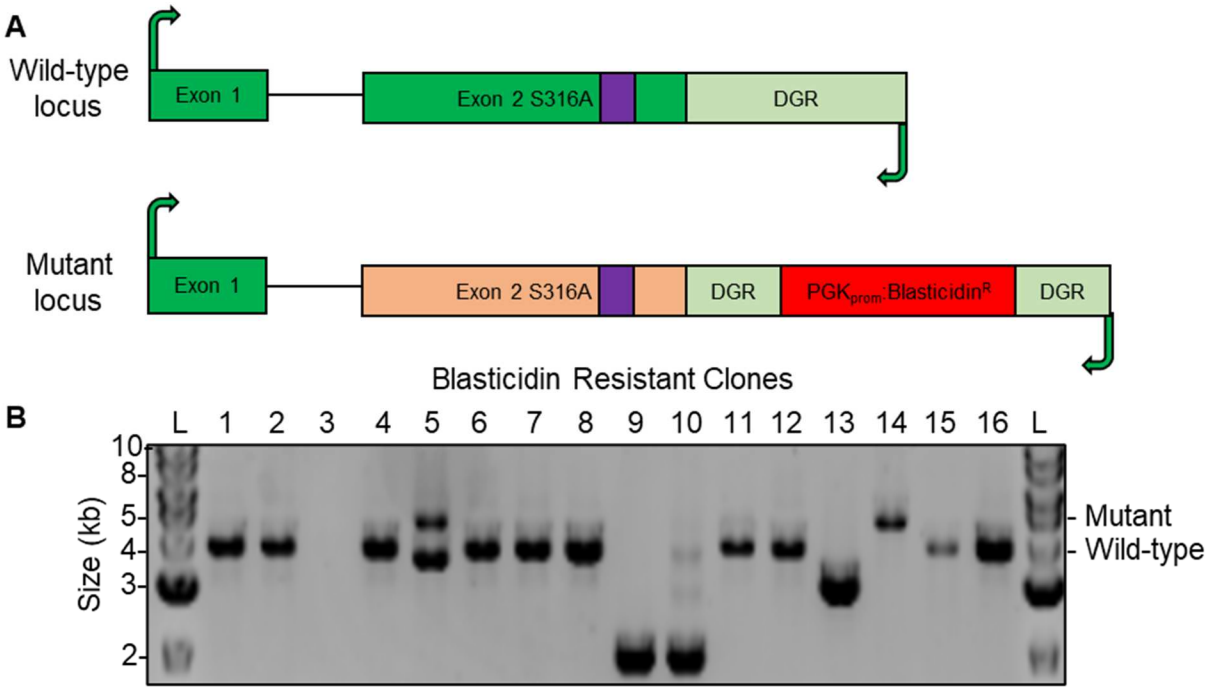

Figure 3.14. Analysis of genomic insertion of the TTP-Blast repair template. (A) Schematic of amplification strategy testing for blasticidin insertion at the correct locus. Green arrows represent PCR primer annealing locations at TTP exon 1 and the downstream genomic region (DGR) 1.0 kbp downstream of TTP exon 2. Desired mutants will contain a 5.0 kbp amplicon compared to a 4.0 kbp wild-type amplicon. (B) Agarose gel showing amplicon size for clones (labelled “Blasticidin Resistance Clones”) that conferred blasticidin resistance. DNA ladder (L) was used to determine band size.

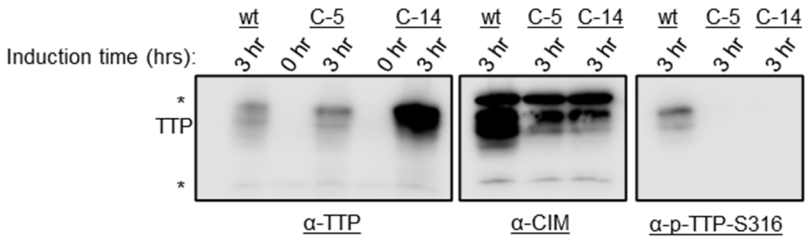

Figure 3.15. Validation of TTP-S316A expression in RAW 264.7 cells. Western blot monitoring levels of TTP and its phosphorylation in LPS induced wild-type (wt) mutant clones #5 and #14 RAW 264.7 macrophage cells. *: non-specific bands.

3.6 Materials and Methods

Cell Culture

HEK293T and RAW264.7 cells were cultured in Dulbecco's modified Eagle's medium (DMEM; Gibco) with 10% fetal bovine serum (FBS) and 1% Penicillin-Streptomycin. For experiments shown in Figures 3.2, 3.5-3.8, 3.11, and 3.15, RAW264.7 cells were treated with DMEM containing 100 ng/ml lipopolysaccharide (LPS) for the indicated times and collected in Laemmli sample lysis buffer (2% SDS, 10% Glycerol, 60 mM Tris-HCl pH 6.8, 5% β-Mercaptoethanol).

Plasmids

pSpCas9(BB)-2A-GFP (PX458) expressing guide RNAs for the TTP-CIM locus were generated as before (137). Briefly, PX458 plasmids were treated with *Bbs*I restriction enzymes, cleaned up with Qiaquick PCR purification kit (Qiagen), and ligated with annealed oligonucleotides containing *Bbs*I overhangs and sequences corresponding to the appropriate gRNA: 5'-CACCGGAAGATGGGGAGACGCCTTG-3' and 5'-AAACCAAGGCGTCTCCCC ATCTTCC 3'. The pHAGE plasmids (a generous gift from the Bennett lab) included pHDM-G, pHDM-HGPM2, pHDM-tat1b, pRC-CMV-rev1b encoding for the vesicular stomatitis virus G glycoprotein, Gag-Pol, tat-accessory protein, and rev-accessory protein respectively. Genomic DNA for the TTP locus was amplified by PCR and inserted into the pDONR-223 by Gateway BP-Clonase (ThermoFisher) to generate pDONR-TTP plasmid. pDONR-TTP-S316A constructs were generated using the Q5 site-directed mutagenesis kit (NEB). pDONR-TTP constructs were recombined with pDEST-pHAGE-tetO-N-FLAG-HA-PGK-BLAST (a generous gift from Dr. Eric Bennett, UCSD) using Gateway LR Clonase (ThermoFisher), generating the pENTR-TTP-PGK-BLAST construct that would be used with

lentiviral pHAGE constructs to insert the genomic TTP locus into transduced cells. To generate a TTP expression construct with a TNF-α promoter the TNF-α 1.2 kb promoter was amplified by PCR from RAW 264.7 genomic DNA and inserted into a pDONR-TTP plasmid by Gibson cloning (NEB) where the pDONR vector was amplified by PCR to remove the TTP promoter region. The repair template pDONR-TTP-BLAST as shown in Fig 3.13 was generated by amplifying the genomic TTP locus, starting from exon 2 to 1,400 bp downstream intergenic region, and inserting it into a pDONR plasmid using Gateway BP Cloning (ThermoFisher), forming pDONR-TTP-inter. Gibson Cloning (NEB) was performed to insert the PGK:Blasticidin resistance gene, isolated from the pENTR plasmid described above, in the downstream intergenic region of the pDONR-TTP-inter to generate pDONR-TTP-BLAST.

Generation of stable lentivirus infected cell lines

Cells were virally transduced with the 3rd generation vial delivery system using pHAGE plasmids as previously shown (a generous gift from Dr. Eric Bennett, UCSD). Briefly, HEK293T cells split into 6-well plates were transfected with five pHAGE plasmids encoding the Gag-Pol, VSVG, Tat1b, CMV, and gene of interest (GOI). Plasmids containing genes of interest contained a selectable blasticidin resistance gene under the PGK promoter. 0.5 µg of the four helper plasmids and 1.0 µg of pHAGE-GOI plasmids were transfected with 9 µl of TransIT 293T reagent (Mirus). The following day, media was aspirated and replaced with 2 ml fresh DMEM supplemented with 10% FBS. On day 3, media was removed, centrifuged at 1,000*g*, and incubated with 2 µl of 6 mg/ml Polybrene (Millipore-Sigma). 750 µL of virus-containing media was added on top of RAW 264.7 cells with 1.5 ml of DMEM supplemented with 10% FBS. On day 4, virus-containing media was removed and replaced with fresh media to allow cells to recover. On day 5, cells were scraped, expanded onto 10-cm plates in fresh media without antibiotic selection. On day 6, media was replaced with DMEM

supplemented with 10% FBS and 5 µg/ml blasticidin. Cells were grown until visible colonies formed at around 10 days and were mechanically picked and placed in 96-well plates. Clones were expanded by vigorous pipetting to resuspend cells and transferred to 12-well plates. When confluent, cells were again expanded and also split into 12-well plates to test for TTP induction by LPS (see above). Clones that expressed inducible TTP were frozen down in FBS supplemented with 10% DMSO.

Generation of TTP mutants with intergenic selectable marker in RAW 264.7 Cells.

For experiments shown in Figures 3.13 - 3.15 cells were split 1:10 onto 6-well plates and co-transfected with PX458-Guide8 and repair templates the following day according to previously recommended protocols (137). The repair template, DONR-TTP-BLAST, was previously linearized by PCR, cleaned using Qiaquick PCR purification kit. The following day, cells were expanded onto 10-cm plates containing 5 µg/ml blasticidin. Two days later, media was changed with fresh media supplemented with 5 µg/ml blasticidin. Clones were mechanically picked and placed into 96-well plates. Confluent colonies were expanded into 12-well plates. While expanding into 6-well plates, aliquots of 50 µl of cell suspension were added to 96-well plates for genomic DNA extraction (see below). Clones that appeared positive for insertion were split into 12-well plates and treated with LPS for the indicated times and collected in Laemmli sample lysis buffer for Western blot analysis.

Genomic DNA extraction

To extract genomic DNA from clones, confluent cells in 12-well plates were mechanically resuspended with vigorous pipetting and 50 µl of the suspension were added into wells of a 96-well plate containing 150 µl of DMEM (10%FBS). The following day, media was aspirated from each well,150 µl of QuickExtract (Lucigen) was added, and samples were incubated at 37^{o}C for 1 hour. Lysed cells were transferred into 96-well PCR plates. Samples were then

incubated at 65°C for 15 minutes, mixed and spun down, and then incubated at 98°C for 10 minutes. Samples were stored at -20°C until analysis by PCR.

Antibodies

Rabbit polyclonal anti-pS316-TTP antibody was generated with the synthesized oligo peptide PRRLPIFNRI(p)SVSE by Pocono Rabbit Farm & Laboratory (USA). The antiserum was purified by affinity chromatography by first collecting antibody binding to a PRRLPIFNRI(p)SVSE-peptide column, and, after elution, collecting the flow-through from a subsequent unphosphorylated PRRLPIFNRISVSE-peptide column. Antibodies bound to the last column were eluted as rabbit polyclonal anti-TTP-CIM. Western blots were probed with the following antibodies at the indicated concentrations: rabbit polyclonal anti-TTP (Sigma-Aldrich, T5327; 1:500), rabbit polyclonal anti-CNOT1 (Proteintech, 14276-1-AP; 1:200), rabbit polyclonal anti-UPF1 ((138),1:1,000), mouse monoclonal anti-GAPDH (Cell Signaling Technology, 97166, 1:1,000).

Quantitative qRT-PCR

1 µg of total RNA extracted with Trizol (Invitrogen) was reverse transcribed using random hexamers with Superscript III according to the manufacturer's protocol (Invitrogen). Quantification of cDNA by qPCR was performed using Fast SYBR Green Master Mix (Applied Biosystems) on a StepOnePlus system (Applied Biosystems). Experiments were performed in triplicate. For each qRT-PCR reaction, 10-fold serial dilutions of cDNA were used to calculate PCR efficiency of primer pairs used. The following DNA oligos were used at 200 nM. GAPDH_F: CAT GGC CTT CCG TGT TCC TA; GAPDH_R: CCT GCT TCA CCA CCT TCT TGA T; TNF-α_F: GGT GCC TAT GTC TCA GCC TCTT; TNF-α_R: GCC ATA GAA CTG ATG AGA GGG AG.

Fluorescence Activated Cell Sorting of CRISPR-Cas9 transfected cells

RAW 264.7 cells were split 1:10 onto 6-well plates. The following day, cells were transfected with PX458 (containing appropriate gRNAs) follows previously established protocols (137). Two days later, transfected cells were washed with phosphate buffered saline (PBS) and treated with Accutase (Millipore Sigma) and gently resuspended by pipetting. Cells were filtered through a strainer. Cell suspension was spun down at 1,000*g* for 5 minutes and resuspended in ice-cold PBS containing the viability marker, 7-AAD. Single-cell sorting was performed using the FACS Aria II (BD) into 180 µl of conditioned DMEM supplemented with 10% FBS and 1% Penicillin and Streptomycin. Media changes were performed every four days and confluent colonies were expanded into 12-well plates. For ssODN transfected experiments, cells were expanded to 6-well plates, aliquots were set aside for genomic DNA analysis (see above). For TTP knockout experiments, colonies were split onto 12-well plates and subsequently treated with LPS for the indicated times and analyzed by Western blotting.

3.7 Acknowledgements

Thank you to Dr. Eric Bennett for providing lentiviral pHAGE plasmids. Thank you to Georg Stoecklin for providing α-p-TTP-Ser178 antibody.

Chapter 4. Conclusions and Future Directions

4.1 Conclusions

Investigating the coordination of regulated mRNA decay offers insight into fundamental concepts of gene expression. With its many decay factors and mechanistic avenues, the process of mRNA decay is a complex waltz of situational prerequisites and conditional checkpoints facilitated by factors that function in *cis* and *trans* within a given mRNA transcript. The outcomes of our understandings resonate as translational discoveries that offer clinical solutions to biomedical problems. For example, how cell signaling affects the expression of ARE-containing pro-inflammatory transcripts is an important clinical question that may offer solutions to chronic inflammatory disease. The work presented here contributes to our understanding of how mRNA decay is regulated in a setting relevant to inflammation.

The RNA-binding protein TTP is best known for its role in mediating the inflammatory response by promoting the degradation of mRNAs for pro-inflammatory cytokines. During the early hours of the inflammatory response TTP is seen to be in an inactive, phosphorylated, state. Despite 30 reported sites of phosphorylation, the functional consequence of TTP's phosphorylated state have only been described for two serine residues, serine 52 and 178 (mouse numbering) which are targeted by MK2, a kinase acting downstream in the p38 MAPK pathway. In Chapter 2, I demonstrated that the conserved serine residue within the CIM, a motif important for association of the CCR4-NOT deadenylase complex, is not a target of MK2 as had been previously reported. Furthermore, I demonstrated that the CIM is sufficient to promote mRNA deadenylation and decay. Experiments probing the functional role of the CIM in TTP-mediated decay revealed that the N-terminal domain of TTP promotes mRNA decay in a manner that does not require CIM-mediated interaction with the CCR4-NOT deadenylation complex. Importantly, the activity of TTP was further enhanced by an

alanine mutation to the conserved serine 316 (mouse numbering). These results suggested the CIM remains active in conditions where TTP is targeted by MK2. Tethering assays where TTP was co-transfected with MK2 revealed an enhanced stabilization of a target transcript upon removal of the CIM compared to wild-type TTP. I also found TTP to coordinate the association of the CCR4-NOT complex through both the CIM and the conserved tryptophan residues, previously reported to associate with CNOT9, and combined mutations of these residues further stabilized target transcripts compared to single mutations.

To confidently assess the functional effect of TTP mutations it is important to recreate the endogenous environment of the inflammatory response. In Chapter 3, I reported my attempts at developing TTP mutants in the RAW 264.7 mouse macrophage cell line. The development of a $TTP^{-/-}$ RAW 264.7 mouse macrophage cell line is an important step in understanding the functional role of TTP mutations in an immune-relevant system. In addition to serving as a control for TTP-mediated regulation during the inflammatory response, I utilized $TTP^{-/-}$ RAW 264.7 cells to generate stable add-back TTP cell lines using a lentiviral delivery system. Although I successfully reintroduced TTP expression that was inducible upon treatment with LPS, these were unable to approach expression levels seen in wild-type cells despite introduction of up to 4.0 kbp of the TTP promoter region or with the complete TNF-α promoter region. These results suggest additional elements, located downstream of the TTP gene or outside of the TTP locus, are necessary to promote the efficient induction of TTP under LPS induction.

In addition to efforts at generating add-back TTP conditions, I also performed CRISPR-Cas9 mediated gene editing of the TTP locus in RAW 264.7 cells. Although targeting the CIM using a combination of ssODNs and repair templates was unsuccessful, these attempts did lead to the serendipitous generation of RAW 264.7 cells in which the TTP gene lacks the conserved CIM region, which can be used for downstream analysis. More promising results came from the generation of a repair template which contained a selectable

marker under its own promoter, downstream of the TTP gene. Preliminary results observing PCR amplification of the genomic locus and TTP expression by Western blotting suggest this method can produce desired TTP mutations in RAW 264.7 cells.

4.2 TTP lacking known CCR4-NOT associations stabilizes but does not completely eliminate mRNA decay.

Because of its role in promoting the association with the CCR4-NOT deadenylase complex (76), it was assumed that the functional loss of the TTP-CIM would drastically hinder TTP-mediated mRNA decay. However, both *in vitro and in vivo* experiments have revealed that the loss of the TTP-CIM does not abolish mRNA decay and promotes a mild inflammatory phenotype in mice (76, 81). In Chapter 2, the functional consequence of losing the CIM in the context of full-length TTP recapitulates these previous observations; however, removing the CIM from tethering experiments examining the TTP C-terminal domain considerably stabilized target transcripts. These results suggest that the TTP N-terminal domain (NTD) can promote mRNA decay in a CIM-independent manner, and probing the functional redundancy seen in the TTP-NTD will help us better understand the coordination of mRNA decay by TTP.

Previous work has suggested that the TTP NTD can promote the association with deadenylation factors (74). To probe whether the NTD can promote mRNA decay independent of the association of the CCR4-NOT complex, tethering assays looking at the NTD in combination with knockdown of components of the CCR4-NOT complex can be performed. Targeting CNOT1 with siRNAs, for example, will reveal if CCR4-NOT is still driving mRNA decay. Additionally, TTP has been demonstrated to promote the association of the CCR4-NOT complex through conserved tryptophan residues, some of which are found in the NTD; therefore, knockdown experiments of CNOT1 can be performed in combination with tryptophan mutants. Results from these experiments can reveal whether the tryptophan-

mediated association of the CCR4-NOT complex in the NTD is sufficient to promote mRNA decay in $TTP_{\Delta CIM}$ conditions. Furthermore, siCNOT1 knockdown experiments in combination with tryptophan mutations may reveal if there are other TTP motifs that promote the association of CCR4-NOT complex.

Similarly, the TTP-NTD has been previously reported to promote association with decapping factors(74). To test whether NTD-mediated decay is promoted by deadenylation-independent decapping, tethered decay assays looking at both full length TTP or NTD truncation mutants in combination with knockdown of EDC4 or other decapping factors can be performed. In addition, NTD mutated in the conserved tryptophan residues can also be tested in conditions where decapping factors have been knocked down.

TTP has also been reported to associate with argonaute (Ago) proteins (139, 140). This association has been demonstrated to be affected by the p38 MAPK pathway acting on TTP (140). To test whether Ago proteins associate with the TTP NTD, AGO2 knockdown experiments can be performed along with tethering decay assays.

4.3 Does 14-3-3 help displace CNOT1?

Although mutation of the conserved tryptophan residues reduced the association of TTP with the CCR4-NOT complex through decreased recruitment of both CNOT9 as well as CNOT1, we did not observe a drastic stabilization of targeted transcripts in conditions where active MK2 was co-transfected with TTP_{3W} mutations. These results suggest that the loss of the CIM-mediated interactions is an important component of this MK2-mediated stabilization and not the loss of CNOT9/CCR4-NOT association per se.

In Chapter 2, immunoprecipitation experiments observing TTP serine mutants treated with okadaic acid showed a decrease in 14-3-3 association occurs upon mutation of the Ser 316 residue within the CIM. These results suggest that 14-3-3 associates with TTP through the CIM, in addition to the previously characterized serine 52 and 178 residues (mouse

numbering)(83). This evidence is further supported by the decrease in association of 14-3-3 in $TTP_{\Delta CIM}$ conditions. 14-3-3 adaptor protein association has been demonstrated to correlate with decreased association of decay factors with TTP (83, 116). Lastly, conditions where TTP activity was hindered by active MK2, mRNA decay was accelerated with TTP_{S316A} mutants. These results suggest that 14-3-3 associates at the TTP-CIM through phosphorylation at Ser 316 and may be involved in repressing TTP-mediated decay. To test this hypothesis, tethering decay assays looking at TTP mutated at serines 52 and 178, TTP_{2A}, and TTP serine mutants with an additional S316A mutation, TTP_{3A}, can be tested in conditions using the 14-3-3 inhibitor R18. It would be predicted that TTP and TTP_{2A} treated with R18 would promote decay faster than untreated conditions. Additionally, TTP_{3A} mutants should promote decay at similar rates in treated and untreated conditions.

Furthermore, it was previously demonstrated in the BRF1-CIM that replacing the serine residue corresponding to TTP-S316 with a potential phosphomimetic aspartate mutation led to an increase in association of the decapping factor DCP1a. Although we found no increase in association of another decapping factor EDC4 upon treatment of TTP with okadaic acid, we did not extensively test to see if DCP1a association increases with phosphorylation of TTP-S316. Furthermore, we did not test if a phosphomimetic mutation would affect the association of a decapping factor in the context of TTP. These reported associations could be explained by experimental artifacts being introduced, or could be due to difference between members of the ZFP36 family. Because TTP and BRF1 are structurally distinct, it may be that the CIM motif can also recruit DCP1A. To test this, pull-down experiments looking at TTP-CTD and GFP-CIM should be run along with full-length TTP using okadaic acid, PKCα, or another CIM kinase such as RKS1 or PKA.

4.4 Does the CIM affect TTP localization through stabilizing 14-3-3 association?

My observations in Chapter 2 revealed that the CIM is a site that promotes the association of 14-3-3 proteins. Alanine mutation of serine 316 caused a decrease in 14-3-3 association and deletion of the CIM also contributed to the loss of 14-3-3 protein binding, as seen in immunoprecipitation experiments. These results offer an exciting new avenue for understanding the dynamics of 14-3-3-mediated regulation of TTP. 14-3-3 proteins have been demonstrated to prevent TTP from associating with stress granules during sodium arsenite treatment due to increased phosphorylation of TTP. Results from chapter 2 suggest that phosphorylation at the CIM may contribute to these changes in TTP localization. To test this, immunofluorescence experiments can be performed as before where stress granules are induced under conditions of TTP phosphorylation mutants. Furthermore, conditions where $TTP_{\Delta CIM}$ is present can also be tested where it is predicted that the loss of association of 14-3-3 proteins would lead to greater association of TTP with stress granules. It may also be necessary to test whether conditions of TTP-CTD, where TTP lacks serine 52, is capable of preventing associations with stress granules as well. These conditions can also be done with the TTP mutants: ΔCIM, S52, S316, and S52/S316A as well. Similarly, Chapter 2 revealed that the CIM can promote deadenylation and decay, and this decay rate was accelerated in S316A mutant conditions. It would be interesting to test if the GFP-CIM constructs that were generated in chapter 2 are also capable of associating with, or promoting the development of, stress granules or p-bodies. Immunofluorescence staining can be performed looking for markers of these granules.

4.5 TTP nuclear localization and roles in alternative polyadenylation and splicing.

Results from Chapter 3 demonstrated the generation of $TTP^{-/-}$ RAW 264.7 macrophage cells by CRISPR-Cas9 editing strategies. As shown in Figure 3.6 in uninduced cells, while no TTP signal was detected in $TTP^{-/-}$ cells, low levels of TTP were detected wild-

type RAW 264.7 macrophage cells. Previous work has revealed that TTP is expressed at low levels in uninduced macrophage cells and is localized in the nucleus (51). Currently, little is known about the nuclear role of TTP; however, it has been demonstrated that the nuclear activity of TTP prevents the transactivation of estrogen receptor alpha, progesterone receptor, glucocorticoid receptors, and androgen receptors, and has been demonstrated to recruit histone deacetylases to inhibit NF-κB activity (141–143). Furthermore, CCR4-NOT, which interacts with TTP in the cytoplasm to promote mRNA decay, is also reported to act as a transcription factor (15). In addition, it has been demonstrated to play a role in alternative splicing in HeLa cells (136). Interestingly, PAR-CLIP studies revealed that around 60% of TTP binding sites occurred in the introns of target transcripts (144). Finally, previous work in the lab hints at a possible role in promoting alternative polyadenylation of ARE-containing transcripts. To test the role of TTP in the nucleus, RNA sequencing experiments looking at wild-type uninduced cells compared to knockouts will be able to address these reported findings on alternative transcripts. Furthermore, ChIP analyses may reveal genomic regions where TTP associations affect transcriptional regulation.

4.6 CRISPR-Cas9 mediated gene editing using a selectable marker.

The development of a repair template containing a selectable marker located in the downstream region of TTP described in Chapter 3 will allow for easier selection of desired mutations expressed from an endogenous promoter within the immune relevant RAW 264.7 macrophage cells. Although this repair template is promising, there are modifications that can still be made to make a more promising delivery vector. If new gRNAs are generated that are far upstream from the CIM, it may not promote the integration of the selectable marker. One possible solution is co-transfection of an additional Cas9 plasmid expressing a guide RNA that targets near the insertion region of the selectable marker. This would allow for two cut sites at the TTP locus to be generated and increase gene editing at this area of interest.

Furthermore, nickase mutant Cas9 plasmids can be utilized to lower off-target effects, if desired. Targeting the intergenic region in addition to TTP exon 2 would, of course, require mutating the repair template to prevent re-targeting after proper insertion occurs.

The generation of novel TTP mutants may require new gRNAs and with that, novel repair templates that create silent mutations to areas targeted by gRNAs would need to be generated. One possible solution is generating a guide RNA sequence that may allow for both integration of the selectable marker as well as any TTP mutation within exon 2. Targeting something critical like the Zinc-finger binding domain, or the sequence that bridges both ZFDs would be an ideal position to investigate.

Lastly, if selectable markers cause unintended pleiotropic effects. Novel strategies using CRISPR-Cas9 targeting of the TTP locus can be implement. For example, novel guide RNAs that target further downstream of the *BsmBI* recognition sequence can be developed to limit the occurrence of false positives during restriction digest clonal testing. Targeting the 3'UTR of TTP with the use of a repair template that contains silent mutations for *BsmBI* can yield less false positive results as less DNA repair events can affect this site. Another solution would also be to introduce a repair template containing a novel restriction cut site that can be used to test for appropriate repair template insertions.

4.7 CIM-tagging RNA binding proteins.

Chapter 2 demonstrated that tagging an MS2-GFP with the CIM accelerated decay of a targeted mRNA, and this activity was further accelerated upon mutation of the conserved serine 316 residue to an alanine to prevent phosphorylation.

These results suggest that tagging an RNA binding protein with the small CIM motif may be sufficient to destabilize bound target transcripts. This can be tested in catalytically inactive Cas13 proteins that are unable to promote cleavage of bound target transcripts. Uniquely targeted Cas13-CIM targets can be analyzed for mRNA stability by RT-qPCR to

see if the addition of the CIM to an RNA binding protein is sufficient to promote decay of a gRNA-targeted mRNA. This could provide a system for mRNA-specific degradation.

Additionally, TTP shares target transcripts with the mRNA stabilizing factor, HuR, which also binds to ARE-containing transcripts. It is unknown whether HuR stabilizes target mRNAs due to simple competition with destabilizing factors for ARE-binding, or whether HuR more actively promotes mRNA stabilization. Tethering decay assays can determine whether MS2-HuR-CIM fusion constructs can promote mRNA decay compared to MS2-HuR conditions. If CIM-tagging HuR does not promote mRNA decay, this suggests that HuR stabilizing effects may be active, for example mediated by interactions that stabilize the poly-A tail. If HuR-CIM does promote mRNA decay, this suggests that the stabilizing effect mediated by HuR is due to physically preventing destabilizing factors from associating to ARE-containing transcripts. An additional exciting avenue from these results would be in conditions like the inflammatory response where TTP is unable to promote mRNA decay due to targeting by the p38 MAPK pathway, could HuR-CIM promote the destabilization of endogenous TTP targets? These types of experiments could help provide insights into mechanisms by which ARE-binding proteins compete with one another to control the stability of ARE-mRNAs.

References

1. Schwartz DC, Parker R. 2000. mRNA Decapping in Yeast Requires Dissociation of the Cap Binding Protein, Eukaryotic Translation Initiation Factor 4E. Mol Cell Biol 20:7933–7942.

2. Lim J, Ha M, Chang H, Kwon SC, Simanshu DK, Patel DJ, Kim VN. 2014. Uridylation by TUT4 and TUT7 marks mRNA for degradation. Cell 159:1365–1376.

3. Zuber H, Scheer H, Ferrier E, Sement FM, Mercier P, Stupfler B, Gagliardi D. 2016. Uridylation and PABP Cooperate to Repair mRNA Deadenylated Ends in Arabidopsis. Cell Rep 14:2707–2717.

4. Scheer H, Zuber H, De Almeida C, Gagliardi D. 2016. Uridylation Earmarks mRNAs for Degradation.. . and More. Trends Genet 32:607–619.

5. Wang Z, Kiledjian M. 2001. Functional Link between the Mammalian Exosome and mRNA DecappingCell.

6. Garneau NL, Wilusz J, Wilusz CJ. 2007. The highways and byways of mRNA decay. Nat Rev Mol Cell Biol 8:113–126.

7. Schoenberg DR, Maquat LE. 2012. Regulation of cytoplasmic mRNA decay. Nat Rev Genet 13:448–448.

8. Chowdhury A, Tharun S. 2009. Activation of decapping involves binding of the mRNA and facilitation of the post-binding steps by the Lsm1-7-Pat1 complex. Rna 15:1837–1848.

9. Ozgur S, Chekulaeva M, Stoecklin G. 2010. Human Pat1b Connects Deadenylation with mRNA Decapping and Controls the Assembly of Processing Bodies †. Mol Cell Biol 30:4308–4323.

10. Coller J, Parker R. 2005. General translational repression by activators of mRNA decapping. Cell 122:875–886.

11. Tharun S, He W, Mayes AE, Lennertz P, Beggs JD, Parker R. 2000. Yeast Sm-like proteins function in mRNA decapping and decay. Nature 404:515–518.

12. Bouveret E, Rigaut G, Shevchenko A, Wilm M, Séraphin B. 2000. A Sm-like protein complex that participates in mRNA degradation. EMBO J 19:1661–1671.

13. Gao M, Wilusz CJ, Peltz SW, Wilusz J. 2001. A novel mRNA-decapping activity in HeLa cytoplasmic extracts is regulated by AU-rich elements. EMBO J 20:1134–1143.

14. Yamashita A, Chang T-C, Yamashita Y, Zhu W, Zhong Z, Chen C-YA, Shyu A-B. 2005. Concerted action of poly(A) nucleases and decapping enzyme in mammalian mRNA turnover https://doi.org/10.1038/nsmb1016.

15. Collart MA. 2016. The Ccr4-Not complex is a key regulator of eukaryotic gene expression https://doi.org/10.1002/wrna.1332.

16. Tucker M, Staples RR, Valencia-Sanchez MA, Muhlrad D, Parker R. 2002. Ccr4p is the catalytic subunit of a Ccr4p/Pop2p/Notp mRNA deadenylase complex in Saccharomyces cerevisiae. EMBO J 21:1427–1436.

17. Tucker M, Valencia-Sanchez MA, Staples RR, Chen J, Denis CL, Parker R. 2001. The Transcription Factor Associated Ccr4 and Caf1 Proteins Are Components of the Major Cytoplasmic mRNA Deadenylase in Saccharomyces cerevisiae. Cell 104:377–386.

18. Machida K, Shigeta T, Yamamoto Y, Ito T, Svitkin Y, Sonenberg N, Imataka H. 2018. Dynamic interaction of poly(A)-binding protein with the ribosome. Sci Rep 8.

19. Tarun SZ, Sachs AB. 1996. Association of the yeast poly(A) tail binding protein with translation initiation factor eIF-4G. EMBO J 15:7168–7177.

20. Imataka H, Gradi A, Sonenberg N. 1998. A newly identified N-terminal amino acid sequence of human eIF4G binds poly(A)-binding protein and functions in poly(A)-dependent translation. EMBO J 17:7480–7489.

21. Webster MW, Chen YH, Stowell JAW, Alhusaini N, Sweet T, Graveley BR, Coller J, Passmore LA. 2018. mRNA Deadenylation Is Coupled to Translation Rates by the Differential Activities of Ccr4-Not Nucleases. Mol Cell 70:1089-1100.e8.

22. Yi H, Park J, Ha M, Lim J, Chang H, Narry V, Correspondence K, Kim VN. 2018. PABP Cooperates with the CCR4-NOT Complex to Promote mRNA Deadenylation and Block Precocious Decay Molecular Cell PABP Cooperates with the CCR4-NOT Complex to Promote mRNA Deadenylation and Block Precocious Decay. Mol Cell 70:1081-1088.e5.

23. Wu Q, Medina SG, Kushawah G, Devore ML, Castellano LA, Hand JM, Wright M, Bazzini AA. 2019. Translation affects mRNA stability in a codon-dependent manner in human cells. Elife 8.

24. Buschauer R, Matsuo Y, Sugiyama T, Chen YH, Alhusaini N, Sweet T, Ikeuchi K, Cheng J, Matsuki Y, Nobuta R, Gilmozzi A, Berninghausen O, Tesina P, Becker T, Coller J, Inada T, Beckmann R. 2020. The Ccr4-Not complex monitors the translating

ribosome for codon optimality. Science (80-) 368.

25. Presnyak V, Alhusaini N, Chen YH, Martin S, Morris N, Kline N, Olson S, Weinberg D, Baker KE, Graveley BR, Coller J. 2015. Codon optimality is a major determinant of mRNA stability. Cell 160:1111–1124.

26. Radhakrishnan A, Green R. 2016. Connections Underlying Translation and mRNA Stability. J Mol Biol 428:3558–3564.

27. Kubacka D, Kamenska A, Broomhead H, Minshall N, Darzynkiewicz E, Standart N. 2013. Investigating the Consequences of eIF4E2 (4EHP) Interaction with 4E-Transporter on Its Cellular Distribution in HeLa Cells. PLoS One 8:72761.

28. Chapat C, Jafarnejad SM, Matta-Camacho E, Hesketh GG, Gelbart IA, Attig J, Gkogkas CG, Alain T, Stern-Ginossar N, Fabian MR, Gingras AC, Duchaine TF, Sonenberg N. 2017. Cap-binding protein 4EHP effects translation silencing by microRNAs. Proc Natl Acad Sci U S A 114:5425–5430.

29. Peter D, Ruscica V, Bawankar P, Weber R, Helms S, Valkov E, Igreja C, Izaurralde E. 2019. Molecular basis for GIGYF-Me31B complex assembly in 4EHP-mediated translational repression. Genes Dev 33:1355–1360.

30. Weber R, Chung MY, Keskeny C, Zinnall U, Landthaler M, Valkov E, Izaurralde E, Igreja C. 2020. 4EHP and GIGYF1/2 Mediate Translation-Coupled Messenger RNA Decay. Cell Rep 33.

31. Morita M, Ler LW, Fabian MR, Siddiqui N, Mullin M, Henderson VC, Alain T, Fonseca BD, Karashchuk G, Bennett CF, Kabuta T, Higashi S, Larsson O, Topisirovic I, Smith RJ, Gingras A-C, Sonenberg N. 2012. A Novel 4EHP-GIGYF2 Translational Repressor Complex Is Essential for Mammalian Development. Mol Cell Biol 32:3585–3593.

32. Tao X, Gao G. 2015. Tristetraprolin Recruits Eukaryotic Initiation Factor 4E2 To Repress Translation of AU-Rich Element-Containing mRNAs. Mol Cell Biol 35:3921–3932.

33. Kedersha N, Stoecklin G, Ayodele M, Yacono P, Lykke-Andersen J, Fitzler MJ, Scheuner D, Kaufman RJ, Golan DE, Anderson P. 2005. Stress granules and processing bodies are dynamically linked sites of mRNP remodeling. J Cell Biol 169:871–884.

34. Protter DSW, Parker R. 2016. Principles and Properties of Stress granules HHS Public Access. Trends Cell Biol 26:668–679.

35. Hao S, Baltimore D. 2009. The stability of mRNA influences the temporal order of the

induction of genes encoding inflammatory molecules. Nat Immunol 10:281–288.

36. Schwanhüusser B, Busse D, Li N, Dittmar G, Schuchhardt J, Wolf J, Chen W, Selbach M. 2011. Global quantification of mammalian gene expression control. Nature 473:337–342.

37. Nicholson AL, Pasquinelli AE. 2019. Tales of Detailed Poly(A) Tails https://doi.org/10.1016/j.tcb.2018.11.002.

38. Mayr C. 2019. What are 3′ utrs doing? Cold Spring Harb Perspect Biol 11.

39. Xu N, Chen C-YA, Shyu A-B. 1997. Modulation of the Fate of Cytoplasmic mRNA by AU-Rich Elements: Key Sequence Features Controlling mRNA Deadenylation and Decay. Mol Cell Biol 17:4611–4621.

40. Caput D, Beutler B, Hartog K, Thayer R, Brown-Shimer S, Cerami A. 1986. Identification of a common nucleotide sequence in the 3'-untranslated region of mRNA molecules specifying inflammatory mediators. Proc Natl Acad Sci U S A 83:1670–1674.

41. Anderson P. 2008. Post-transcriptional control of cytokine production. Nat Immunol 9:353–359.

42. Otsuka H, Fukao A, Funakami Y, Duncan KE, Fujiwara T. 2019. Emerging evidence of translational control by AU-rich element-binding proteins. Front Genet 10:332.

43. Barreau C, Paillard L, Osborne HB. 2005. AU-rich elements and associated factors: Are there unifying principles? Nucleic Acids Res.

44. Shaw G, Kamen R. 1986. A Conserved AU Sequence from the 3' Untranslated Region of GM-CSF mRNA Mediates Selective mRNA DegradationCell.

45. Frevel MAE, Bakheet T, Silva AM, Hissong JG, Khabar KSA, Williams BRG. 2003. p38 Mitogen-Activated Protein Kinase-Dependent and -Independent Signaling of mRNA Stability of AU-Rich Element-Containing Transcripts. Mol Cell Biol 23:425–436.

46. Bakheet T, Williams BRG, Khabar KSA. 2006. ARED 3.0: the large and diverse AU-rich transcriptome. Nucleic Acids Res 34:D111–D114.

47. Stumpo DJ, Lai WS, Blackshear PJ. 2010. Inflammation: Cytokines and RNA-based regulation. Wiley Interdiscip Rev RNA.

48. Kontoyiannis D, Pasparakis M, Pizarro TT, Cominelli F, Kollias G. 1999. Impaired on/off regulation of TNF biosynthesis in mice lacking TNF AU- rich elements:

Implications for joint and gut-associated immunopathologies. Immunity 10:387–398.

49. Lai WS, Blackshear PJ. 2001. Interactions of CCCH zinc finger proteins with mRNA. Tristetraprolin-mediated AU-rich element-dependent mRNA degradation can occur in the absence of a poly(A) tail. J Biol Chem 276:23144–23154.

50. Lai WS, Stumpos J, Blacksheart PJ. 1990. Rapid Insulin-stimulated Accumulation of an mRNA Encoding a Proline-rich Protein*. J Biol Chem 265:16556–16563.

51. DuBois RN, McLane MW, Ryder K, Lau LF, Nathans D. 1990. A growth factor-inducible nuclear protein with a novel cysteine/histidine repetitive sequence. J Biol Chem 265:19185–19191.

52. Carballo E, Gilkeson GS, Blackshear PJ. 1997. Bone marrow transplantation reproduces the tristetraprolin-deficiency syndrome in recombination activating gene-2 (-/-) mice. Evidence that monocyte/macrophage progenitors may be responsible for TNFα overproduction. J Clin Invest 100:986–995.

53. Lai WS, Carballo E, Thorn JM, Kennington EA, Blackshear PJ. 2000. Interactions of CCCH zinc finger proteins with mRNA. Binding of tristetraprolin-related zinc finger proteins to AU-rich elements and destabilization of mRNA. J Biol Chem 275:17827–17837.

54. Chen YL, Jiang YW, Su YL, Lee SC, Chang MS, Chang CJ. 2013. Transcriptional regulation of tristetraprolin by NF-κB signaling in LPS-stimulated macrophages. Mol Biol Rep 40:2867–2877.

55. Lai WS, Thompson MJ, Taylor GA, Liu Y, Blackshear PJ. 1995. Promoter Analysis of Zfp-36, the Mitogen-inducible Gene Encoding the Zinc Finger Protein Tristetraprolin*.

56. Taylor GA, Thompson MJ, Lai WS, Blackshear PJ. 1995. Phosphorylation of tristetraprolin, a potential zinc finger transcription factor, by mitogen stimulation in intact cells and by mitogen-activated protein kinase in vitro. J Biol Chem.

57. Taylor GA, Carballo E, Lee DM, Lai WS, Thompson MJ, Patel DD, Schenkman DI, Gilkeson GS, Broxmeyer HE, Haynes BF, Blackshear PJ. 1996. A pathogenetic role for TNFα in the syndrome of cachexia, arthritis, and autoimmunity resulting from tristetraprolin (TTP) deficiency. Immunity 4:445–454.

58. McGrath PT, Xu Y, Ailion M, Garrison JL, Butcher RA, Bargmann CI. 2011. Parallel evolution of domesticated Caenorhabditis species targets pheromone receptor genes. Nature 477:321–325.

59. Carballo E, Lai WS, Blackshear PJ. 1998. Feedback Inhibition of Macrophage Tumor Necrosis Factor-α Production by Tristetraprolin. Science (80-) 281:1001–1005.

60. Ogilvie RL, Abelson M, Hau HH, Vlasova I, Blackshear PJ, Bohjanen PR. 2005. Tristetraprolin Down-Regulates IL-2 Gene Expression through AU-Rich Element-Mediated mRNA Decay. J Immunol 174:953–961.

61. Lai WS, Carballo E, Strum JR, Kennington EA, Phillips RS, Blackshear PJ. 1999. Evidence that tristetraprolin binds to AU-rich elements and promotes the deadenylation and destabilization of tumor necrosis factor alpha mRNA. Mol Cell Biol 19:4311–23.

62. Carballo E, Lai WS, Blackshear PJ. 2000. Evidence that tristetraprolin is a physiological regulator of granulocyte-macrophage colony-stimulating factor messenger RNA deadenylation and stability. Blood 95:1891–1899.

63. Stoecklin G, Ming X-F, Looser R, Moroni C. 2000. Somatic mRNA Turnover Mutants Implicate Tristetraprolin in the Interleukin-3 mRNA Degradation Pathway. Mol Cell Biol 20:3753–3763.

64. Lai WS, Parker JS, Grissom SF, Stumpo DJ, Blackshear PJ. 2006. Novel mRNA targets for tristetraprolin (TTP) identified by global analysis of stabilized transcripts in TTP-deficient fibroblasts. Mol Cell Biol 26:9196–208.

65. Michel SLJ, Guerrerio AL, Berg JM. 2003. Selective RNA Binding by a Single CCCH Zinc-Binding Domain from Nup475 (Tristetraprolin)†. Biochemistry 42:4626–4630.

66. Lai WS, Stumpo DJ, Qiu L, Faccio R, Blackshear PJ. 2017. A knock-in tristetraprolin (TTP) zinc finger point mutation in mice: Comparison with complete TTP deficiency. Mol Cell Biol MCB.00488-17.

67. Tchen CR, Brook M, Saklatvala J, Clark AR. 2004. The stability of tristetraprolin mRNA is regulated by mitogen-activated protein kinase p38 and by tristetraprolin itself. J Biol Chem 279:32393–32400.

68. Patial S, Curtis AD, Lai WS, Stumpo DJ, Hill GD, Flake GP, Mannie MD, Blackshear PJ. 2016. Enhanced stability of tristetraprolin mRNA protects mice against immune-mediated inflammatory pathologies. Proc Natl Acad Sci 113:1865–1870.

69. Stoecklin G, Gross B, Ming XF, Moroni C. 2003. A novel mechanism of tumor suppression by destabilizing AU-rich growth factor mRNA. Oncogene 22:3554–3561.

70. Marderosian M, Sharma A, Funk AP, Vartanian R, Masri J, Jo OD, Gera JF. 2006. Tristetraprolin regulates cyclin D1 and c-Myc mRNA stability in response to rapamycin in an Akt-dependent manner via p38 MAPK signaling. Oncogene 25:6277–6290.

71. Bakheet T, Frevel M, Williams BRG, Greer W, Khabar KSA. 2001. ARED: human AU-rich element-containing mRNA database reveals an unexpectedly diverse functional

repertoire of encoded proteins. Nucleic Acids Res 29:246–254.

72. Gruber AR, Fallmann J, Kratochvill F, Kovarik P, Hofacker IL. 2011. AREsite: A database for the comprehensive investigation of AU-rich elements. Nucleic Acids Res 39.

73. Fenger-Grøn M, Fillman C, Norrild B, Lykke-Andersen J. 2005. Multiple processing body factors and the ARE binding protein TTP activate mRNA decapping. Mol Cell 20:905–915.

74. Lykke-Andersen J, Wagner E. 2005. Recruitment and activation of mRNA decay enzymes by two ARE-mediated decay activation domains in the proteins TTP and BRF-1. Genes Dev 19:351–361.

75. Reznik B, Clement SL, Lykke-Andersen J. 2014. hnRNP F Complexes with Tristetraprolin and Stimulates ARE-mRNA Decay https://doi.org/10.1371/journal.pone.0100992.

76. Fabian MR, Frank F, Rouya C, Siddiqui N, Lai WS, Karetnikov A, Blackshear PJ, Nagar B, Sonenberg N. 2013. Structural basis for the recruitment of the human CCR4-NOT deadenylase complex by tristetraprolin. Nat Struct Mol Biol 20:735–9.

77. Fu R, Olsen MT, Webb K, Bennett EJ, Lykke-Andersen J. 2016. Recruitment of the 4EHP-GYF2 cap-binding complex to tetraproline motifs of tristetraprolin promotes repression and degradation of mRNAs with AU-rich elements. Rna 22:373–382.

78. Chen CY, Gherzi R, Ong SE, Chan EL, Raijmakers R, Pruijn GJM, Stoecklin G, Moroni C, Mann M, Karin M. 2001. AU binding proteins recruit the exosome to degrade ARE-containing mRNAs. Cell.

79. Lai WS, Kennington EA, Blackshear PJ. 2003. Tristetraprolin and Its Family Members Can Promote the Cell-Free Deadenylation of AU-Rich Element-Containing mRNAs by Poly(A) Ribonuclease. Mol Cell Biol 23:3798–3812.

80. Qi M-Y, Wang Z-Z, Zhang Z, Shao Q, Zeng A, Li X-Q, Li W-Q, Wang C, Tian F-J, Li Q, Zou J, Qin Y-W, Brewer G, Huang S, Jing Q. 2012. AU-Rich-Element-Dependent Translation Repression Requires the Cooperation of Tristetraprolin and RCK/P54. Mol Cell Biol 32:913–928.

81. Lai WS, Stumpo DJ, Wells ML, Gruzdev A, Hicks SN, Nicholson CO, Yang Z, Faccio R, Webster MW, Passmore LA, Blackshear PJ. 2019. Importance of the Conserved Carboxyl-Terminal CNOT1 Binding Domain to Tristetraprolin Activity In Vivo https://doi.org/10.1128/MCB.00029-19.

82. Bulbrook D, Brazier H, Mahajan P, Kliszczak M, Fedorov O, Marchese FP, Aubareda

A, Chalk R, Picaud S, Strain-Damerell C, Filippakopoulos P, Gileadi O, Clark AR, Yue WW, Burgess-Brown NA, Dean JLE. 2018. Tryptophan-Mediated Interactions between Tristetraprolin and the CNOT9 Subunit Are Required for CCR4-NOT Deadenylase Complex Recruitment. J Mol Biol 430:722–736.

83. Stoecklin G, Stubbs T, Kedersha N, Wax S, Rigby WF, Blackwell TK, Anderson P. 2004. MK2-induced tristetraprolin:14-3-3 complexes prevent stress granule association and ARE-mRNA decay. EMBO J 237600163:1313–1324.

84. Kedersha N, Stoecklin G, Ayodele M, Yacono P, Lykke-Andersen J, Fitzler MJ, Scheuner D, Kaufman RJ, Golan DE, Anderson P. 2005. Stress granules and processing bodies are dynamically linked sites of mRNP remodeling. J Cell Biol 169:871–884.

85. Franks TM, Lykke-Andersen J. 2007. TTP and BRF proteins nucleate processing body formation to silence mRNAs with AU-rich elements. Genes Dev 21:719–735.

86. Cao H, Dzineku F, Blackshear PJ. 2003. Expression and purification of recombinant tristetraprolin that can bind to tumor necrosis factor-alpha mRNA and serve as a substrate for mitogen-activated protein kinases. Arch Biochem Biophys 412:106–120.

87. Mahtani KR, Brook M, Dean JLE, Sully G, Saklatvala J, Clark AR. 2001. Mitogen-Activated Protein Kinase p38 Controls the Expression and Posttranslational Modification of Tristetraprolin, a Regulator of Tumor Necrosis Factor Alpha mRNA Stability 21:6461–6469.

88. Carballo E, Lai WS, Blackshear PJ. 2000. Evidence that tristetraprolin is a physiological regulator of granulocyte-macrophage colony-stimulating factor messenger RNA deadenylation and stability. Blood 95:1891–1899.

89. Johnson BA, Geha M, Blackwell TK. 2000. Similar but distinct effects of the tristetraprolin/TIS11 immediate-early proteins on cell survival. Oncogene 19:1657–1664.

90. Johnson BA, Stehn JR, Yaffe MB, Keith Blackwell T. 2002. Cytoplasmic localization of tristetraprolin involves 14-3-3-dependent and -independent mechanisms. J Biol Chem 277:18029–18036.

91. Cao H, Deterding LJ, Venable JD, Kennington EA, Yates JR, Tomer KB, Blackshear PJ. 2006. Identification of the anti-inflammatory protein tristetraprolin as a hyperphosphorylated protein by mass spectrometry and site-directed mutagenesis. Biochem J 394:285–297.

92. Winzen R, Kracht M, Ritter B, Wilhelm A, Chen CYA, Shyu A Bin, Müller M, Gaestel M, Resch K, Holtmann H. 1999. The p38 MAP kinase pathway signals for cytokine-induced mRNA stabilization via MAP kinase-activated protein kinase 2 and an AU-rich

region-targeted mechanism. EMBO J 18:4969–4980.

93. Chrestensen CA, Schroeder MJ, Shabanowitz J, Hunt DF, Pelo JW, Worthington MT, Sturgill TW. 2004. MAPKAP Kinase 2 Phosphorylates Tristetraprolin on in Vivo Sites Including Ser178, a Site Required for 14-3-3 Binding. J Biol Chem 279:10176–10184.

94. Brook M, Tchen CR, Santalucia T, McIlrath J, Arthur JSC, Saklatvala J, Clark AR. 2006. Posttranslational Regulation of Tristetraprolin Subcellular Localization and Protein Stability by p38 Mitogen-Activated Protein Kinase and Extracellular Signal-Regulated Kinase Pathways. Mol Cell Biol 26:2408–2418.

95. Hitti E, Iakovleva T, Brook M, Deppenmeier S, Gruber AD, Radzioch D, Clark AR, Blackshear PJ, Kotlyarov A, Gaestel M. 2006. Mitogen-Activated Protein Kinase-Activated Protein Kinase 2 Regulates Tumor Necrosis Factor mRNA Stability and Translation Mainly by Altering Tristetraprolin Expression, Stability, and Binding to Adenine/Uridine-Rich Element. Mol Cell Biol 26:2399–2407.

96. Hsieh HH, Chen YA, Chang YJ, Wang HH, Yu YH, Lin SW, Huang YJ, Lin S, Chang CJ. 2021. The functional characterization of phosphorylation of tristetraprolin at C-terminal NOT1-binding domain. J Inflamm (United Kingdom) 18:1–16.

97. Rataj F, Planel S, Desroches-Castan A, Le Douce J, Lamribet K, Denis J, Feige JJ, Cherradi N. 2016. The cAMP pathway regulates mRNA decay through phosphorylation of the RNA-binding protein TIS11b/BRF1. Mol Biol Cell 27:3841–3854.

98. Clark AR, Dean JLE. 2016. The control of inflammation via the phosphorylation and dephosphorylation of tristetraprolin: a tale of two phosphatases. Biochem Soc Trans 44:1321–1337.

99. Bell SE, Sanchez MJ, Spasic-Boskovic O, Santalucia T, Gambardella L, Burton GJ, Murphy JJ, Norton JD, Clark AR, Turner M. 2006. The RNA binding protein Zfp36l1 is required for normal vascularisation and post-transcriptionally regulates VEGF expression. Dev Dyn 235:3144–3155.

100. Ramos SBV, Stumpo DJ, Kennington EA, Phillips RS, Bock CB, Ribeiro-Neto F, Blackshear PJ. 2004. The CCCH tandem zinc-finger protein Zfp36l2 is crucial for female fertility and early embryonic development. Development 131:4883–4893.

101. Sanduja S, Blanco FF, Dixon DA. 2011. The roles of TTP and BRF proteins in regulated mRNA decay. Wiley Interdiscip Rev RNA.

102. Stumpo DJ, Broxmeyer HE, Ward T, Cooper S, Hangoc G, Yang JC, Shelley WC, Richfield EK, Ray MK, Yoder MC, Aplan PD, Blackshear PJ. 2009. Targeted disruption of Zfp36l2, encoding a CCCH tandem zinc finger RNA-binding protein, results in defective hematopoiesis. Blood 114:2401–2410.

103. Ball CB, Rodriguez KF, Stumpo DJ, Ribeiro-Neto F, Korach KS. 2014. The RNA-Binding Protein, ZFP36L2, Influences Ovulation and Oocyte Maturation. PLoS One 9:97324.

104. Galloway A, Saveliev A, Łukasiak S, Hodson DJ, Bolland D, Balmanno K, Ahlfors H, Monzón-Casanova E, Mannurita SC, Bell LS, Andrews S, Díaz-Muñoz MD, Cook SJ, Corcoran A, Turner M. 2016. RNA-binding proteins ZFP36L1 and ZFP36L2 promote cell quiescence. Science (80-) 352:453–459.

105. Hodson DJ, Janas ML, Galloway A, Bell SE, Andrews S, Li CM, Pannell R, Siebel CW, MacDonald HR, De Keersmaecker K, Ferrando AA, Grutz G, Turner M. 2010. Deletion of the RNA-binding proteins ZFP36L1 and ZFP36L2 leads to perturbed thymic development and T lymphoblastic leukemia. Nat Immunol 2010 118 11:717–724.

106. Hyatt LD, Wasserman GA, Rah YJ, Matsuura KY, Coleman FT, Hilliard KL, Pepper-Cunningham ZA, Ieong M, Stumpo DJ, Blackshear PJ, Quinton LJ, Mizgerd JP, Jones MR. 2014. Myeloid ZFP36L1 Does Not Regulate Inflammation or Host Defense in Mouse Models of Acute Bacterial Infection. PLoS One 9:e109072.

107. Blackshear PJ, Perera L. 2014. Phylogenetic distribution and evolution of the linked RNA-binding and NOT1-binding domains in the tristetraprolin family of tandem CCCH zinc finger proteins. J Interf Cytokine Res 34:297–306.

108. Adachi S, Homoto M, Tanaka R, Hioki Y, Murakami H, Suga H, Matsumoto M, Nakayama KI, Hatta T, Iemura SI, Natsume T. 2014. ZFP36L1 and ZFP36L2 control LDLR mRNA stability via the ERK-RSK pathway. Nucleic Acids Res 42:10037–10049.

109. Otsuka H, Fukao A, Tomohiro T, Adachi S, Suzuki T, Takahashi A, Funakami Y, Natsume T, Yamamoto T, Duncan KE, Fujiwara T. 2020. ARE-binding protein ZFP36L1 interacts with CNOT1 to directly repress translation via a deadenylation-independent mechanism. Biochimie 174:49–56.

110. Maitra S, Chou CF, Luber CA, Lee KY, Mann M, Chen CY. 2008. The AU-rich element mRNA decay-promoting activity of BRF1 is regulated by mitogen-activated protein kinase-activated protein kinase 2. Rna 14:950–959.

111. Schmidlin M, Lu M, Leuenberger SA, Stoecklin G, Mallaun M, Gross B, Gherzi R, Hess D, Hemmings BA, Moroni C. 2004. The ARE-dependent mRNA-destabilizing activity of BRF1 is regulated by protein kinase B. EMBO J 23:4760–4769.

112. Benjamin D, Schmidlin M, Min L, Gross B, Moroni C. 2006. BRF1 Protein Turnover and mRNA Decay Activity Are Regulated by Protein Kinase B at the Same Phosphorylation Sites. Mol Cell Biol 26:9497–9507.

113. Graham JR, Hendershott MC, Terragni J, Cooper GM. 2010. mRNA Degradation Plays a Significant Role in the Program of Gene Expression Regulated by

Phosphatidylinositol 3-Kinase Signaling. Mol Cell Biol 30:5295–5305.

114. Hao S, Baltimore D. 2009. The stability of mRNA influences the temporal order of the induction of genes encoding inflammatory molecules. Nat Immunol 10:281–288.

115. Fu R, Olsen MT, Webb K, Bennett EJ, Lykke-Andersen J. 2016. Recruitment of the 4EHP-GYF2 cap-binding complex to tetraproline motifs of tristetraprolin promotes repression and degradation of mRNAs with AU-rich elements. RNA 22:373–382.

116. Sun L, Stoecklin G, Van Way S, Hinkovska-Galcheva V, Guo RF, Anderson P, Shanley TP. 2007. Tristetraprolin (TTP)-14-3-3 complex formation protects TTP from dephosphorylation by protein phosphatase 2a and stabilizes tumor necrosis factor-α mRNA. J Biol Chem 282:3766–3777.

117. Taylor GA, Carballo E, Lee DM, Lai WS, Thompson MJ, Patel DD, Schenkman DI, Gilkeson GS, Broxmeyer HE, Haynes BF, Blackshear PJ. 1996. A pathogenetic role for TNFa in the syndrome of cachexia, arthritis, and autoimmunity resulting from tristetraprolin (TTP) deficiency. Immunity 4:445–454.

118. Sandler H, Kreth J, Timmers HTM, Stoecklin G. 2011. Not1 mediates recruitment of the deadenylase Caf1 to mRNAs targeted for degradation by tristetraprolin. Nucleic Acids Res 39:4373–4386.

119. Cuenda A, Rousseau S. 2007. p38 MAP-Kinases pathway regulation, function and role in human diseases. Biochim Biophys Acta - Mol Cell Res 1773:1358–1375.

120. Marchese FP, Aubareda A, Tudor C, Saklatvala J, Clark AR, Dean JLE. 2010. MAPKAP kinase 2 blocks tristetraprolin-directed mRNA decay by inhibiting CAF1 deadenylase recruitment. J Biol Chem 285:27590–27600.

121. Clement SL, Scheckel C, Stoecklin G, Lykke-Andersen J. 2011. Phosphorylation of Tristetraprolin by MK2 Impairs AU-Rich Element mRNA Decay by Preventing Deadenylase Recruitment. Mol Cell Biol 31:256–266.

122. Ronkina N, Shushakova N, Tiedje C, Yakovleva T, Tollenaere MAX, Scott A, Batth TS, Olsen JV, Helmke A, Bekker-Jensen SH, Clark AR, Kotlyarov A, Gaestel M. 2019. The Role of TTP Phosphorylation in the Regulation of Inflammatory Cytokine Production by MK2/3. J Immunol 203:2291–2300.

123. Clement SL, Lykke-Andersen J. 2008. A tethering approach to study proteins that activate mRNA turnover in human cells. Methods Mol Biol 419:121–133.

124. Tollenaere MAX, Tiedje C, Rasmussen S, Nielsen JC, Vind AC, Blasius M, Batth TS, Mailand N, Olsen J V., Gaestel M, Bekker-Jensen S. 2019. GIGYF1/2-Driven Cooperation between ZNF598 and TTP in Posttranscriptional Regulation of

Inflammatory Signaling. Cell Rep 26:3511-3521.e4.

125. Tran DDH, Koch A, Saran S, Armbrecht M, Ewald F, Koch M, Wahlicht T, Wirth D, Braun A, Nashan B, Gaestel M, Tamura T. 2016. Extracellular-signal regulated kinase (Erk1/2), mitogen-activated protein kinase-activated protein kinase 2 (MK2) and tristetraprolin (TTP) comprehensively regulate injury-induced immediate early gene (IEG) response in in vitro liver organ culture. Cell Signal 28:438–447.

126. Xue Y, Liu Z, Gao X, Jin C, Wen L, Yao X, Ren J. 2010. GPS-SNO: Computational prediction of protein s-nitrosylation sites with a modified GPS algorithm. PLoS One 5:115–1.

127. Gschwendt M, Dieterich S, Rennecke J, Kittstein W, Mueller HJ, Johannes FJ. 1996. Inhibition of protein kinase C μ by various inhibitors. Differentiation from protein kinase c isoenzymes. FEBS Lett 392:77–80.

128. Nakajima K, Tohyama Y, Kohsaka S, Kurihara T. 2004. Protein kinase Cα requirement in the activation of p38 mitogen-activated protein kinase, which is linked to the induction of tumor necrosis factor α in lipopolysaccharide-stimulated microglia. Neurochem Int 44:205–214.

129. Pennington K, Chan T, Torres M, Andersen J. 2018. The dynamic and stress-adaptive signaling hub of 14-3-3: emerging mechanisms of regulation and context-dependent protein–protein interactions. Oncogene 37:5587–5604.

130. Luo Y, Na Z, Slavoff SA. 2018. P-Bodies: Composition, Properties, and Functions. Biochemistry 57:2424–2431.

131. Deleault KM, Skinner SJ, Brooks SA. 2008. Tristetraprolin regulates TNF TNF-α mRNA stability via a proteasome dependent mechanism involving the combined action of the ERK and p38 pathways. Mol Immunol 45:13–24.

132. Schwede A, Ellis L, Luther J, Carrington M, Stoecklin G, Clayton C. 2008. A role for Caf1 in mRNA deadenylation and decay in trypanosomes and human cells. Nucleic Acids Res 36:3374–3388.

133. Lykke-Andersen J. 2002. Identification of a Human Decapping Complex Associated with hUpf Proteins in Nonsense-Mediated Decay. Mol Cell Biol 22:8114–8121.

134. Sanduja S, Blanco FF, Young LE, Kaza V, Dixon DA. 2012. The role of tristetraprolin in cancer and inflammation. Front Biosci (Landmark Ed 17:174–88.

135. Tiedje C, Diaz-Munoz MD, Trulley P, Ahlfors H, Laaß K, Blackshear PJ, Turner M, Gaestel M. 2016. The RNA-binding protein TTP is a global post-transcriptional regulator of feedback control in inflammation. Nucleic Acids Res 44:7418–7440.

136. Tu Y, Wu X, Yu F, Dang J, Wang J, Wei Y, Cai Z, Zhou Z, Liao W, Li L, Zhang Y. 2019. Tristetraprolin specifically regulates the expression and alternative splicing of immune response genes in HeLa cells. BMC Immunol 20.

137. Ran FA, Hsu PDPPD, Wright J, Agarwala V, Scott D a, Zhang F. 2013. Genome engineering using the CRISPR-Cas9 system. Nat Protoc 8:2281–308.

138. Lykke-Andersen J, Shu M Di, Steitz JA. 2000. Human Upf Proteins Target an mRNA for Nonsense-Mediated Decay When Bound Downstream of a Termination Codon. Cell 103:1121–1131.

139. Jing Q, Huang S, Guth S, Zarubin T, Motoyama A, Chen J. 2005. Involvement of MicroRNA in AU-Rich Element-Mediated mRNA Instability their participation in regulating the stability of ARE-RNA is supported by experimental observation (Stoecklin et. Cell 120:623–634.

140. Qi MY, Song JW, Zhang Z, Huang S, Jing Q, Matera AG. 2018. P38 activation induces the dissociation of tristetraprolin from Argonaute 2 to increase ARE-mRNA stabilization. Mol Biol Cell 29:988–1002.

141. Rodríguez-Gómez G, Paredes-Villa A, Cervantes-Badillo MG, Gómez-Sonora JP, Jorge-Pérez JH, Cervantes-Roldán R, León-Del-Río A. 2021. Tristetraprolin: A cytosolic regulator of mRNA turnover moonlighting as transcriptional corepressor of gene expression. Mol Genet Metab https://doi.org/10.1016/j.ymgme.2021.03.015.

142. Barrios-García T, Gómez-Romero V, Tecalco-Cruz Á, Valadéz-Graham V, León-Del-Río A. 2016. Nuclear tristetraprolin acts as a corepressor of multiple steroid nuclear receptors in breast cancer cells. Mol Genet Metab Reports 7:20–26.

143. Barrios-García T, Tecalco-Cruz A, Gómez-Romero V, Reyes-Carmona S, Meneses-Morales I, León-Del-Río A. 2014. Tristetraprolin represses estrogen receptor α transactivation in breast cancer cells. J Biol Chem 289:15554–15565.

144. Sedlyarov V, Fallmann J, Ebner F, Huemer J, Sneezum L, Ivin M, Kreiner K, Tanzer A, Vogl C, Hofacker I, Kovarik P. 2016. Tristetraprolin binding site atlas in the macrophage transcriptome reveals a switch for inflammation resolution. Mol Syst Biol 12.